An Exponential Chaotic Differential Evolution Algorithm for Optimizing Bridge Maintenance Plans

Eslam Mohammed Abdelkader*[1], Osama Moselhi[2], Mohamed Marzouk[3], and Tarek Zayed[4]

ABSTRACT

Bridges are one of the fundamental infrastructure assets that are vital for economic growth and public welfare. Over the past few decades, the numbers of deteriorating bridges have drastically escalated raising concerns for serviceable, safe and functional transportation networks. This state of affairs poses a paramount challenge especially when coupled with the need to address social and environmental constraints. Accordingly, this current research paper proposes an automated three-component model for bridge maintenance optimization at both project and network levels. The first component aims at identifying the physical characteristics of the tackled bridge inventory. The second component encompasses designing a multi-objective optimization model to determine the optimal set of maintenance plans through four principal objective functions. These functions comprise maximization of performance condition of bridge elements, minimization of agency and user costs, minimization of duration of traffic disruption and minimization of environmental impact. In the multi-objective optimization model, an exponential chaotic differential evolution (ECDE) algorithm is introduced in an attempt to circumvent the drawbacks of convergence speed and search behavior of classical meta-heuristics. The third component combines criteria importance through inter-criteria correlation (CRITIC), complex proportional assessment (COPRAS) and grey relational analysis (GRA) to select the most optimum maintenance plan for each study period. Comparison results revealed that ECDE-based Sinusoidal algorithm managed to improve the performance diagnostics of classical meta-heuristics by values ranged from 49.2% to 73.1% over the multi-year maintenance plans. The results of benchmark test functions exemplified that ECDE-based Sinusoidal algorithm performed better than genetic and differential evolution algorithms by 114.2% and 79.5%, respectively. The developed integrated model is expected to assist infrastructure managers in executing optimized and sustainable maintenance budget plans within various planning scenarios.

Keywords: Bridges; maintenance optimization; project and network levels; multi-objective; exponential chaotic differential evolution; multi-criteria decision making; complex proportional assessment

[1] Assistant lecturer, Structural Engineering Department, Faculty of Engineering, Cairo University, Egypt.
[2]Professor and Director of the Centre for Innovation in Construction and Infrastructure Engineering and Management (CICIEM), Department of Building, Civil, and Environmental Engineering, Concordia University, Montreal, QC, Canada.
[3] Professor of Construction Engineering and Management, Structural Engineering Department, Faculty of Engineering, Cairo University, Egypt.
[4] Professor, Department of Building and Real Estate, the Hong Kong Polytechnic University, Hung Hom, Hong Kong.

1. INTRODUCTION

In the recent few years, infrastructure asset management has been recognized as an integrated strategic approach that aims at maximizing the public safety, serviceability and functionality of the assets by making full use of limited allocated resources. It merges engineering fundamentals with sound business approaches and economic foundations endeavoring to establish cost-effective intervention decisions across the lifecycle of the asset [1,2]. Bridges are critical and vital links of transportation infrastructure that should be efficiently preserved within acceptable performance requirements over the lifetime of the bridge despite harsh operating conditions. They experience severe deterioration agents which accelerate their aging and depreciation including extreme weather conditions, freeze-thaw cycles, excessive distress loads due to traffic overload, etc. Repairing these bridges requires a significant investment, whereas the available budget cannot cover the expenses of maintaining all the networks' bridges simultaneously. This calls for establishing bridge management systems (BMSs) that aid transportation agencies in structuring optimal programs and strategies of maintenance, repair and rehabilitation (MR&R) while satisfying their structural and resources constraints. The proper allocation of MR&R budget minimizes the accumulation of backlog of bridge intervention actions, whereas the backlog of maintenance activities can create a massive increase in the repair costs to the extent that repairing the deteriorating bridges is more expensive than building new ones [3].

In Canada, the immediate and serious implications of bridge collapses have directed the public attention to the essence of managing bridge maintenance from structural, economic, societal, and environmental perspectives. Bridges encounter expeditious deterioration that necessitates urgent structural intervention to prevent them from further deterioration and to improve the bridge elements better than existing ones. It is estimated that approximately that one third of the bridges in Canada suffer from functional or structural deficiencies. Furthermore, they consumed nearly 57% of their useful lifetime, which marks the second highest consumption rate among the five main assets after the wastewater treatment infrastructures. The five main assets encompass highways and roads, bridges and overpasses, water supply systems, wastewater treatment and sewer systems [4,5].

From provincial perspective, bridges in Quebec have the highest average age followed by Nova Scotia and then Ontario. On the other hand, Prince Edward Island has the lowest average age. It can be noticed that the consumption rate of bridge in Quebec is nearly 15% higher that the consumption rate of the Canadian national bridges, which can be explained by the fact that most of the bridges in Quebec were constructed between the 1960s and 1980s [6,7]. Additionally, it is provided that the backlog of bridge maintenance, rehabilitation and replacement is estimated to be equal to $10 billion [8]. In view of above, the present research study proposes a multi-objective optimization model that uses exponential chaotic differential evolution optimization algorithm for the optimum allocation of bridge MR&R actions in both project and network levels while accommodating the competing objective functions of condition, cost, environmental impact and traffic disruption.

2. LITERATURE REVIEW

A cost-effective maintenance schedule is necessary for delegated agencies in order to obtain the exact information about the need and timing of maintenance activities for a certain planning horizon. Additionally, it enables them enable to manage the imbalance between the extensive needs for maintenance, repair and rehabilitation actions, and the limited available funds. Several studies were carried out for bridge maintenance planning and prioritization through modeling several objective functions. The literature review is divided into three main sections, namely optimization-based models, multi-criteria decision making models and summarized research gaps.

2.1 Optimization-based Models

Alsharqawi et al. [9] proposed a budget optimization model to identify the most appropriate maintenance, repair and rehabilitation actions for reinforced concrete bridge decks. Genetic algorithm was implemented to find the optimum intervention actions based on satisfying cost and level of service requirements. Weibull distribution was modeled to simulate the deterioration process of bridge decks along the study period. Weighted comprehensive criteria method was used to search for the Pareto optimal solutions according to assigning relative weights to the bi-objective functions. It was shown that increasing level of services could be fulfilled by increasing the budget cost by 51%. Ghodoosi et al. [10] developed an optimization model that comprised genetic algorithm to select the cost-effective intervention actions. In the developed model, a biquadratic regression function was incorporated to model the reliability of the bridge superstructure across the planning horizon. The fitness function involved minimization of the equal uniform annual worth of MR&R expenditures for a composite reinforced concrete superstructure.

Shim et al. [11] proposed a bi-objective optimization model for the budget allocation of MR&R decisions over six years of planning horizon. Stochastic Markov decision process was employed to predict the deterioration of the network of bridge decks based on the national bridge inventory. In the developed model, two interrelated objective functions were considered, which were minimizing the percentage area of structurally deficient deck, and minimizing the total annual MR&R expenditures. The proposed multi-objective optimization modrl was based on modification of "Normal Boundary Intersection" algorithm. They highlighted that it could better generate efficient Pareto optimal solutions when compared against normal boundary intersection, normal constraint, goal attainment and weighted sum techniques. Wu et al. [12] presented a life-cycle optimization model for highway bridge maintenance. Semi-Markov decision process was deployed to simulate the deterioration of bridges of the 2012 national bridge inventory dataset for the state of Texas. Then, the optimum maintenance strategies can be identified relying on the deterioration pattern and the repair costs. They highlighted that the developed model could provide more effective decision-making plans in the light of limited repair funds for maintaining critical bridges.

Badawy [13] presented a single-objective genetic algorithm to obtain the optimum maintenance plan of the expansion joints. Markovian models were used to obtain the future performance of the expansion joints, whereas the transition probability matrix was calibrated based on minimizing the differences between the predicted condition and the inspected condition. The optimum intervention actions were identified based on the maximization of the annual condition index of the expansion joints while satisfying a total budget constraint.

2.2 Multi-criteria Decision Making Models

Allah Bukhsh et al. [14] proposed a framework for multi-year maintenance planning for a group of bridges. Markov decision process was applied to forecast the deterioration process of the bridge, such that percentage prediction method was used to calibrate the transition probability matrices. In the developed framework, multi-attribute utility theory was utilized to rank the bridges through a universal score that simulates the preferences of the decision makers. A five-year optimal maintenance plan was established capitalizing on the genetic algorithm given a certain condition threshold and budget constraint. They pointed out that the developed framework can aid asset managers in implementing various maintenance scenarios within different performance and financial requirements. Dromey et al. [15] developed a model to rank the rehabilitation priority of bridges based on a set of characteristic attributes. Linear regression analysis was utilized to predict the annual degradation in the condition ratings of the bridges. The prioritization index was established based on ten influencing factors including: overall structural condition, number of spans, bridge material, rehabilitation cost, etc. Afterwards, stepwise multiple regression analysis was conducted to generate the best combination of independent variables that constitute the prioritization index. They highlighted that the developed model could serve as a robust process to optimize the annual investments designated for bridge network rehabilitation.

Gao et al. [16] proposed a method to rank the concrete bridge repairs based on the VIKOR (VlseKriterijumska Optimizcija I Kaompromisno Resenje in Serbian). The final multi-criteria ranking index was obtained based on a set of attributes including: average daily traffic, average daily truck traffic, service years, service environment alongside the sufficiency rating attributes. The sufficiency ratings attributes encompassed the ratings of deck, substructure, superstructure, culvert, etc. The relative importance weighting of the criteria set was computed based on the criteria importance through inter-criteria correlation. They suggested that the developed ranking system could efficiently rank the bridge maintenance order. Contreras-Nieto et al. [17] introduced a geographical information system-based model for the prioritization of bridge maintenance plans. The ranking system was formed based on the average daily traffic alongside the weighted average rating that considered deck, substructure, superstructure and scour. They evaluated the bridges based on a set of four attributes, namely bridge resiliency, riding comfort, safety and serviceability, whereas their relative importance weighting was obtained using Analytical Hierarchy Process.

Mahdi et al. [18] introduced a decision support system for identifying optimum maintenance plan of bridges stepping on bridge overall priority index. The evaluation of the bridge depends on three performance indicators, namely structural performance, functional performance and external factors. The optimal maintenance budget allocation is generated through a dynamic programming-based model that aimed at minimizing the total repair cost, and subject to performance and financial constraints. Markiz and Jrade [19] introduced a stochastic fuzzy logic decision support system combined with bridge information management system (BrIMS) to predict the bridge deterioration and to sort the MR&R actions. The priority rankings of the bridge components were established using quality function deployment and technique of order preference similarity to the ideal solution (TOPSIS). The deterioration process of the bridge elements was simulated using time-dependent gamma shock models, such that the gamma function parameters were estimated through regression analysis. It was revealed that the developed deterioration model could efficiently mimic the future performance of the bridge elements with a percentage of error ranged from 10% to 15%.

Nurani et al. [20] investigated the implementation of analytical hierarchy process (AHP), fuzzy AHP and technique of order preference similarity to the ideal solution for the identification of bridge maintenance priorities. The ranking platform was established based on the average daily traffic alongside the bridge damage condition, which was based on the aggregated weighted average of the condition of the different components. Results revealed that AHP and TOPSIS produced close priority rankings to each other. Rashidi et al. [21] developed a decision support system to select the optimum remediation strategies for steel bridges. Simplified analytical hierarchy process ($\mathrm{S-AHP}$) was used to compute the weighting vector of the six main attributes of the decision making model, namely service life, safety, cost, environmental impact, traffic disruption and aesthetic appeal. They considered four different alternatives of rehabilitation actions: splice plates, steel plate strengthening, fiberglass reinforced plastic strengthening and partial member replacement. They concluded that safety had the highest global importance among the different attributes. Additionally, it can provide decision makers with reliable recommendations for the prioritization and selection of remediation actions of deteriorated bridges.

Nurdin et al. [22] introduced a multi-criteria decision making framework for the determination of maintenance and rehabilitation priorities of bridges. In this model, AHP was applied to model the weighting vector of the relevant attributes, namely condition, traffic volume and policy. Bridge condition was found to be of the highest weight (49.1%) while traffic volume constituted the lowest weight (18.5%). Subsequently, the intervention action, either maintenance or rehabilitation, was assigned as per the prioritization index. Yoon and Hastak [23] developed a multi-tiered method for the prioritization of bridge deck rehabilitation relying on urgency scale and total prioritization scale. The urgency scale was based on computing the timeframe that the rehabilitation process of the bridge deck can be delayed until its structural condition goes beyond the acceptable limit. The total prioritization scale integrates the normalized magnitudes of the performance, economic and criticality scales.

2.3 Summarized Research Gaps

Bibliometric co-occurrence map is structured for the purpose of creating a comprehensive overview of the bridge maintenance planning and prioritization. This is accomplished using VOSviewer platform which enables to extract and analyse the co-occurrences of keywords related to a given topic. Van Eck and Waltman [24] defined the number of co-occurrences of two keywords as the number of publications in which the keywords were mentioned together either in the title, abstract or the keywords list. The scientometric analysis facilitates delineating the drawbacks of the previous studies which paves the way for establishing more efficient maintenance optimization models. Figure 1 depicts a bibliometric co-occurrence map for the bridge maintenance planning and prioritization using VOSviewer 1.6.14. The created bibliometric map is used to highlight the frequencies of the developed genetic algorithm-based models. It is obtained capitalizing on a total of 101 articles published from 1997 to 2020 that induces a network of 222 keywords. In view of the previous studies, most of them supported either element-level, project-level or network-level decisions separately. Despite their interrelatedness, the previous literature lacks the integration of the different levels of decision-making. This absence of integration between the different levels of decision-making process can yield inefficient maintenance budget allocation models [25]. It is worth mentioning that the integration of the different levels is a more complicated task because of the necessity to model the various deterioration patterns of the bridge components instead of dealing with one type of them, which were usually bridge decks.

INSERT FIGURE 1

Some studies relied on single-objective optimization models for maintenance budget allocation. Single-objective optimization models focus on one fitness function at the expense of other functions. This induces a significant sacrifice in the performance of the optimization model and the quality of the generated optimal solutions. Most of the maintenance planning models dealt with short-term maintenance planning, whereas the previous models lack the exploration of long-term strategic planning. The allocation of MR&R decisions in short-term study periods is a simplified process and experience less interruptions when compared against the long-term maintenance planning. It is expected that the short-term maintenance models will diverge when applied to the more exhaustive nature of the combinatorial optimization model associated with long-term planning. This elicited from the amplified increase in the possible solutions of MR&R decisions. As such, the short-term periods are not sufficient to validate the performance capacity of the maintenance optimization models. Additionally, previous researches were concerned with relatively smaller number of bridge elements, which causes these models to be incomprehensive enough to model current transportation networks of large numbers of bridge elements.

Some models assumed that the deterioration behavior experienced by the bridge elements after the application of the intervention action will be in the same manner as before its application. In this context, the deterioration rates of the bridge elements are predicted to decelerate when intervention action is applied. Additionally, some models optimize the MR&R actions for the entire bridge rather than the different elements of the bridge. Dealing with the bridge as a single unit regardless the physical condition of the bridge elements may create misleading maintenance schedule. This stems from the fact that different bridge elements experience different deterioration rates over the course of the study period, which implies that they will reach their critical stages at different periods. Furthermore, the maintenance decision support systems that capitalized on a universal ranking index for prioritization purposes may be inefficient because of their incapability to monitor the degradation of the various bridge elements. It can be also noticed that multi-criteria decision-making-based maintenance models are mainly concerned with prioritization of intervention actions at a certain instance of time based on the current condition ratings of bridge elements. In this regard, they fail to generate a MR&R schedule over a certain planning horizon while accommodating a set of conflicting objective functions.

Some of the developed planning solutions presume deterministic unit costs and don’t deal with them as stochastic random variables. Failure to address the inherent uncertainties of the performance indices in the decision-making model can yield inferior maintenance plans.

Moreover, it was found that previous studies mostly focused on agency costs in their maintenance evaluation models and ignored the user-incurred costs. Nonetheless, user costs can substantially outweigh the direct agency costs in the bridges carrying high volumes of traffic. The accurate quantification and integration of user costs with agency cost can establish more comprehensive maintenance decision-making strategies.

Besides, many previous efforts viewed the maintenance management of bridges from the perspective of traditional pillars of structural condition and cost meanwhile ignoring other important performance aspects. However, Van dam et al. [(26] suggested that infrastructure management should no longer be modeled from technical perspective solely. Furthermore, transportation networks are profoundly embedded in the community. Thus, management of existing bridges should satisfy the societal and environmental requirements in addition to the technical performance aspects. Additionally, the integration of environmental and societal principles of sustainability with the conventional pillars of asset management will provide decision-makers with a more comprehensive assessment of the implications of their maintenance decisions on the three main pillars of sustainable communities, i.e., economy, society and environment.

Another shortcoming can be interpreted is that some maintenance optimization models impose constraints like the total budget and ignore the presence of annual budget constraints. In this regard, the maintenance budget is usually assigned annually. Furthermore, the maintenance optimization model may satisfy the total budget constraint and violate the annual budget constraints. This causes that the importance of assigning this constraint is better demonstrated in the presence of large numbers of bridge elements. Some of the developed maintenance optimization plans experience large number of intervention actions within small portion of the planning horizon because they overlooked the maximum number of visits when formulating the optimization model. This induces significant traffic disruption to the users of the bridge. Furthermore, some of the developed annual MR&R cost profiles witness substantial fluctuations. Nonetheless, transportation agencies are interested in establishing timely maintenance plans with balanced expenditures over the planning period. In this context, a constraint needs to be assigned to stabilize the fluctuations of the annual MR&R cost profiles. As such, the critical shortcomings of previous research studies motivated the authors to create a bridge maintenance optimization model that manages to give due consideration for the physical, economic, social and environmental impacts for the intervention actions.

3. PROPOSED MODEL

The main objective of the present research paper is to develop an automated platform that supports both project and network-levels decisions for maintenance budget allocation over a certain planning horizon. The framework of the proposed model is depicted in Figure 2. As can be seen, the proposed method is divided into three main components namely, data input architecturing, multi-objective optimization and hybrid multi-criteria decision-making. In the first component, the first stage is identifying the characteristics of the tackled bridge inventory, which encompasses the age, type and number of the bridge in the bridge network in addition to the type and number of bridge components in each bridge. In the present study, the lifetime performance of the bridge is demonstrated in the form of three main components, namely deck, pier and abutment. Additionally, the proposed model is designed to deal with both short-term and long-term study periods. In this context, the maintenance planning categorizes the intervention strategies into four main types which are: no intervention, minor repair, major rehabilitation and replacement.

The deterioration modeling plays a monumental role in the multi-year maintenance planning at the different decision-making levels. This deterioration mechanism has to be properly captured for the different bridge components, whereas each bridge component has a different deterioration trend the other. In the present study, Markov decision process is employed to emulate the deterioration process of the bridge elements because of its capability to handle the uncertainties and vagueness of the deterioration mechanism stemming from the presence of un-observed explanatory variables and in-accurate inspection procedures. With respect to the bridge decks, a hybrid Bayesian-based approach is adopted to calibrate the transition probability matrix, whereas the deterioration process is assumed to be non-homogenous from a realistic point of view because bridge decks follow a varying deterioration pattern over the course of their service life. In the deterioration model, the likelihood functions of the in-state probabilities were computed using Bayesian belief network capitalizing on its capability to model the dependencies between the bridge defects. Markov chain Monte Carlo Metropolis-Hastings algorithm was then employed to derive the posterior probabilities stepping on the integration of the likelihood and prior probabilities. In the last stage, a stochastic optimization model based on genetic algorithm was used to obtain the transition probabilities for each zone. More details about this model can be adopted from Mohammed Abdelkader et al. [27]. Regarding the pier and abutment, the transition probabilities are obtained from Hasan [28].

It should be mentioned that the applied MR&R decision governs both the improvement in the physical condition rating of the bridge element as well as the performance of the bridge element after the employment of the intervention action. The fundamental premise of the condition improvement functions is that the level of condition performance of the bridge element is improved by an amount that is triggered by the type of the intervention decision. Furthermore, it is worth noting that deterioration transition probability matrices of the bridge element are marked by the application of MR&R action. As such, four deterioration models corresponding to the four intervention actions are constructed for each bridge component. One of the main objectives of the present study is to address the socio-environmental implications of the maintenance intervention strategies alongside the conventional economic aspects. As such, the user costs, environmental emissions footprint and work zone duration need to be computed. In this context, the work zone duration denotes the length of a time a work activity occupies a certain location. According to the manual on uniform traffic devices (MUTCD), the work duration can be categorized into five main groups namely, mobile, short-duration, short-term stationary, intermediate-term stationary and long-term stationary. The short-duration stands for a work-zone that occupies a location up to one hour while long-term stationary refers to work-zone that occupies a location for more than three days [29].

The costs in the bridge's lifecycle cost analysis can be divided into agency costs and user costs. Agency costs refer to the costs incurred by the agency or owner over the lifetime of the facility. User costs refer to costs incurred by the users of the facility as a result of the maintenance operation, which causes traffic disruption or congestion to the normal traffic flow in the facility [30]. The proposed model tackles both agency and user costs in order to establish a holistic analytical platform that enables decision-makers to select the lowest costing alternative. In the present study the user cost of a work zone is evaluated with respect to travel delay costs, vehicle operating costs and the accident costs [31]. Latin hypercube sampling is utilized in the developed model to emulate the encountered inherent uncertainties associated with maintenance costs, duration of traffic disruption and environmental impact. In this regard, maintenance costs, environmental emissions footprint and work zone durations are assumed to be normally distributed with different means and standard deviations. Normal distribution is preferred due to its simplicity and accurate simulation of unforeseen conditions in construction industry [32,33,34,35]. For each candidate solution during each optimization iteration, one thousand samples were randomly picked using Lain hyper cube sampling from their respective distributions to ensure convergence [36,37,38]. The mean values of the distributions of total life-cycle maintenance cost, total duration of traffic distributions and total environmental impact are computed and appended as objective function values for the designated candidate solution in the optimization iteration.

Latin hypercube is stratified sampling scheme that enables better coverage and exploration of the domain of the variations of the input variables. It is preferred over Monte Carlo sampling because of its time-efficiency in addition to its higher capacity of establishing efficient probability distributions using less number of iterations and less sampling error [39]. In Latin hypercube sampling, the parameter space of the input factor is divided in to N non-overlapping bins of equal marginal probabilities 1/ N. In the first iteration, one of the bins is selected randomly to be sampled from. Till the remaining N iterations, one of the bins which was not selected from sampling is picked to be sampled from. The process continues until all the N bins are picked for sampling over the N iterations [40]. It was stated earlier that the uncertainties of the deterioration process is modeled using the Makrovian model. As such, the proposed method is capable of addressing the uncertainties of the technical, economic, societal and environmental aspects of the maintenance intervention actions, which constitute the main pillars of sustainability-based decision-making process.

The second component is the multi-objective optimization, whereas the proposed model deals with multiple objective of maintenance planning. This component is designated for optimizing the MR&R plans through a set of principal objectives which encompass maximization the minimum physical condition rating of the bridge elements, minimization the total intervention costs, minimization the total duration of traffic disruption and minimization of the total environmental impact of the intervention actions. The multi-objective maintenance planning model involves a set of condition and cost constraints that comply with the technical and budget constraints imposed by the transportation agencies. The proposed model employs exponential chaotic differential evolution optimization algorithm to optimize the MR&R actions.

Several modifications were reported in the literature to improve the search behavior of multi-objective optimization algorithms like the uses of hypervolume indicator coupled with local search procedures [41], multi-directional prediction strategy [42], decomposition-based archiving approach [43], preference polyhedron with interval parameters [44] and chaotic operators [45]. To the authors' best of knowledge, chaotic optimization has not been previously investigated for maintenance budget allocation of the different assets. In the chaotic processing, the diversity and convergence of the differential evolution are optimized while preserving its original characteristics. The use of chaotic disturbance mechanism enriches the search behavior of the differential evolution capitalizing on amplifying both of its exploration and exploitation. This prevents the differential evolution algorithm from being stagnated in local minima and premature convergence especially in the presence of multimodal search spaces that encompass multiple local minima. In this regard, the multimodal search space is considered as a substantial challenge for the optimization algorithm to explore in an attempt to find the global optimum solution. The proposed method investigates nine different chaotic maps to find out the most efficient one.

Another advantage of the chaotic mapping is the generated improvement in the diversity of the population. This takes place because the values of the operators are calibrated adaptively over the course of the optimization process which in turn improves the convergence of the differential evolution algorithm. Additionally, the chaotic search saves the computational time consumed in fine-tuning the algorithm's operators to be used in improving the computational efficiency of optimization. Another competitive advantage of the optimization algorithms is that it is less sensitive than the conventional optimization algorithms to the initial setting of values which successively enhances the stability and robustness of the optimization search mechanism [46,47,48]. In the present study, the chaotic operations are employed for optimizing the initialization of population and generating chaotic variable sequence for the mutation scaling factor and crossover probability. The strategy of the exponential chaotic mutation scaling factor is formulated based on the integration of exponential distribution function and chaotic maps. The exponential scheme facilitates the efficient exploration of the search space so that the search agents move faster and at distant positions from each other, which in turn aids in converging to the global optimum solution within less number of iterations.

The proposed model investigates nine different chaotic maps to find out the most efficient one. These chaotic maps are logistic, Singer, sinusoidal, sine, iterative, Chebyshev, cubic, logistic-sine and circle. The chaotic optimization algorithm is validated through comparisons against state of art meta-heuristics namely, genetic algorithm (GA), particle swarm optimization (PSO) algorithm, invasive weed optimization (IWO) algorithm, differential evolution (DE) algorithm, Jaya algorithm, teaching learning optimization (TLO) algorithm and biogeography-based optimization (BBO) algorithm. The evaluation process of the developed multi-objective optimization model is three-folded. In the first fold, the evaluation comparisons are carried out capitalizing on a set of performance metrics including: minimum and average fitness function values in addition to hypervolume indicator, generational distance, inverted generational distance, spacing and maximum Pareto front error. Hypervolume indicator measures the region in the objective space that is covered by the non-dominated solutions [49]. This size or region is bounded by a reference point and it selected to be the point associated with the worst objective function values (nadir point) [50,51]. Spacing metric calculates the relative distance between any subsequent non-dominated solutions [52]. Generational distance measures the average distance of solutions from the true Pareto front [53]. Inverted generational distance evaluates the average minimum distance from each reference point in the true Pareto front and the closest solution obtained by the optimization algorithm [54]. In the metrics of generational distance, inverted generational distance and maximum Pareto front error, a reference point set needs to be identified. In this regard, the true Pareto front of the present multi-objective optimization problem is unknown. Hence, each algorithm was run five times independently and then all non-dominated solutions obtained by all the tackled conventional and exponential chaotic-based meta-heuristics over all the runs, are gathered and appended. Non-dominated sorting operators are then implemented to obtain the non-dominated reference set [55,56]. Maximum Pareto front error calculates the largest distance between any vector in the approximate Pareto front and the nearest vector in the true Pareto front [57]. These performance metrics are capable of judging three main aspects of optimization algorithms which are: diversity, accuracy and cardinality. The second fold is designed for the purpose of evaluating the significance levels of the optimal solution. In this regard, Shapiro-Wilk test is used at first to study the normality of the data at significance level (α) of 0.05. Subsequently, parametric or non-parametric tests are performed relying on the assessment of normality of the data for statistical significance comparison. The third aims at establishing an integrative reflection on the performances of the multi-objective evolutionary algorithms (MOEA) with respect to the accuracy and stability. This is addressed though the average ranking method that is fed by the output generated from the first fold.

The developed chaotic exponential chaotic differential evolurion algorithm is further validated against the classical meta-heuristics of genetic algorithm and differential evolution algorithm using the benchmark test functions of Schwefel 2.26 [58], Rastrigin [59], Griewank [60], Beale [61] and three-hump camel [62]. The used benchmark test functions include a combination of multi-modal functions such as Schwefel 2.26, Rastrigin, Griewank and three-hump camel meanwhile Beale is a uni-modal function [63,64,65]. Multi-modal functions are associated with several local extreme points, whereas they are used to reflect the exploration abilities of meta-heursitics and diversity preservation which facilitate local minima entrapment. The uni-modal functions test the convergence speed and exploitation abilities of meta-heuristics [66,67].

The third component is the hybrid multi-criteria decision-making which is designed for the purpose of selecting the most optimum MR&R plan for each study period among the set of Pareto optimal solutions. In this component, the weights of the performance aspects are obtained objectively based on the criteria importance through inter-criteria correlation technique to overcome the subjective preferences in the weights' assignment. In this algorithm, the information of the criteria is signified by not only the standard deviation of the criteria but also the correlation between the attributes. In this study, a hybrid multi-criteria decision-making (MCDM) approach is proposed to provide a robust and comprehensive ranking of the Pareto optimal solutions. In this regard, complex proportional assessment (COPRAS) and grey relational analysis (GRA) are coupled to generate a final ranking of the Pareto optimal solutions using the average ranking method. COPRAS and GRA are selected because they proved their efficiency in dealing with complex problems of decision-making such as improvement of surface water distribution systems [68], sustainability assessment of cities [69], studying the characteristics of asphalt binder [70] and risk assessment of deep foundation excavation [71]. Furthermore, they require less parameters than other MCDM approaches in their computational procedures. Additionally, the two MCDM approaches are of different computational nature which paves the way for creating a comprehensive ranking of the solutions. The multi-objective optimization model is automated using a computerized platform that encompasses a hybridization of C#.net and Matlab programming languages to facilitate the users' implementation. It is expected that the automated paradigm is capable of exploiting the compatibility and versatility capabilities of C#.net alongside the superior computational capacity of the Matlab.

INSERT FIGURE 2

4. MULTI-OBJECTIVE OPTIMIZATION MODEL

The proposed multi-objective optimization model considers both project and network-level decisions in the planning of MR&R actions while satisfying the condition rating and budget constraints. In this context, it enables to determine which bridge component to repair, what intervention action to apply and when to perform the intervention action. The solution structure of the multi-objective maintenance planning model is depicted in Figure 3. As shown in Figure 3, the search agent or the candidate solution is structured in the form of a string of elements, whose length denotes the number of decision variables of the multi-objective optimization model. The variable X_{ijt} takes integer values range from one to four depending on the type of the intervention action, whereas X_{ijt} of 1, 2, 3 and 4 correspond to no intervention, minor repair, major rehabilitation and replacement, respectively. For instance, minor repair of bridge deck includes crack sealing, patching and removing of spalled or delaminated concrete. Major rehabilitation includes strengthening by adding additional plates or girders in addition to increasing bridge deck thickness. Additionally, it is worth noting that the proposed model can tackle project and network-level decisions by modeling the timely MR&R plans for element i in bridge j at time t. In the present study, a set of principal multiple objectives are modeled for the purpose of multi-year maintenance planning. The objective functions tend to maximize the condition performance level of the bridge elements, minimize the total life-cycle maintenance costs, minimize the duration of traffic disruption and minimize the environmental impact as displayed in Equations (1), (2) ,(3) and (4), respectively.

$$\mathrm{CR} = \mathrm{Max}\begin{cases} \min \mathrm{cond}_{\mathrm{deck}} = F[\mathrm{Mt_d}, \mathrm{t_d}] \ |\text{for } d = 1, 2, 3 \ldots\ldots\ldots\ldots\ldots D \\ \min \mathrm{cond}_{\mathrm{pier}} = F\left[\mathrm{Mt_p}, \mathrm{t_p}\right] \ |\text{for } p = 1, 2, 3 \ldots\ldots\ldots\ldots\ldots P \\ \min \mathrm{cond}_{\mathrm{abutment}} = F[\mathrm{Mt_{ab}}, \mathrm{t_{ab}}] \ |\text{for } ab = 1, 2, 3 \ldots\ldots\ldots\ldots\ldots AB \end{cases} \tag{1}$$

$$TLCC = Min \sum_{t=1}^{T} \sum_{j=1}^{J} \sum_{i=1}^{I} \frac{TAC_{ijt}}{(1+r)^t} + \frac{TUC_{ijt}}{(1+r)^t} \tag{2}$$

$$TDTT = Min \sum_{t=1}^{T} \sum_{j=1}^{J} \sum_{i=1}^{I} DTT_{ijt} \tag{3}$$

$$TEI = Min \sum_{t=1}^{T} \sum_{j=1}^{J} \sum_{i=1}^{I} EI_{ijt} \tag{4}$$

Subject to the following constraints:

$$CR \geq CR_{min} \tag{5}$$

$$TLCC \leq BUD_{available} \tag{6}$$

$$TC_t \leq BUD_t \tag{7}$$

$$STD_{MC} \leq STD_{thre} \tag{8}$$

$$Num_{Interv} \leq Num_{thre} \tag{9}$$

Such that;

$$\begin{aligned} EI_{ijt} = {} & T1 \times \left(\frac{Eghg}{Eghg_{sum}}\right) + T2 \times \left(\frac{Eap}{Eap_{Sum}}\right) + T3 \times \left(\frac{Epm}{Epm_{Sum}}\right) + T4 \times \left(\frac{Eep}{Eep_{Sum}}\right) \\ & + T5 \times \left(\frac{Eod}{Eod_{Sum}}\right) \\ & + T6 \times \left(\frac{Es}{Es_{Sum}}\right) \end{aligned} \tag{10}$$

$$STD_{MC} = \sqrt{\frac{\sum_{r=1}^{N} (AVG\_MC - TC_t)^2}{N}} \tag{11}$$

Where;

CR represents the minimum condition rating for all bridge components in all bridges across the planning horizon. It is worth mentioning that the minimum function is adopted instead of the average function because the average function fails to capture the presence of failure in the bridge elements. $\min \mathrm{cond}_{\mathrm{deck}}$, $\min \mathrm{cond}_{\mathrm{pier}}$ and $\min \mathrm{cond}_{\mathrm{abutment}}$ represent the condition performances of deck, pier and abutment, respectively. Mt_{d}, Mt_{p} and $\mathrm{Mt}_{\mathrm{ab}}$ represent the type of intervention action applied to deck, pier and abutment, respectively. t_{d}, t_{p} and t_{ab} depict the time sequences of intervention action applied to deck, pier and abutment, respectively. D, P and AB stand for the total numbers of decks, piers and abutments, respectively.

TLCC depicts the total life-cycle maintenance costs and it is equal to the summation of the discounted maintenance costs applied at time instant t. $\mathrm{TAC}_{\mathrm{ijt}}$ and $\mathrm{TUC}_{\mathrm{ijt}}$ depict the total agency and user costs of the intervention action for element i in bridge j at time t. r stands for the monetary discount rate and it is assumed 6% [72]. TDTT represents the total duration of traffic disruption. $\mathrm{DTT}_{\mathrm{ijt}}$ stands for the duration of traffic disruption encountered from the MR&R action performed to element i in bridge j at time t. The work zone durations for the different intervention actions are derived from Lindly and Clark [73] and resource planning developed in the previous section.

TEI is the total environmental impact from the intervention action. $\mathrm{EI}_{\mathrm{ijt}}$ stands for the environmental impact of the MR&R action performed to element i in bridge j at time t. It is equal to the weighted aggregation of the potentials of the various environmental emissions produced during the intervention process. T1, T2, T3, T4, T5 and T6 indicate the severity percentages of greenhouse gases, sulfur dioxide, particular matter, eutrophication particles, ozone depleting particles and smog, respectively. Eghg, Eap, Epm, Eep, Eod and Es represent potentials of greenhouse gases, sulfur dioxide, particular matter, eutrophication particles, ozone depleting particles, and smog, respectively. $\mathrm{Eghg}_{\mathrm{sum}}$, $\mathrm{Eap}_{\mathrm{Sum}}$, $\mathrm{Epm}_{\mathrm{Sum}}$, $\mathrm{Eep}_{\mathrm{Sum}}$, $\mathrm{Eod}_{\mathrm{Sum}}$, and $\mathrm{Es}_{\mathrm{Sum}}$ represent potential sum of the greenhouse gases, sulfur dioxide, particular matter, eutrophication particles, ozone depleting particles, and smog, respectively. T1, T2, T3, T4, T5 and T6 are assumed 0.3, 0.1, 0.1, 0.1, 0.3 and 0.1, respectively. The potentials of the six environmental emissions are obtained Athena impact Estimator 5.4.0103 and the developed resource planning method. More information about the modeling of the environmental emissions can be found in Marzouk et al. [74].

CR_{min} is the minimum allowable condition rating any bridge element is allowed to reach. $BUD_{available}$ denotes the available budget limit for all intervention actions of all bridge elements. TC_t denotes the total maintenance cost at instant t. BUD_t is the yearly budget limit of the intervention actions. STD_{MC} represents the standard deviation of the MR&R expenditures over the planning horizon. STD_{thre} is a threshold that corresponds to the maximum allowable standard deviation of the MR&R costs. AVG_MC is the average maintenance costs over the planning horizon. This constraint is imposed to establish a balanced MR&R cost profile as much as possible through minimizing the variations and fluctuations of the MR&R expenditures over the course of the study period. Num_{Interv} is the number of intervention actions for all bridge elements. Num_{thre} is the maximum allowable number of visits over the time horizon. This constraint is assigned to decrease the number of intervention visits, which in turn minimizes the traffic disruption. It is worth mentioning that all the afore-mentioned constraints are imposed as hard ones so that any solution which doesn't satisfy the constraint's requirements during the optimization process is filtered out.

INSERT FIGURE 3

4.1 Maximization of Bridge's Condition Rating

In the developed multi-objective optimization model, deterioration modeling is essential to forecast the future condition of decks, abutments and girders over the designated planning horizon. The used deterioration model in this research paper was presented in a previous publication by the authors which can be found in Mohammed Abdelkader et al. [27]. The inputs to this model are the inspection records and the outputs are the transition probabilities and deterioration curve. It is a stochastic time-based model that was formulated to alleviate the shortcomings of deterministic and state-based models. In this model, a Bayesian belief networks were utilized to the degree of influence of the bridge defects on the condition rating and degradation process of bridge element. It considered five types of bridge defects, namely corrosion, delamination, cracking, spalling and scaling. Transition times were assumed to follow probability distributions and they were used to calculate the conditional probabilities in the

Bayesian belief network. The output of the Bayesian belief network was the likelihood functions of the in-state probabilities. Markov chain Monte Carlo Metropolis-Hastings algorithm was then employed to derive the posterior distributions of in-state probabilities by integrating their likelihood and prior probabilities. The deterioration process was assumed to be non-homogenous, whereas the entire service life was divided into zones and transition probability matrix was assigned to each zone. A stochastic optimization model was designed to compute the optimum transition probability matrices for each zone which were appended and used in the present research paper.

As mentioned earlier, one of the key objectives of the multi-objective optimization model is to maximize the performance condition rating of the bridge elements. This is accomplished through the deterioration modeling of the bridge elements, which enables to emulate the condition rating of the bridge element over time. In this context, the transition probabilities of the deterioration model are mapped according to the preventive or corrective MR&R action. If the bridge deck undergoes no MR&R action, the transition probability matrix can be defined using Equation (12). The transition probability matrices of minor repair, major rehabilitation and replacement are displayed in Equations (13), (14) and (15), respectively [75].

$$P^{t,t+1} = \begin{bmatrix} P_{11} & 1-P_{11} & 0 & 0 \\ 0 & P_{22} & 1-P_{2} & 0 \\ 0 & 0 & P_{33} & 1-P_{33} \\ 0 & 0 & 0 & 100\% \end{bmatrix} \tag{12}$$

$$P^{t,t+1} = \begin{bmatrix} P_{11} & 1-P_{11} & 0 & 0 \\ P_{11} & 1-P_{11} & 0 & 0 \\ 0 & P_{22} & 1-P_{22} & 0 \\ 0 & 0 & P_{33} & 1-P_{33} \end{bmatrix} \tag{13}$$

$$P^{t,t+1} = \begin{bmatrix} P_{11} & 1-P_{11} & 0 & 0 \\ P_{11} & 1-P_{11} & 0 & 0 \\ P_{11} & 1-P_{11} & 0 & 0 \\ 0 & P_{22} & 1-P_{22} & 0 \end{bmatrix} \tag{14}$$

$$P^{t,t+1} = \begin{bmatrix} P_{11} & 1-P_{11} & 0 & 0 \\ P_{11} & 1-P_{11} & 0 & 0 \\ P_{11} & 1-P_{11} & 0 & 0 \\ 0 & P_{11} & 1-P_{11} & 0 \end{bmatrix} \tag{15}$$

Where;

P_{11}, P_{22} and P_{33} represent the probabilities that a bridge element remain in condition state 1, condition state 2 and condition state 3, respectively.

The condition improvement functions are mapped stepping on the type of MR&R action. After applying the minor repair, the condition states 2, 3 and 4 are improved to the condition states 1, 2 and 3, respectively. . After the implementation of major rehabilitation, the condition states 2, 3 and 4 are enhanced to the condition states 1, 1 and 2, respectively. If the bridge element is replaced, it will return to its condition state [75,76].

4.2 Minimization of Maintenance Costs

The maintenance cost is divided into two main components, namely agency and user costs. Agency costs are monetary values incurred by the agency as a result of applying the intervention actions. They are usually estimated as cost per unit area. Table 1 represents the agency cost of the intervention actions for the bridge deck [77]. The second component of the maintenance costs is the user cost, which represents the cost incurred by the users or the travelling public during the maintenance activity. This cost is fundamentally attributable to the restriction imposed on the use of the bridge as a result of the MR&R action. This restriction or construction work induces additional costs and delays because of the additional travel time and vehicle operating costs. The user costs depend primarily on the duration of work zone, average daily traffic and the increase in the accident rate because of the work zone, whereas the increase in the pre-mentioned parameters can result in as substantial increase in the user costs. In the case of bridges associated with high volumes of traffic, the user cost may exceed the agency costs. In the present study the user cost of a work zone is evaluated with respect to travel delay costs, vehicle operating costs and the accident costs [31].

INSERT TABLE 1

4.2.1 Travel delay costs

The first component of the users cost is the travel delay cost, which refers to the cost incurred by users as a result of the traffic disruption caused by the MR&R activities. The travel delay costs usually occur because of the increase in travel time due to congestion delays and speed reductions. The travel delay cost can be computed as follows.

$$\mathrm{TDC} = \left(\frac{\mathrm{L}}{\mathrm{S_a}} - \frac{\mathrm{L}}{\mathrm{S_n}}\right) \times \mathrm{t_{mrr}} \times \left[\left((\mathrm{ADT} - \mathrm{ADTT}] \times \mathrm{C_{pass}}\right) + \left((\mathrm{ADTT}] \times \mathrm{C_{tru}}\right)\right] \tag{16}$$

Where;

TDC represents the travel delay costs. L indicates the length of the affected bridge. $\mathrm{S_a}$ represents the traffic speed during the work zone. $\mathrm{S_n}$ represents the normal traffic speed. ADT and ADTT indicate the average daily traffic and average daily truck traffic. $\mathrm{C_{pass}}$ and $\mathrm{C_{tru}}$ represent the hourly time value of passenger car driver and truck driver per vehicle. $\mathrm{t_{mrr}}$ indicates the duration of the work zone.

4.2.2 Vehicle operating cost

Vehicle operating cost refers to the cost incurred by the vehicle drivers as a result of the additional time of operating the vehicle because of the traffic disruption created by the work zone. The vehicle operating cost includes: acceleration in the vehicle deprecation, the increase in vehicle operating cost, increase in the fuel consumption and the increase in the tire wear. The vehicle operating cost can be expressed as follows.

$$\mathrm{VOC} = \left(\frac{\mathrm{L}}{\mathrm{S_a}} - \frac{\mathrm{L}}{\mathrm{S_n}}\right) \times \mathrm{t_{mrr}} \times \left[\left((\mathrm{ADT} - \mathrm{ADTT}] \times \mathrm{C_{vov\_pass}}\right) + \left((\mathrm{ADTT}] \times \mathrm{C_{voc\_tru}}\right)\right] \tag{17}$$

Where;

VOC represents the vehicle operating costs. $\mathrm{C_{vov\_pass}}$ and $\mathrm{C_{voc\_tru}}$ denote the operating cost of passenger car and truck, respectively.

4.2.3 Accident cost

Accident cost is the cost incurred due to the increase in the accident rate as a result of the MR&R activities. It encompasses the cost of injuries and damage to properties. The accident cost can be obtained using Equation (18).

$$\mathrm{AC} = \mathrm{L} \times \mathrm{ADT} \times \left[\left((\mathrm{A_a} - \mathrm{A_n}] \times \mathrm{t_{mrr}} \times \mathrm{C_{acc}}\right)\right] \tag{18}$$

Where;

AC indicates the accident costs. $\mathrm{C_{acc}}$ represents the average cost per accident. $\mathrm{A_n}$ and $\mathrm{A_a}$ denote the normal accident rate and accident rate during the work zone, respectively.

4.2.4 Traffic growth rate

The average daily traffic can be subjected to an annual increase rate because of the economic prosperity and population growth. By assuming a constant increase in the average daily traffic, the ADT at time instant t can be computed using Equation (19).

$$\mathrm{ADT_t} = \mathrm{ADT} \times (1 + \mathrm{g})^{\mathrm{t}} \tag{19}$$

Where;

$\mathrm{ADT_t}$ represents the average daily traffic at a certain time t. g refers to the annual increase rate in the average daily traffic.

5. Exponential Chaotic Differential Evolution Algorithm

A revised algorithm that integrates a chaotic and exponential search mechanism with the differential evolution algorithm is proposed to circumvent the shortcomings of the classical meta-heuristic optimization algorithms. In the recent years, chaotic variable sequences generated from chaotic mapping mechanisms have been successfully applied in partial applications. Chaos can be defined as ubiquitous a dynamic non-linear phenomenon that exhibits infinite periodic movements in non-linear systems, and it is characterized by its irregularity, intrinsic stochastic property, randomicity and ergodicity.

Ergodicity property is an outstanding feature of chaotic systems that describes dynamical systems that has the same behavior averaged over time as averaged over space of all the system's space. This property enables to transit and search every state and node in the finite search space within certain range without repetition through a deterministic formulation. Chaos can be also viewed as a highly unpredictable and unstable motion of dynamical systems in a finite search plane. Thus, a non-linear system can be called chaotic if it exhibits sensitive-dependence on the initial conditions of the chaotic processing, and experiences infinite unstable periodic motions across the non-linear system. This is expected to amplify the search behavior and diversity of the generated solutions in the multimodal objective search space, which in turn prevents the differential evolution from premature convergence to local optimum solutions [78,79,80].. The basic procedures of differential evolution algorithm are described first then the chaotic control mechanism of the parameters of differential evolution algorithm is described.

5.1 Basic Procedures of Multi-objective Differential Evolution Algorithm

The developed multi-objective optimization model employs exponential chaotic differential evolution algorithm to create an optimal maintenance schedule over the multi-year planning horizon. The developed model uses the process of non-dominated sorting to compare individuals and select the most optimal ones [81]. Differential evolution algorithm is a population-based meta-heuristic algorithm that was first proposed by Storn and Price in 1997 to solve non-differentiable and non-linear global optimization problems [82]. The basic procedures of differential evolution are similar to genetic algorithm. However, they differ in the mechanisms of crossover and mutation [83,84]. The basic strategy of non-dominated sorting differential evolution algorithm is presented in the following lines.

The first step is the random generation of initial population in the search space using Equation (10).

$$X_{i,G} = LB + rand[0,1] \times (UB - LB) \tag{20}$$

Where;

i and G stande for the population and generation, respectively. UB and LB are the upper and lower bounds of the design parameter vector. $rand[0,1]$ is a random number uniformly distributed between 0 and 1.

The second step in functioning the differential evolution algorithm is the mutation. Mutation is applied to all vectors in the population, whereas three randomly selected vectors from the population are picked and combined to form the mutation vector. The mutation vector is created by adding the difference between two randomly selected vectors to the third vector. A target vector is chosen from the current population such that a mutation vector is generated for each target vector. The mutation vector is defined using Equation (2).

$$V_{i,G+1} = X_{r1,G} + F\left(X_{r2,G} - X_{r3,G}\right) \qquad \text{such that } r1 \neq r2 \neq r3 \tag{21}$$

Where;

r1, r2, and r3 are three randomly selected integer indices (r1, r2, and r3 ϵ {1, 2, 3………. NP}), and they are different from the index of the target vector. F is called a mutation scale factor that controls the amplification of differential variation between the vectors of $X_{r2,G}$, and $X_{r3,G}$, and it is a real number between 0 and 1.

Crossover is applied after mutation to increase the diversity of the perturbed parameter vectors through exchanging the components of the target vector with the mutation vector. The trial vector is generated using Equation (11). In this regard, if the crossover rate is larger than a uniformly generated number. Hence, $X_{j,i,G}$ in the target vector sent to the trial vector. Otherwise, $V_{j,i,G+1}$ in the mutant vector is sent to the trial vector.

$$U_{j,i,G+1} = \begin{cases} V_{j,i,G+1} & \text{if } CR \geq \text{rand}_j \\ X_{j,i,G}, & \text{if } CR < \text{rand}_j \end{cases} \tag{22}$$

Where;

$U_{j,i,G+1}$ is the trial vector. CR is a crossover probability between 0 and 1. j denotes index of the element in the vector. rand_j is a uniform random number between [0,1].

The selection operator is used to determine whether or not the trial vector should be a member of the population in the next generation, whereas the trial vector is compared against the target vector and the vector with a better objective function value, is picked to be copied to the next generation. The selection operator is expressed using Equation (23). In the case of minimization cost functions, if the objective function value of the trial vector is less than the target vector then the trial vector is selected over the target vector. Otherwise, the target vector is retained. $\leq$

$$X_{i,G+1} = \begin{cases} U_{i,G+1} & \text{if } \left(U_{i,G+1}\right) > (X_{i,G}) \\ X_{i,G}, & \text{if} \left(U_{i,G+1}\right) > (X_{i,G}) \end{cases} \tag{23}$$

Where;

$\left(U_{i,G+1}\right) > (X_{i,G})$ means that the solution of the trial vector dominates the target vector in the multi-objective optimization sense, and $\left(U_{i,G+1}\right) \leq (X_{i,G})$ means that the target vector dominates the trial vector. The operators of non-domination rank and crowding distance adopted from Deb et al. (2002) are utilized to compare between fitness functions of trial and target vectors and select the best solutions in the forthcoming generations. In the non-domination rank, the individuals in the population are divided into fronts, and the individuals that are not dominated by another solution constitute the front of rank 1. Then, the individuals which are only dominated by the first front are assigned a rank 2, and the recursive process is iterated until all individuals are assigned to a front with a designated rank. Crowding distance aims at diversifying the population's distribution and it is used to compare solutions belonging to the same front, and the solutions with higher crowding distance are consider as higher than the solutions with lower crowding distance.

The three operators of crossover, mutation and selection are implemented sequentially at each generation until stopping criteria is satisfied, i.e., reaching maximum number of generations.

5.2 Types of Chaotic Maps

In this research, nine different types of chaotic map sequences are experimented, namely logistic map, sine map, sinusoidal map, singer map, circle map, cubic map, iterative map, Chebyshev map, logistic-sine map.

5.2.1 Logistic map

Logistic map is one of the most well-known chaotic functions, which was introduced by Robert May in 1976. This chaotic mechanism is usually featured in non-linear dynamics of biological population witnessing chaotic behavior. Additionally, this mechanism generates chaotic sequences in the range (0, 1). Logistic chaotic map can be expressed as follows [85].

$$\mathrm{x}_{\mathrm{k}+1} = \beta \times \mathrm{x}_{\mathrm{k}} \times (1 - \mathrm{x}_{\mathrm{k}}) \tag{24}$$

Where;

x_{k} is the chaotic number at iteration k. β is a control parameter equal to 4.

5.2.2 Sine map

Sine map is a unimodal chaotic mapping mechanism that can be mathematically expressed as follows [86].

$$\mathrm{x}_{\mathrm{k}+1} = \frac{\beta}{4} \times \sin(\pi \mathrm{x}_{\mathrm{k}}) \tag{25}$$

Where;

β is a control parameter such that $0 \leq \beta \leq 4$.

5.2.3 Sinusoidal map

The sinusoidal chaotic sequence ensures that the chaotic behavior with the span (0, 1). Sinusoidal map can be formally defined as follows [87].

$$x_{k+1} = \beta \times {x^2}_k \times \sin(\pi x_k) \tag{26}$$

Where;

β is 2.3 to better simulate the variations of the chaotic variable.

5.2.4 Singer map

Singer is a one-dimensional chaotic system that can be mathematically expressed as follows [46].

$$x_{k+1} = \beta \times (7.86x_k - 23.31{x^2}_k + 28.75{x^3}_k - 13.302875{x^4}_k) \tag{27}$$

Where;

$\beta \in (0.9, 1.08)$

5.2.5 Circle map

Circle chaotic mapping function was proposed by Andrey Kolmogorov in the form of a simplified model for driven mechanical rotors. It delineates a model of phase locked loop in electronics. Circle mapping mechanism generates chaotic sequences within the range (0, 1). It can be mathematically defined as follows [78].

$$x_{k+1} = x_k + b - \frac{a}{2\pi} \times \sin(2\pi x_k)\mathrm{mod}(1) \tag{28}$$

Where;

b=0.2 and a=0.5. $\mathrm{mod}(1)$ refers to a remainder operator of the division of the chaotic number by 1.

5.2.6 Cubic map

Cubic map is one of the most common mapping mechanisms in generating chaotic sequences in several applications such as cryptography. It is a polynomial function of degree 2. This mapping function generates sequences within the range (0, 1). It can be formally defined as follows [87].

$$x_{k+1} = \beta \times x_k \times (1 - x^2{}_k) \tag{29}$$

Where;

β is equal to 2.59.

5.2.7 Iterative map

Iterative map with infinite collapses maps (ICMIC) generates variable sequence within the range (-1, 1). It can be mathematically represented as follows [46].

$$x_{k+1} = \sin\left(\frac{\beta \times \pi}{x_k}\right) \tag{30}$$

Where;

$\beta \in (0, 1)$ and it is usually selected greater than 0.6 to create good chaotic sequences. The results are then normalized to generate a chaotic sequence within the range (0, 1).

5.2.8 Chebyshev map

Chebyshev map is a common symmetric that is normally utilized in the applications of digital communication, security problems and neural network. Chebyshev map creates variable sequence within the range (-1, 1), and it can be formally expressed using Equation (31) [88].

$$x_{k+1} = \cos\left(\beta \times \cos^{-1}(x_k)\right) \tag{31}$$

Where;

β is equal to 5

5.2.9 Logistic-sine map

Logistc-sine map is a chaotic model that utilizes both logistic map and sine map to generate chaotic variable sequences. Logistic-sine chaotic model can be mathematically represented as follows [89].

$$x_{k+1} = \left(\beta \times x_k \times (1 - x_k) + \frac{(4-\beta)}{4} \times \sin(\pi x_k)\right) \mathrm{mod}(1) \tag{32}$$

Where;

β is a chaotic multiplier that is assumed 0.86.

5.3 Differential Evolution with Chaotic Sequences

The population initialization, mutation scaling factor and crossover probability are key factors affecting the convergence of the differential evolution algorithm and quality of final solutions. As such, the developed method adopts chaotic population initialization and chaotic operators to alleviate the shortcomings of conventional meta-heuristics through amplifying the search mechanism of the differential evolution optimization algorithm. This due to the fact the chaotic variables can travel ergodically over the whole search space of interest. Random initialization is the most commonly-utilized approach to generate initial population. However, this approach may lead search agents to be far away from the population. In this context, chaotic population initialization is at first carried out to enhance the diversity of the initial population which enables the differential evolution to prevent local optimum solutions and find global optimum solutions. This is accomplished by generating an D-Dimensional vector $Z_0 = [Z_{01}, Z_{02}, Z_{03} \ldots\ldots\ldots Z_{0D}]$, such that each of its elements is random number in the range [0, 1]. Then, chaotic queues $[Z_1, Z_2, Z_3 \ldots\ldots\ldots Z_{NP}]$ are generated based on the designated chaotic map. Then, the chaotic queues are mapped to the desired optimized parameters' range.

With respect to the crossover probability and mutation scaling factor, the chaotic dynamics is incorporated for the purpose of their tuning. As mentioned earlier, the search performance of the differential evolution is significantly influenced by the control parameters of crossover probability and mutation scaling factor, whereas proper setting of their values plays a monumental role in the success of their important. The difficulty arises from the methods of selection of optimum parameter values which are usually capitalized on empirical evidence and practical experience. These trial and fine-tuning-based methods require high computational effort because of the large number of runs needed for the optimum setting of parameters of differential evolution scheme. Additionally, these control parameters are constant across the whole exploration process. Thus, the mutation scaling factor and crossover probability can't guarantee the optimization's ergodicity in the search space. In the light of forgoing, the crossover probability and mutation scaling factor are modeled and tuned as chaotic variables to substitute the random numbers of the classical algorithm through establishing a self-adaptive dynamic parameter control mechanism. It is expected that this chaotic dynamics-based mechanism is capable of amplifying the search behaviour by improving the balance between the exploration and exploitation during the disturbance process. The chaotic sequences of the crossover probability based on the circle map can be formally expressed as follows.

$$\mathrm{CR}_{\mathrm{G}+1} = \mathrm{CR}_{\mathrm{G}} + \mathrm{b} - \frac{\mathrm{a}}{2\pi} \times \sin(2\pi \mathrm{CR}_{\mathrm{G}}) \mathrm{mod}(1) \quad \text{such that } \mathrm{G} = [1,2,3 \ldots \ldots \ldots \mathrm{G}_{\mathrm{max}}] \tag{33}$$

With respect to the mutation scaling factor, it is tuned based on hybridization of the merits of both chaotic sequences and exponential distribution. From one side, the nature of exponential scheme presents a faster mechanism to explore the design space. From the other side, chaotic behavior avoids optimization problems from stagnation in local optimum. This in turn is expected to accomplish faster convergence and better solutions. The strategy of exponentially-decreasing chaotic mutation scaling factor based on the logistic-sine map is formulated as follows.

$$\begin{aligned} \mathrm{F}_{\mathrm{G}+1} = {} & [(\mathrm{e}^{\frac{-2\mathrm{G}}{\mathrm{G}_{\mathrm{max}}}}) \times (\mathrm{F}_{\mathrm{max}} - \mathrm{F}_{\mathrm{min}})] \\ & + [[\left(\beta \times \mathrm{F}_{\mathrm{G}} \times (1 - \mathrm{F}_{\mathrm{G}}) + \frac{(4-\beta)}{4} \times \sin(\pi \mathrm{F}_{\mathrm{G}})\right) \mathrm{mod}(1)] \\ & \times \mathrm{F}_{\mathrm{min}}] \end{aligned} \tag{34}$$

Where;

$\mathrm{F}_{\mathrm{min}}$ and $\mathrm{F}_{\mathrm{max}}$ stand for the initial and final mutation scaling factors, respectively. $\mathrm{mod}(.)$ is the modulus operator.

6. Hybrid Multi-criteria Decision-making

Hybrid multi-criteria decision-making algorithm is designed for selecting the best solutions among the set of Pareto optimal solutions. In this context, CRITIC technique is utilized to compute the weighting importance vector of the condition performance level, total life-cycle maintenance costs, the duration of traffic disruption and the environmental impact [90]. This objective weighting approach is data dependent, and deals directly with the decision matrix when deriving the weights of attributes. Thus, it doesn't need pairwise comparison matrices or decision-maker's judgements like subjective referencing-based techniques. The objective weight of the attributes signifies the real features and amount of information stored in each one. This technique is based on two dimensions generated from the measures of performance of criteria in the multi-criteria decision analysis, namely comparative intensity and conflict. The first dimension is captured by the standard deviation which analyzes the measure performance of the evaluated alternatives in each criteria separately. The second dimension is tackled by the correlation coefficient between each pair of attributes. COPRAS and GRA are incorporated to sort the optimal solutions based on a different theoretical concept, whereas COPRAS relies on the utility degrees of the different alternatives for their ranking. On the other hand, GRA is established based on the grey theory, and it utilizes the grey relational grade to analyze the reference series and the alternative series. Each technique produces a distinct ranking from the other. Thus, average ranking (AR) method is applied to derive the final global ranking of the optimal solutions for the sake of accurate and comprehensive assessment. It provides an integrative view of the performances of an algorithm from the perspectives of accuracy and robustness. This is accomplished through computing the mean and standard deviation of the ranks of the optimal solutions obtained from the two multi-criteria decision making techniques [91].

6.1 Criteria Importance through Inter-criteria Correlation

The computational procedures of the CRITIC technique are discussed in the following lines [90]. The first stage is to normalize the decision matrix where the purpose of this step is to convert the measures of performance into non-dimensional ones since the dimensions and attributes of different attributes are different. The normalized decision matrix is computed using Equation (35).

$$y_{ij} = \frac{x_{ij} - \min\{x_{ij}, i = 1,2, \dots \dots \dots m\}}{\max\{x_{ij}, i = 1,2, \dots \dots \dots m\} - \min\{x_{ij}, i = 1,2, \dots \dots \dots m\}} \qquad (35)$$

Where;

x_{ij} represents the measure of performance of the $i-\text{th}$ alternative with respect to $j-\text{th}$ attribute.

As mentioned earlier, this method relies on the contrast intensity and conflict to compute the weights of attributes. Equation (36) is utilized to quantify the amount of information of each attribute stored in the decision matrix based on the contrast intensity and conflict.

$$Q_j = \sigma_j \sum_{j=1}^{m} (1 - r_{jk}) \qquad (36)$$

Where;

σ_j represents the standard deviation of the $j-\text{th}$ attribute. r_{jk} indicates the linear correlation coefficient between the $j-\text{th}$ and $k-\text{th}$ attributes. It is worth mentioning that a criteria with a high standard deviation and lower correlation coefficient with the other implies a higher weight of the criteria because a higher value of Q_j indicates more importance assigned to the $j-\text{th}$ criteria.

The final weights of the attributes are obtained by normalizing the amount of information transmitted by the attributes as follows.

$$W_j = \frac{Q_j}{\sum_{j=1}^{m} Q_j} \qquad (37)$$

Where;

W_j stands for the weight of the attribute.

6.2 Complex Proportional Assessment

COPRAS algorithm was first proposed by Zavadskas et al. in 1994 [92], and it is able to evaluate design attributes and assign priorities in the light of presence of conflicting criteria. It presumes direct and proportional dependencies of significance and utility degrees of the investigated decision alternatives on a system of design attributes. The significance of investigated design alternatives is identified based on analyzing their positive and negative characteristics while taking into consideration the mutually conflicting criteria [93,94]. Its computational steps are presented in the following lines [92].

The first step is the normalization process in order to transform the performance scores of the input decision matrix into comparable dimensionless values as shown in Equation (38).

$$d_{ij} = \frac{x_{ij}}{\sum_{i=1}^{m} x_{ij}} \tag{38}$$

Where;

d_{ij} is the normalized performance score of the $i-th$ alternative and $j-th$ attribute. x_{ij} is the performance score of the $i-th$ alternative and $j-th$ attribute. m is the number of decision alternatives. m stands for number of decision alternatives.

The second step is to derive the weighted normalized decision matrix by multiplying the performance scores of decision alternative by their respective weighting values as expressed in Equation (39).

$$v_{ij} = p_{ij} \times w_j \tag{39}$$

Where;

v_{ij} denotes the weighted normalized value of the $i-th$ alternative and $j-th$ attribute.

The third step is to compute the sums of weighted normalized values for both the beneficial and cost attributes by applying Equations (3) and (4).

$$s+_i = \sum_{j=1}^{n} v^{+}{}_{ij} \tag{40}$$

$$s-_i = \sum_{j=1}^{n} v^{-}{}_{ij} \tag{41}$$

Where;

Higher values are more desirable in the case of beneficial criteria ($s +_i$), and lower values are preferred in the case of cost criteria ($s -_i$).

The fourth step is to calculate the relative priority or significance of each decision alternative on the basis of their positive and negative characteristics using Equation (42).

$$Q_i = s +_i + \frac{s-_{min} \times \sum_{i=1}^{m} s-_i}{s-_i \times \sum_{i=1}^{m} (s-_{min}/s-_i)} = s +_i + \frac{\sum_{i=1}^{m} s-_i}{s-_i \times \sum_{i=1}^{m} (1/s-_i)} \tag{42}$$

The fifth step is to calculate the utility degree for each alternative which is used to generate a complete ranking of design alternatives. The quantitative utility degrees can be obtained using Equation (6).

$$N_i = \frac{Q_i}{Q_{max}} \times 100\% \tag{43}$$

Where;

Q_{max} denotes the maximum utility degree accomplished by all the decision alternatives. The values of utility degree vary from 0% to 100%, whereas higher values of Q_i imply a better decision alternative.

6.3 Grey Relational Analysis

Grey relational analysis is inspired by grey system theory which was introduced to address uncertainties, incomplete and imprecise information in grey systems [95].The main procedures of grey relational analysis are described in the following lines [96].

The first step is grey relation generation in order to obtain the comparability sequence. The normalization of performance values for the benefit and cost criteria is conducted using Equations (44) and (45), respectively.

$$y_{ij} = \frac{x_{ij} - \min\{x_{ij}, i = 1,2, \dots \dots \dots m\}}{\max\{x_{ij}, i = 1,2, \dots \dots \dots m\} - \min\{x_{ij}, i = 1,2, \dots \dots \dots m\}} \tag{44}$$

$$y_{ij} = \frac{\max\{x_{ij}, i = 1,2, \dots \dots \dots m\} - x_{ij}}{\max\{x_{ij}, i = 1,2, \dots \dots \dots m\} - \min\{x_{ij}, i = 1,2, \dots \dots \dots m\}} \tag{45}$$

The second step is the definition of reference sequence which lies with the range of [0, 1]. The reference sequence is the largest normalized performance value in the case of benefit criteria, and it is the smallest normalized performance value in the case of cost criteria. In this regard, a closer sequence to the reference sequence indicates a better sequence.

The third step is to compute the grey relational coefficient using Equation (46).

$$\gamma(y_{0j}, y_{ij}) = \frac{\Delta_{min} + \xi\Delta_{max}}{\Delta_{ij} + \xi\Delta_{max}} \tag{46}$$

Where;

$\Delta_{ij} = |y_{0j} - y_{ij}|$

$\Delta_{min} = \min\{\Delta_{ij}, i = 1,2, \ldots \ldots \ldots m; j = 1,2, \ldots \ldots \ldots n\}$

$\Delta_{max} = \max\{\Delta_{ij}, i = 1,2, \ldots \ldots \ldots m; j = 1,2, \ldots \ldots \ldots n\}$

ξ is a distinguishing coefficient between 0 and 1, and it is assumed 0.5 in this research study [97,98].

The fourth step is to calculate the grey relational grade as shown in Equation (47).

$$r(y_0, y_i) = \sum_{j=1}^{n} w_j \times \gamma(y_{0j}, y_{ij}) \tag{47}$$

Where;

Grey relational grade signifies the closeness between the comparability sequence and reference (ideal) sequence. In this context, an alternative associated with higher value of grey relational grade is a better one.

7. MODEL IMPLEMENTATION

The developed model is performed for optimum maintenance planning of a group of bridge elements in Quebec. The targeted bridge elements encompass ten bridge decks, seven piers and five abutments that were selected from seventeen bridges. A five-year, twenty five-year and thirty-five year maintenance plans are created for the sake of testing the capacity of the developed maintenance planning model to handle both short-term and long-term strategic planning. The age of the bridge elements ranges from 1970 to 2004 with average age of 27.05 years for the five-year and twenty five-year study periods. More deteriorated bridges of average 33.09 years are considered in the case of thirty-five year study period to better experiment with the capabilities of the developed maintenance optimization method. The parameters of the user costs are as follows. The affected length per bridge is 600 meters. The normal traffic speed is

100 km/hr. The reduced traffic speeds in the case of minor repair, major repair and replacement are 80, 50 and 30, respectively. The initial average daily traffic is 10,000 vehicles per day. The percentage of trucks from average daily traffic is 3.1%. The traffic growth is selected to be 1.1%/year. Hourly time value of passenger car driver and truck driver are assumed $14.21/hr and $29.22/hr, respectively. The operating costs of passenger car and truck are 17.24/hr and $39.67/hr, respectively. The normal accident rate and accident rate during the work zone are assumed 1.56% and 2.58%, respectively. The average cost per accident is assumed $126,120.

After the definition and quantification of the performance aspects of maintenance management of bridges, the second model is a multi-objective optimization model that exploits the use of exponential chaotic differential evolution algorithm for the sake of structuring optimum maintenance schedule of bridges over the multi-year planning period while accommodating the multiple performance constraints. The initial value of all chaotic maps is assumed 0.7 (Sayed et al., 2018; Saxena et al., 2018). Figures 4 and 5 describe the behavior of the nine chaotic maps for 500 iterations. As can be seen, the chaotic dynamics enable the chaotic operators to travel ergodically across the search space. For instance, the chaotic sequences of control parameters in the singer map exhibit rapid transitions within close number of iterations. In the sinusoidal map, the chaotic variable sequences vary from 0.5 to 0.95. This provides an advantage over constant control parameters through providing full and efficient exploration of the search space. Figure 6 demonstrates the interface designated for the multi-objective maintenance model. In it, the user is asked to define the length of study period, maximum number of visits for each element, minimum acceptable performance condition of element, maximum available budget, maximum yearly-budget and maximum standard deviation of costs. With respect to the parameters of the exponential chaotic differential evolution algorithm, the user is asked to specify the initial population size, maximum number of iterations, minimum and maximum scaling factors, value of initial chaotic number, and type of chaotic mechanism.

INSERT FIGURE 4

INSERT FIGURE 5

INSERT FIGURE 6

In order to provide a fair comparison between the different meta-heuristic optimization algorithms, the initial population size is assumed 50. The numbers of iterations for the five-year, twenty five-year and thirty-five year study periods are assumed 1000, 1500 and 1700, respectively. Different initializations of parameters were experimented for the different meta-heuristics in order to search for their optimum setting of values. Each meta-heuristic was run five times independently in order to avoid unstable solutions due to random initialization of population. The set of optimal solutions obtained from the multi-objective optimization model based on ECDE-based logistic sine map, differential evolution and teaching learning optimization for the twenty five-year study horizon are depicted in Figures 7 and 8. The variables “CI”, “TC” “EI” and “TD” denote performance condition index, maintenance costs, duration of traffic disruption and environmental impact, respectively. Four figures are generated to cover all possible combinations of the four performance aspects of the multi-objective optimization model. The generated maintenance plans should satisfy a minimum performance condition threshold of 64.04. The maximum available budget is $1,000,000 in five-year study plan, and $2,000,000 for the twenty five-year and thirty five-year study plans. Furthermore, the maximum yearly-budget and maximum standard deviation of costs are set to $250,000 and $20,000, respectively in the five-year period. In the twenty five-year and thirty five-year periods, the maximum yearly-budget and maximum standard deviation of costs are $1,000,000 and $500,000, respectively. As can be seen, the ECDE algorithm is capable of achieving significant reduction in the maintenance expenditures, traffic disruption and adverse environmental implications when compared against the classical meta-heuristics meanwhile fulfilling designated performance condition requirements. For the thirty five-year maintenance plan, the optimal solutions of the ECDE-based cubic, ECDE-based logistic-sine, ECDE-based circle and ECDE-based sine algorithms are presented in Figure 9. It should be mentioned that all the exponential chaotic optimization models achieved environmental impact of zero. Thus, the performance aspects of condition, maintenance cost and traffic disruption are displayed. In this context, it can be inferred that the exponential chaotic differential evolution algorithms attained promising results in terms of the four governing performance metrics. Furthermore, it should be reported that the classical optimization algorithms failed to find the optimum solutions within the boundaries and constraints for the maintenance planning model of thirty five-year study period.

INSERT FIGURE 7

INSERT FIGURE 8

INSERT FIGURE 9

Tables 2 and 3 are presented to establish an in-depth comparison between the different meta-heuristic algorithms for the maintenance planning of the thirty five-year study period. They are evaluated capitalizing on the minimum fitness function values (Min), average fitness function values (Avg), hypervolume indicator (HV), generational distance (GD), inverted generational distance (IGD), spacing (S) and maximum Pareto front error (MPFE). It should be mentioned that the best performing meta-heuristic optimization algorithm is the one which yields higher values of hypervolume indicator, in addition to lower values of generational distance, inverted generational distance, spacing and maximum Pareto front error. The bold values represent the best achieved values of the performance indicators. It can be interpreted that the ECDE-based logistic algorithm achieved the highest minimum condition rating, ECDE-based Chebyshev algorithm achieved the lowest minimum total maintenance cost. Additionally, ECDE-based sinusoidal algorithm, ECDE-based cubic algorithm, ECDE-based logistic-sine algorithm and ECDE-based circle algorithm yielded the lowest minimum environmental impact. With respect to the average performance of the objective function values, ECDE-based circle algorithm provided the highest average condition rating. Moreover, ECDE-based sinusoidal algorithm achieved the lowest average maintenance cost and environmental impact.

In terms of hypervolume indicator, ECDE-based sinusoidal algorithm provided the largest hypervolume indicator (98.4%). On the other hand, ECDE-based cubic algorithm attained the lowest hypervolume indicator (96.4%). ECDE-based logistic, ECDE-based sinusoidal and ECDE-based Chebyshev algorithms provided the best generational distance, inverted generational distance and maximum Pareto front error. On the other hand, ECDE-based cubic algorithm provided the highest generational distance and inverted generational distance. Additionally, ECDE-based circle algorithm attained the worst maximum Pareto front error. With respect to spacing metric, ECDE-based logistic, ECDE-based sinusoidal, ECDE-based sine, ECDE-based iterative, ECDE-based Chebyshev and ECDE-based circle algorithms provided the lowest spacing. Nonetheless, ECDE-based logistic-sine algorithm provided the highest spacing. It can be also noticed that different ECDE-based algorithms obtain different optimization results. This is due to that each ECDE-based algorithm incorporate different chaotic sequence function to find the global optimum solution which causes their exploration-exploitation search behavior to be different from each other.

INSERT TABLE 2

INSERT TABLE 3

The average ranking method is utilized to establish a comprehensive and unified comparison between the meta-heuristic optimization algorithms. This comparison integrates their performances with respect to the three study periods. The results of the average ranking method are recorded in Table 4 and displayed in Figure 10. As shown in Figure 10, there is significant improvement in both the mean of rankings and standard deviation of rankings attained by the exponential chaotic differential evolution algorithm when compared against the conventional optimization algorithms. According to the results listed in Table 4, it can be found that ECDE-based sinusoidal algorithm achieved the first rank followed by the ECDE-based logistic algorithm and then the ECDE-based iterative algorithm. In this context, ECDE-based sinusoidal algorithm achieved $\mu_{\mathbf{a}}$ and σ_a of 2.41 and 2.03, respectively. With respect to the conventional optimization algorithms, DE provided the tenth rank followed by the TLO and then IWO while Jaya attained the least ranking. The rankings of GA and PSO are fourteenth and fifteenth, respectively. Furthermore, GA exhibited the highest unstable performance across the different multi-objective optimization problems. In this regard, $\mu_{\mathbf{a}}$ and σ_a of GA are 7.45 and 3.87, respectively. In addition, $\mu_{\mathbf{a}}$ and σ_a of PSO are 7.55 and 3.61, respectively. This evinces that the exponential chaotic differential evolution optimization algorithm substantially outranks classical meta-heuristics and it demonstrates more stable performance than them.

INSERT TABLE 4

INSERT FIGURE 10

A hybrid multi-criteria decision-making algorithm is designed to select the most compromise solution among the set of Pareto optimal solutions. In this context, CRITIC technique is used for deriving the weights of the attributes CR, TLCC, TDTT and TEI. Table 5 reports the quantity of information and final weights of each criterion. It was concluded that CR has the highest relative weight, and the remaining attributes of TLCC, TDTT and TEI exhibit approximately equal weights. In this regard, the final weights of CR, TLCC, TDTT and TEI are 30.07%, 20.03%, 26.68% and 23.22%, respectively. Furthermore, COPRAS and GRA are applied to rank the Pareto optimal solutions. Each type of the multi-criteria decision-making induces a distinct ranking from the other. In this regard, AR method is employed to formulate a consensus ranking of the Pareto optimal solutions Sample of the optimal solutions for the five-year, twenty five-year and thirty five-year maintenance planning horizons are recorded in Tables 6, 7 and 8, respectively. The best maintenance plan for the five-year study period induces CR, TLCC, TDTT and TEI of 72.87, $388,05.06, 0 and 11.89, respectively. For the twenty five-year planning horizon, the best solution comprises CR, TLCC, TDTT and TEI of 64.09, $363,20.8, 0 and 11.89, respectively. Additionally, The most optimum maintenance plan for the thirty five-year study period induces CR, TLCC, TDTT and TEI of 64.09, $100,148.4, 0 and 33.68, respectively. By analyzing the rankings of the optimum solutions, it can be inferred that the disagreement between the rankings of the optimum solutions increases with the increase in the complexity of the multi-objective optimization model, i.e., more lengthy planning horizon. This state of affair necessitates the employment of the AR method for the purpose of obtaining compromise solution.

INSERT TABLE 5

INSERT TABLE 6

INSERT TABLE 7

INSERT TABLE 8

The profile of the twenty five-year maintenance plans of a bridge deck obtained from the ECDE-based logistic-sine algorithm and the ECDE-based sinusoidal algorithm are presented in Figure 11. As shown in Figure 11, the exponential chaotic differential evolution algorithms are capable of formulating efficient maintenance plans that can accommodate the different performance aspects. Additionally, it is capable of establishing maintenance profiles with minimum interruptions and cost-effective profile with balanced expenditures over the planning horizon. The maintenance profiles of maintenance plans generated from the ECDE-based singer algorithm and TLO algorithms are presented in Figure 12. These schedules are designated for maintenance planning of a bridge deck over a study period of thirty five years. It can be inferred that the ECDE-based singer algorithm experience significant less traffic disruption when compared against the TLO algorithm, whereas ECDE-based singer and TLO algorithms induce 1 and 4 interruptions, respectively along the planning horizon. Furthermore, the ECDE-based singer algorithm is capable of formulating better cost-effective profiles with less perturbations and variations.

INSERT FIGURE 11

INSERT FIGURE 12

Figure 13 show maintenance cash flow of the bridge network over the five-year planning horizon. The cash flow is generated based on the optimum maintenance plan obtained by ECDE-based sinusoidal algorithm. The optimum maintenance plan comprised carrying out six intervention actions: five minor repair actions for the bridge decks in 2021 and one minor repair action for the bridge deck in 2022. In this regard, the total cost of the maintenance plan was valued to be $38,805.1. The maintenance cash flow of the bridge network over twenty five-year planning horizon is presented in Figure 14. The ECDE-based sinusoidal algorithm selected to conduct six minor repair actions for the bridge decks: two minor repair actions at 2028, and four minor repair actions at 2026, 2029, 2031 and 2033. The cost of intervention actions was valued to worth $36,320.8. The maintenance cash flow over the thirty five-year study period is depicted in Figure 15. The optimum maintenance schedule encompassed seventeen minor repair actions for the bridge decks: seven minor repair actions at 2022, 2038, 2041, 2042, 2045, 2047 and 2052 in addition two minor repair actions at each of 2024, 2025, 2026, 2029 and 2031. It is worth mentioning that no intervention action was applied to abutments and piers because of their low deterioration rate when compared against decks so there condition rating was far away minimum allowable performance condition threshold value.

INSERT FIGURE 13

INSERT FIGURE 14

INSERT FIGURE 15

In order to further validate the developed model, the multi-objective optimization model is re-designed to accommodate seven girders rather than the piers. More deteriorated bridges were considered such that their age was 33.5 years. The minimum allowable condition was raised to

85.5 to better demonstrate the features of the developed maintenance optimization model in abutments and piers. The maximum available budget was $ 10,000,000, and the maximum yearly budget was valued to be $ 2,000,000. The maximum standard deviation of maintenance costs was set to be $5,000,000. Figure 16 depicts the cash flow of the bridge network over the five-year study period. Based on the ECDE-based sinusoidal algorithm, the optimum maintenance plan incorporated ten intervention actions to be performed at the first year. This included six major rehabilitation actions for decks, one minor repair action for abutment and three major rehabilitation actions for girders. The total cost of intervention actions was valued to be $493,551.56.

INSERT FIGURE 16

Table 9 reports the performances of ECDE-based sinusoidal, differential evolution and genetic algorithms over the five-year study. It can be noticed that the developed ECDE-based sinusoidal algorithm was able to satisfy the performance condition requirements while maintaining lower total life-cycle maintenance cost, total duration of traffic disruption and total environmental impact. In addition, the number of intervention actions of the developed ECDE-based sinusoidal algorithm was less than differential evolution and genetic algorithm. Differential evolution exhibited the second highest performance while genetic algorithm had the least performance and it was accompanied by the largest number of intervention actions. In this regard, the values of CR, TLCC, TDTT, TEI and number of intervention actions were 86.41, $493,551.56, 0, 126.14 and 10, respectively. Based on the genetic algorithm, the respective values of CR, TLCC, TDTT, TEI and number of intervention actions were 90.62, $4,453,917.27, 2.89, 466.63 and 96, respectively.

INSERT TABLE 9

Figures 17 to 21 display the convergence curves of the ECDE-based sinusoidal, genetic and differential evolution algorithms for the benchmark functions of Schwefel 2.26, Rastrigin, Griewank, Beale and three-hump camel. In this regard, the plotted convergence curves are undertaken for the best performance histories obtained over the multiple runs. The global optimum solutions of Rastrigin, Griewank, Beale and three-hump camel are zero, and the global optimum solution of Schwefel 2.26 is -12569.49. The numbers of iterations and search agents over all meta-heuristics are fixed to 1000 and 50, respectively. In addition, the number of dimensions is set to 30 for all test functions. In Schwefel 2.26 function, ECDE -based sinusoidal algorithm accomplished superior results over differential evolution and genetic algorithms, whereas it converged to a very near global optimum solution of -12569.49 at iteration 503. In addition, differential evolution converged to a relatively close global solution of -12568.32 at iteration 998, and genetic algorithm got stagnated in local optimum solution. With regards to Rastrigin function, ECDE -based sinusoidal algorithm obtained the best objective function values, whereas it reached the value 3.6E-03 at iteration 992. Genetic algorithm performed better than differential evolution algorithm, whereas they got stuck in the values 19.9 and 55.72 at iterations 380 and 949, respectively. For the Griewank function, it is noticed that ECDE -based sinusoidal algorithm managed to reach the global optimum solution at iteration 851. Differential evolution reached an objective function value of 1.12E-11 at iteration 998, and genetic algorithm prematurely converged to a local optimum solution.

In Beale function, ECDE -based sinusoidal algorithm was able to converge fast to the global optimum solution at iteration 208. Differential evolution and genetic algorithm failed to visit the global optimum point. In this regard, differential evolution stabilized at the value of 6.53E-22 at the iteration 987, and genetic algorithm got stuck at the value 3.02E-11 early at the iteration 48. With respect to three-hump camel function, ECDE -based sinusoidal algorithm was able to perform much better than differential evolution and genetic algorithm whereas it managed to find a very close global solution of 2.59E-244 at iteration 991. In this regard, differential evolution and genetic algorithm stabilized at the values of 4.13E-73 and 1.96E-73 at the iterations 997 and 168, respectively. In view of the above, it can be observed that the ECDE -based sinusoidal algorithm substantially converged faster than genetic algorithm and differential evolution algorithm in both multi-modal and uni-modal test function, and it managed to accurately find the global optimum solution in almost all of them. However, genetic and differential evolution algorithms failed to converge to the actual global optimum solution and they were rapidly getting trapped in premature convergence more clearly in the benchmark functions of Rastrigin, Griewank and three-hump camel.

INSERT FIGURE 17

INSERT FIGURE 18

INSERT FIGURE 19

INSERT FIGURE 20

INSERT FIGURE 21

Table 10 summarizes the best, worst, average and standard deviation of the objective function values. These values are reported based on five independent runs. It can be noticed that ECDE -based sinusoidal algorithm precisely reached the global optimum solution in the test functions of Griewank and Beale. ECDE -based sinusoidal algorithm produced very close values to the global optimum solution in the test functions of Schwefel 2.26, Rastrigin and three-hump camel. In this regard, the best objective function values scored by the ECDE -based sinusoidal algorithm differ by 1.34E-02, 3.6E-03 and 4.13E-73 in the functions of Schwefel 2.26, Rastrigin and three-hump camel, respectively. It can be also seen that the developed ECDE -based sinusoidal algorithm significantly outperformed genetic and differential evolution algorithm across the five test functions such that it accomplished lower best, worst and average objective function value in addition to a lower standard deviation. The average objective function value of ECDE -based sinusoidal algorithm was better by 114.26% and 79.51% when compared against genetic and differential evolution algorithms, respectively. In addition, it is found that the best objective function values of ECDE -based sinusoidal algorithm was lower by 106.54% and 80% than the ones of genetic and differential evolution algorithms, respectively. Hence, it can be argued that the developed ECDE -based sinusoidal algorithm exhibits high exploration and exploitation search abilities which improved its convergence speed, population diversity and prevented it from being trapped in local minima solutions. Nevertheless, classical meta-heuristics failed to solve efficiently the multi-modal and uni-modal functions because they are highly susceptible to be stagnated in local minima and premature convergence With regards to standard deviation, it can be derived that the developed ECDE -based sinusoidal algorithm obtained lower standard deviation by 94.89% and 96.72% with respect to the genetic and differential evolution algorithms, respectively. This superiority illustrates the robustness of the developed ECDE -based sinusoidal algorithm since it is experiences very few perturbations in its performance across the different runs. At the level of classical meta-heuristics, it can be inferred that differential evolution algorithm yielded better optimum solutions than genetic algorithm in the functions of Schwefel 2.26, Griewank and Beale. However, it is outperformed by it in Rastrigin and three-hump camel functions. This demonstrates the higher variations in the performance of classical meta-heuristics and their case-dependency nature mostly when attempting to solve higher-dimension optimization problem accompanied by the presence of several local minima points.

INSERT TABLE 10

Four experiments are carried out to validate the performance of the developed ECDE -based sinusoidal algorithm against some of the existing research works. These experiments comprise different numbers of iterations, population sizes, benchmark functions and multiple dimensions to better test the developed algorithm. In the first experiment, the developed ECDE -based sinusoidal algorithm is compared against the improved clonal selection algorithm (ICSAT) proposed by Ülker [99]. In this experiment, the number of iterations, population size and dimension size are assumed as 5000, 30 and 30, respectively. Figure 22 shows the convergence curves of ECDE -based sinusoidal algorithm for Rastrigin and Schwefel 2.26 functions. These curves are plotted for the best performance histories among the thirty independent runs. It is found that the ECDE -based sinusoidal algorithm converged to the global optimum solution of zero at iteration 2390 in the Rastrigin function. In addition, they reached a very near global solution of -12569.49 at iteration 920 in the Schwefel 2.26 function. The average and best objective function values of the thirty runs are given in Table 11. It can be inferred that the ECDE -based sinusoidal algorithm outperformed ICSAT algorithm providing lower best and average objective function values in both Rastrigin and Schwefel 2.26 functions. For instance, the best objective function values of ECDE -based sinusoidal and ICSAT algorithms in the Rastrigin function are 0 and 9.84, respectively. In the Schwefel 2.26 function, the average objectives function values of ECDE -based sinusoidal and ICSAT algorithms are -12569.49 and 1.49E-5, respectively.

INSERT FIGURE 22

INSERT TABLE 11

In the second experiment, the developed ECDE -based sinusoidal algorithm is compared against the Jaya-Bat algorithm introduced by Kaur et al. [100]. The comparative analysis is performed using Rastrigin and Griewank functions, and the population size is set to 40. In the Rastrigin function, the numbers of dimensions and iterations are 10 and 2000, respectively. With regards to the Griewank function, the numbers of dimensions and iterations are 30 and 1000, respectively. Figure 23 demonstrate the convergence of ECDE -based sinusoidal algorithm in the Rastrigin and Griewank functions. The ECDE -based sinusoidal algorithm found the global optimum solution in the Rastrigin function at iteration 529. It was also found a very near global optimum solution of 1.11E-16 in the Griewank function at iteration 846. The best, worst, average and standard deviation of objective function values are presented in Table 12. It is revealed that ECDE -based sinusoidal algorithm accomplished better objective function values with lower standard deviation than Jaya-bat algorithm in both Rastrigin and Griewank functions. In Rastrigin function, the average objective function values of ECDE -based sinusoidal algorithm and Jaya-bat algorithm are 7.79E-06 and 4.94, respectively. With respect to the Griewank function, the values of standard deviation of ECDE -based sinusoidal algorithm and Jaya-bat algorithm are 1.27E-13 and 1.9E-03, respectively.

INSERT FIGURE 23

INSERT TABLE 12

The third experiment encompasses verifying the performances of the developed ECDE -based sinusoidal algorithm against the improved particle swarm optimization (IPSO) algorithm presented by Xia et al. [101]. A set of thirty independent runs are undertaken, and the population size, number of dimensions and number of iterations are 40, 20 and 5000, respectively. Figure 24 illustrate the convergence of the developed ECDE -based sinusoidal algorithm in Rastrigin and Griewank functions. As can be seen, ECDE -based sinusoidal algorithm converged to zero in both Rastrigin and Griewank functions at iterations 1503 and 987, respectively. Table 13 provides the average objective function values of ECDE -based sinusoidal and IPSO algorithms. The average objective function values of ECDE -based sinusoidal in Rastrigin and Griewank functions are zero while the average objective function values obtained by IPSO algorithm are 3.54 and 2.53E-03 in Rastrigin and Griewank functions, respectively.

INSERT FIGURE 24

INSERT TABLE 13

In the fourth experiment the efficiency of the developed ECDE -based sinusoidal algorithm is investigated through its comparison against the golden eagle optimizer (GEO) introduced by

Mohammadi-Balani et al. [102]. Thirty runs were executed and the number of iterations and population size are assumed 1000 and 50, respectively. The performance comparison is done based on Beale, three-hump camel, Rastrigin and Griewank functions. In this context, the numbers of dimensions are two in Beale and three-hump camel functions, and they are thirty in Rastrigin and Griewank functions. Figures 25 and 26 show the convergence curves of the ECDE -based sinusoidal algorithm in Beale, three-hump camel, Rastrigin and Griewank functions. It is derived that ECDE -based sinusoidal algorithm found the global optimum solution of zero in both Beale and Griewank functions at iterations 152 and 824, respectively. It also converged to close global optimum solutions of 1.9E-286 and 3.7E-12 in three-hump camel and Rastrigin functions at iterations 984 and 976, respectively. The average and standard deviation of objective function values are provided in Table 14. It can be inferred that the ECDE -based sinusoidal algorithm outperformed the GEO algorithm in terms of quality and consistency of solutions. Both algorithms generated same average and standard deviation of objective function vales in Beale function while ECDE -based sinusoidal algorithm obtained superior results in three-hump camel, Rastrigin and Griewank functions. In the three-hump camel function, the average objective function values of ECDE -based sinusoidal and GEO algorithms are 8.88E-284 and 6.28E-126, respectively. In addition, the average objective function values ECDE -based sinusoidal and GEO algorithms in Rastrigin function are 2.08E-01 and 1.09E01, respectively. It is also noticed that ECDE -based sinusoidal and GEO algorithms scored standard deviation values in Griewank function are equal to 1.99E-17 and 5.53E-03, respectively.

INSERT FIGURE 25

INSERT FIGURE 26

INSERT TABLE 14

8. CONCLUSION

With the increase of percentage of deterioration bridges meanwhile maintenance costs are trending upwards. This calls for proper bridge management systems for the purpose of establishing timely-intervention plans. In this context, this paper introduces a three-tier automated platform for maintenance budget allocation of bridges at both project and network-levels. This study also tackles short-term and long-term strategic planning at the different decision-making levels of BMSs. The developed multi-objective optimization model uses exponential chaotic differential evolution algorithm for the purpose of optimizing the MR&R plans through a set of principal objectives under performance condition and cost constraints. The objective functions are constructed to maximize the condition performance level of the bridge elements, minimize the total life-cycle maintenance costs, minimize the duration of traffic disruption and minimize the environmental impact. Additionally, the developed multi-objective optimization model is designed to ensure balanced cost profiles with less fluctuations as possible.

The applicability of the developed model was tested using a set of various bridge elements and different study periods. Results obtained from the numerical example demonstrated that the developed ECDE-based Sinusoidal algorithm managed to improve the optimization performance aspects by 49.16% with respect to the multi-objective genetic algorithm in the five-year study period. In the twenty five-year study period, ECDE-based logistic algorithm enabled an enhancement of performance aspects by 72.19% with respect to differential evolution algorithm. At the level of thirty five-year study period, classical meta-heuristics failed to find feasible solutions within the assigned constraints of the maintenance planning model. In this regard, ECDE-based logistic-sine algorithm achieved a thirty five-year maintenance plan of CR, TLCC, TDTT and TEI of 68.65, 101866.48, 0 and 33.68, respectively. The results of AR technique revealed that ECDE-based sinusoidal algorithm outranked other meta-heuristics accomplishing the highest and most stable ranking ($\mu_{\mathbf{a}}$=2.41, σ_a=2.03). Classical meta-heuristics obtained significant lower rankings than exponential chaotic differential evolution algorithms. In addition, they experienced high perturbations in their performance across the different study periods (σ_a of GA is 3.87 and σ_a of PSO is 3.61).

In the high-dimensional benchmark test functions, it was derived that the developed ECDE -based sinusoidal algorithm obtained better average objective function values than genetic and differential evolution algorithms by 114.26% and 79.51%., respectively. They were highly vulnerable to premature convergence and local minima entrapment which caused them to fail in finding the global optimum solutions. As such, it is expected that the developed multi-objective optimization model can structure cost-effective and well-balanced maintenance plans which guarantee decision-makers satisfactory healthy condition of bridge elements while accommodating tight budget constraints.

REFERENCES

1. Tao, Z., Zophy, F. G., & Wiegmann, J. (2000). Asset management model and systems integration approach. Transportation Research Record, *1719*(1), 191–199. https://doi.org/10.3141/1719-25.
2. Flintsch, G. W., & Bryant, J. W. (2006). *Asset Management Data Collection for Supporting Decision Processes*. Washington, DC. https://www.fhwa.dot.gov/asset/dataintegration/if08018/assetmgmt_web.pdf (accessed December 20, 2018).
3. Miyamoto, A., Kawamura, K., & Nakamura, H. (2001). Development of a bridge management system for existing bridges. *Advances in Engineering Software*, *32*, 821–833. https://doi.org/10.1016/S0965-9978(01)00034-5.
4. National Research Council Canada. (2013). "*Critical Concrete Infrastructure: Extending the Life of Canada's Bridge Network*". http://www.nrc-cnrc.gc.ca/ci-ic/article/v18n1-5 (accessed December 20, 2018).
5. Statistics Canada. (2009). "*Age of Public Infrastructure: A Provincial Perspective*". http://www.statcan.gc.ca/pub/11-621-m/11-621-m2008067-eng.htm (accessed December 20, 2018).
6. Farzam, A., Nollet, M.-J., & Khaled, A. (2016). "Integration of site conditions information using geographic information system for the seismic evaluation of bridges." *Canadian Society of Civil Engineering Annual Conference: Resilient Infrastructure*, London,Canada, 1-4 June, 1-10. https://doi.org/10.1080/17499518.2021.1952609.
7. Viami International Inc. and the Technology Strategies Group. (2013). "*Market Study for Aluminium Use in Roadway Bridges"*, Montreal, Canada. https://aluminium.ca/uploader/publications/aluminumuseinroadwaybridges-finalreport28-05-13.pdf (accessed December 25, 2018).
8. Sennah, K., Juette, B., Witt, C., & Combar, P. M. (2011). Vehicle Crash Testing On a GFRP-Reinforced PL-3 Concrete Bridge Barrier. *Proceedings of the 4th International Conference on Durability and Sustainability of Fibre Reinforced Polymer Composites for Construction and Rehabilitation*, Québec City, Canada, 20-22 June. http://conf.tac-atc.ca/english/annualconference/tac2011/docs/s1/sennah.pdf (accessed October 10, 2018).
9. Alsharqawi, M., Abu Dabous, S., Zayed, T., & Hamdan, S. (2021). Budget Optimization of

Concrete Bridge Decks under Performance-Based Contract Settings. *Journal of Construction Engineering and Management*, *147*(6), 1–13. https://doi.org/10.1061/(ASCE)CO.1943-7862.0002043.

10. Ghodoosi, F., Abu-Samra, S., Zeynalian, M., & Zayed, T. (2018). Maintenance cost optimization for bridge structures using system reliability analysis and genetic algorithms. *Journal of Construction Engineering and Management*, *144*(2), 1–10. https://doi.org/10.1061/(ASCE)CO.1943-7862.0001435.
11. Shim, H. S., Lee, S. H., & Kang, B. S. (2017). Pareto front generation for bridge deck management system using bi-objective optimization. *KSCE Journal of Civil Engineering*, *21*(5), 1563–1572. https://doi.org/10.1007/s12205-016-2569-8.
12. Wu, D., Yuan, C., Kumfer, W., & Liu, H. (2017). A life-cycle optimization model using semi-markov process for highway bridge maintenance. *Applied Mathematical Modelling*., 43, 45–60. https://doi.org/10.1016/j.apm.2016.10.038.
13. Badawy, A. M. (2017). *Assessment of Bridges' Expansion Joints In Egypt*. M.Sc. thesis, American University in Cairo, Egypt. http://dar.aucegypt.edu/handle/10526/5204 (accessed October 10, 2020).
14. Allah Bukhsh, Z., Stipanovic, I., & Doree, A. G. (2020). Multi-year maintenance planning framework using multi-attribute utility theory and genetic algorithms. *European Transport Research Review*, *12*(1), 1-13. https://doi.org/10.1186/s12544-019-0388-y.
15. Dromey, L., Ruane, K., Murphy, J. J., O'Rourke, B., & Lacey, S. (2020). A bridge-rehabilitation strategy based on the analysis of a bridge-inspection data set. *Infrastructure Asset Management*, *7*(1), 25–35. https://doi.org/10.1680/jinam.18.00028.
16. Gao, Z., Liang, R. Y., & Xuan, T. (2019). VIKOR method for ranking concrete bridge repair projects with target-based criteria. *Results in Engineering*, *3*, 1–9. https://doi.org/10.1016/j.rineng.2019.100018.
17. Contreras-nieto, C., Shan, Y., Lewis, P., & Ann, J. (2019). Bridge maintenance prioritization using analytic hierarchy process and fusion tables. *Automation in Construction*, *101*, 99–110. https://doi.org/10.1016/j.autcon.2019.01.016.
18. Mahdi, I. M., Khalil, A. H., Mahdi, H. A., & Dina, M. M. (2019). Decision support system for optimal bridge' maintenance. *International Journal of Construction Management*, 1–15. https://doi.org/10.1080/15623599.2019.1623991.

19. Markiz, N., & Jrade, A. (2018). Integrating Fuzzy-Logic Decision Support With A Bridge Information Management System (BRIMS) at The Conceptual Stage Of Bridge Design. *Journal of Information Technology in Construction*, *23*, 92–121. http://www.itcon.org/2018/5 (accessed January 10, 2020).
20. Nurani, A. I., Pramudyaningrum, A. T., & Fadhila, S. R. (2017). Analytical Hierarchy Process (AHP), Fuzzy AHP , and TOPSIS for Determining Bridge Maintenance Priority Scale in Banjarsari , Surakarta. *International Journal of Science and Applied Science: Conference Series*, *2*(1), 60–71. https://doi.org/10.20961/ijsascs.v2i1.16680.
21. Rashidi, M., Ghodrat, M., Samali, B., Kendall, B., & Zhang, C. (2017). Remedial Modelling of Steel Bridges through Application of Analytical Hierarchy Process (AHP). *Applied Sciences*, *7*(2), 1–20. https://doi.org/10.3390/app7020168.
22. Nurdin, A., Kristiawan, S. A., & Handayani, D. (2017). Determination of the bridge maintenance and rehabilitation priority scale in kabupaten Pinrang. *Journal of Physics: Conference Series*, *795*, 1–7. https://doi.org/10.1088/1742-6596/795/1/012070.
23. Yoon, Y., & Hastak, M. (2016). Condition Improvement Measurement Using the Condition Evaluation Criteria of Concrete Bridge Decks. *Journal of Transportation Engineering*, *142*(11), 1–8. https://doi.org/10.1061/(ASCE)TE.1943-5436.0000883.
24. Van Eck, N. J., & Waltman, L. (2010). Software survey : VOSviewer , a computer program or bibliometric mapping. *Scientometrics*, *84*, 523–538. https://doi.org/10.1007/s11192-009-0146-3.
25. Thompson, P. D., Sobanjo, J. O., & Kerr, R. (2003). Florida DOT project-level bridge management models. *Journal of Bridge Engineering*, *8*(6), 345–352. https://doi.org/10.1061/(ASCE)1084-0702(2003)8:6(345).
26. Van Dam, K. H., Nikolic, I., & Lukszo, Z. (2012). *Agent-Based Modelling of Socio-Technical Systems*. Springer. https://doi.org/10.1007/978-94-007-4933-7.
27. Mohammed Abdelkader, E., Zayed, T., & Marzouk, M. (2019). A Computerized Hybrid Bayesian-Based Approach for Modeling the Deterioration of Concrete Bridge Decks. *Structure and Infrastructure Engineering*, *25*(19), 1178-1199. https://doi.org/10.1080/15732479.2019.1619782.
28. Hasan, M. S. (2015). Deterioration Prediction of Concrete Bridge Components Using Artificial Intelligence and Stochastic Methods. M.Sc. thesis, RMIT University, Australia.

https://researchrepository.rmit.edu.au/esploro/outputs/doctoral/Deterioration-prediction-of concrete-bridge-components-using-artificial-intelligence-and-stochastic-methods/9921863935901341 (accessed November 10, 2020).

29. Datta, T., Gates, T., Savolainen, P., Kay, J., Parajuli, S., & Nicita, N. (2016). *A Guide to Short - Term Stationary, Short - Duration, and Mobile Work Zone Traffic Control*, *Washington, D.C.* https://www.workzonesafety.org/files/documents/training/fhwa_wz_grant/wsu_STSDM_guide.pdf (accessed November 10, 2020).
30. Singh, D., & Tiong, R. L. K. (2005). Development of life cycle costing framework for highway bridges in Myanmar. *International Journal of Project Management*, *23*(1), 37–44. https://doi.org/10.1016/j.ijproman.2004.05.010.
31. Ehlen, M. A., & Marshall, H. E. (1996). *The Economics of New-Technology Materials: A Case Study of FRP Bridge Decking*, Gaithersburg. https://doi.org/10.6028/NIST.IR.5864.
32. Younes, T., Ni, F. M. W., & Tighe, S. (2020). Risk analysis in paving operations using discrete event simulation: a case study of Taiwan permeable asphalt concrete pavement pilot road project. *International Journal of Pavement Engineering*, *21*(7), 830–840. https://doi.org/10.1080/10298436.2018.1511785.
33. Shang, H., & Sun, L. (2018). Research on Life-Cycle Cost of Bridge Based on the Method of Monte Carlo Simulation. In *International Conference on Construction and Real Estate Management 2018*, 125–131. https://doi.org/10.1061/9780784481752.006.
34. Ökmen, Ö., & Öztas, A. (2010). Construction cost analysis under uncertainty with correlated cost risk analysis model. *Construction Management and Economics*, *28*(2), 203–212. https://doi.org/10.1080/01446190903468923.
35. Cheah, C. Y. J., & Liu, J. (2006). Valuing governmental support in infrastructure projects as real options using Monte Carlo simulation. *Construction Management and Economics*, *24*(5), 545–554. https://doi.org/10.1080/01446190500435572.
36. Aarthipriya, V., Chitra, G., & Poomozhi, J. S. (2020). Risk and its impacts on time and cost in construction projects. *Journal of Project Management*, *5*, 245–254. https://doi.org/10.5267/j.jpm.2020.6.002.

37. Pehlivan, S., & Öztemir, A. E. (2018). Integrated Risk of Progress-Based Costs and Schedule Delays in Construction Projects. *Engineering Management Journal*, *30*(2), 108–116. https://doi.org/10.1080/10429247.2018.1439636.

38. Sakka, Z. I., & El-Sayegh, S. M. (2007). Float Consumption Impact on Cost and Schedule in the Construction Industry. *Journal of Construction Engineering and Management*, *133*(2), 124–130. https://doi.org/10.1061/(ASCE)0733-9364(2007)133:2(124).

39. García-Alfonso, H., & Córdova-Esparza, D.-M. (2018). Comparison of uncertainty analysis of the Montecarlo and Latin Hypercube algorithms in a camera calibration model. *2018 IEEE 2nd Colombian Conference on Robotics and Automation (CCRA)*, 1-5, Barranquilla. https://doi.org/10.1109/CCRA.2018.8588138.

40. Li, J., Li, A., & Feng, M. Q. (2013). Sensitivity and Reliability Analysis of a Self-Anchored Suspension Bridge. *Journal of Bridge Engineering*, *18*(8), 703–711. https://doi.org/10.1061/(ASCE)BE.1943-5592.0000424.

41. Sun, J., Miao, Z., Gong, D., Zeng, X. J., Li, J., & Wang, G. (2020). Interval Multiobjective Optimization with Memetic Algorithms. *IEEE Transactions on Cybernetics*, *50*(8), 3444–3457. https://doi.org/10.1109/TCYB.2019.2908485.

42. Rong, M., Gong, D., Zhang, Y., Jin, Y., & Pedrycz, W. (2019). Multidirectional Prediction Approach for Dynamic Multiobjective Optimization Problems. *IEEE Transactions on Cybernetics*, *49*(9), 3362–3374. https://doi.org/10.1109/TCYB.2018.2842158.

43. Zhang, Y., Gong, D. wei, Sun, J. yong, & Qu, B. yang. (2018). A decomposition-based archiving approach for multi-objective evolutionary optimization. *Information Sciences*, *430–431*, 397–413. https://doi.org/10.1016/j.ins.2017.11.052.

44. Sun, J., Gong, D., & Sun, X. (2011). Solving interval multi-objective optimization problems using evolutionary algorithms with preference polyhedron. *Genetic and Evolutionary Computation Conference, GECCO'11*, 729–736. https://doi.org/10.1145/2001576.2001676.

45. Zhou, Q., He, Y., Zhao, D., Li, J., Li, Y., Williams, H., & Xu, H. (2021). Modified Particle Swarm Optimization with Chaotic Attraction Strategy for Modular Design of Hybrid Powertrains. *IEEE Transactions on Transportation Electrification*, *7*(2), 616–625. https://doi.org/10.1109/TTE.2020.3014688.

46. Anter, A. M., & Ali, M. (2020). Feature selection strategy based on hybrid crow search optimization algorithm integrated with chaos theory and fuzzy c-means algorithm for

medical diagnosis problems. *Soft Computing*, *24*(3), 1565–1584. https://doi.org/10.1007/s00500-019-03988-3.

47. Hekimoğlu, B. (2019). Optimal Tuning of Fractional Order PID Controller for DC Motor Speed Control via Chaotic Atom Search Optimization Algorithm. *IEEE Access*, *7*, 38100–38114. https://doi.org/10.1109/ACCESS.2019.2905961.
48. Mirjalili, S., & Gandomi, A. H. (2017). Chaotic gravitational constants for the gravitational search algorithm. *Applied Soft Computing Journal*, *53*, 407–419. https://doi.org/10.1016/j.asoc.2017.01.008.
49. Zitzler, E., & Thiele, L. (1999). Multiobjective evolutionary algorithms: A comparative case study and the strength Pareto approach. *IEEE Transactions on Evolutionary Computation*, *3*(4), 257–271. https://doi.org/10.1109/4235.797969.
50. Duman, S., Akbel, M., & Kahraman, H. T. (2021). Development of the Multi-Objective Adaptive Guided Differential Evolution and optimization of the MO-ACOPF for wind/PV/tidal energy sources. *Applied Soft Computing Journal*, *112*, 1-35. https://doi.org/10.1016/j.asoc.2021.107814.
51. Boufellouh, R., & Belkaid, F. (2020). Bi-objective optimization algorithms for joint production and maintenance scheduling under a global resource constraint: Application to the permutation flow shop problem. *Computers and Operations Research*, *122*, 1-25. https://doi.org/10.1016/j.cor.2020.104943.
52. Schott, J. R. (1995). *Fault tolerant design using single and multicriteria genetic algorithm optimization*. M.SC thesis, Massachusetts Institute of Technology, United States of America. http://hdl.handle.net/1721.1/11582 (accessed November 20, 2018).
53. Shenfield, A., & Fleming, P. J. (2014). Multi-objective evolutionary design of robust controllers on the grid. *Engineering Applications of Artificial Intelligence*, *27*, 17–27. https://doi.org/10.1016/j.engappai.2013.09.015.
54. Liu, Y., Zhu, N., Li, K., Li, M., Zheng, J., & Li, K. (2020). An angle dominance criterion for evolutionary many-objective optimization. *Information Sciences*, *509*, 376–399. https://doi.org/10.1016/j.ins.2018.12.078.
55. Yu, C., Andreotti, P., & Semeraro, Q. (2020). Multi-objective scheduling in hybrid flow shop: Evolutionary algorithms using multi-decoding framework. *Computers and Industrial Engineering*, *147*, 1–19. https://doi.org/10.1016/j.cie.2020.106570.

56. Bi, X., Yu, D., Liu, J., & Hu, Y. (2020). A preference-based multi-objective algorithm for optimal service composition selection in cloud manufacturing. *International Journal of Computer Integrated Manufacturing*, *33*(8), 751–768. https://doi.org/10.1080/0951192X.2020.1775298.
57. Massaro, A., & Benini, E. (2015). A surrogate-assisted evolutionary algorithm based on the genetic diversity objective. *Applied Soft Computing Journal*, *36*, 87–100. https://doi.org/10.1016/j.asoc.2015.06.026.
58. Sun, Y., Yang, T., & Liu, Z. (2019). A whale optimization algorithm based on quadratic interpolation for high-dimensional global optimization problems. *Applied Soft Computing Journal*, *85*, 1–20. https://doi.org/10.1016/j.asoc.2019.105744.
59. Cheng, L., Wu, X. H., & Wang, Y. (2018). Artificial flora (AF) optimization algorithm. Applied Sciences, 8(3), 1–21. https://doi.org/10.3390/app8030329.
60. Griewank, A. O. (1981). Generalized descent for global optimization. *Journal of Optimization Theory and Applications*, *34*(1), 11–39. https://doi.org/10.1007/BF00933356.
61. Jamil, M., & Yang, X. S. (2013). A literature survey of benchmark functions for global optimisation problems. *International Journal of Mathematical Modelling and Numerical Optimisation*, *4*(2), 150–194. https://doi.org/10.1504/ijmmno.2013.055204.
62. Wu, J., Wang, Y., Burrage, K., Tian, Y., Lawson, B., & Ding, Z. (2020). An improved firefly algorithm for global continuous optimization problems. *Expert Systems With Applications*, *149*, 1–12. https://doi.org/10.1016/j.eswa.2020.113340.
63. Li, Y., Zhao, Y., & Liu, J. (2021). Dynamic sine cosine algorithm for large-scale global optimization problems. *Expert Systems with Applications*, *177*, 1–14. https://doi.org/10.1016/j.eswa.2021.114950.
64. Shah, H., Tairan, N., Garg, H., & Ghazali, R. (2018). Global gbest guided-artificial bee colony algorithm for numerical function optimization. *Computers*, *7*(4), 1-17. https://doi.org/10.3390/computers7040069.
65. El-Sherbiny, A., Elhosseini, M. A., & Haikal, A. Y. (2018). A new ABC variant for solving inverse kinematics problem in 5 DOF robot arm. *Applied Soft Computing Journal*, *73*, 24–38. https://doi.org/10.1016/j.asoc.2018.08.028.
66. Li, G., Shuang, F., Zhao, P., & Le, C. (2019). An improved butterfly optimization algorithm for engineering design problems using the cross-entropy method. *Symmetry*, *11*(8), 1–20.

https://doi.org/10.3390/sym11081049.

67. Mirjalili, S., & Lewis, A. (2016). Obstacles and difficulties for robust benchmark problems: A novel penalty-based robust optimisation method. *Information Sciences*, *328*, 485–509. https://doi.org/10.1016/j.ins.2015.08.041.

68. Tork, H., Javadi, S., & Hashemy Shahdany, S. M. (2021). A new framework of a multi-criteria decision making for agriculture water distribution system. *Journal of Cleaner Production*, *306*, 1–14. https://doi.org/10.1016/j.jclepro.2021.127178.

69. Yi, P., Dong, Q., Li, W., & Wang, L. (2021). Measurement of city sustainability based on the grey relational analysis: The case of 15 sub-provincial cities in China. *Sustainable Cities and Society*, *73*, 1–11. https://doi.org/10.1016/j.scs.2021.103143.

70. Ma, X., Chen, H., Zhang, X., Xing, M., & Yang, P. (2019). Effect of Asphalt Binder Characteristics on Filler-Asphalt Interactions and Asphalt Mastic Creep Properties. *Journal of Materials in Civil Engineering*, *31*(8), 1–11. https://doi.org/10.1061/(ASCE)MT.1943-5533.0002773.

71. Valipour, A., Yahaya, N., Md Noor, N., Antuchevičienė, J., & Tamošaitienė, J. (2017). Hybrid SWARA-COPRAS method for risk assessment in deep foundation excavation project: an Iranian case study. *Journal of Civil Engineering and Management*, *23*(4), 524–532. https://doi.org/10.3846/13923730.2017.1281842.

72. Xie, H. B., Wu, W. J., & Wang, Y. F. (2018). Life-time reliability based optimization of bridge maintenance strategy considering LCA and LCC.*Journal of Cleaner Production*, *176*, 36–45. https://doi.org/10.1016/j.jclepro.2017.12.123.

73. Lindly, J. K., & Clark, P. R. (2004). Characterizing Work Zone Configurations and Effects. Alabama. http://utca.eng.ua.edu/files/2011/08/04406fnl.pdf (accessed November 20, 2018).

74. Marzouk, M., Mohammed Abdelkader, E., & Al-Gahtani, K. (2017). Building information modeling-based model for calculating direct and indirect emissions in construction projects. *Journal of cleaner production*, *152*, 351-363. https://doi.org/10.1016/j.jclepro.2017.03.138.

75. Hong, T., Chae, M. J., Kim, D., Koo, C., Lee, K. S., & Chin, K. H. (2013). Infrastructure Asset Management System for Bridge Projects in South Korea. *KSCE Journal of Civil Engineering*, 17(7), 1551–1561. https://doi.org/10.1007/s12205-013-0408-8.

76. Lee, S., Park, W., Ok, S., & Koh, H. (2011). Preference-based Maintenance Planning for Deteriorating Bridges under Multi-objective Optimisation Framework. *Structure and Infrastructure Engineering*, 7(8), 633–644. https://doi.org/10.1080/15732479.2010.501565.

77. Shim, H. S., & Lee, S. H. (2017). Balanced Allocation of Bridge Deck Maintenance Budget Through multi-objective optimization . *KSCE Journal of Civil Engineering*, *21*(4), 1039-1046. https://doi.org/10.1007/s12205-016-0591-5.

78. Tharwat, A., Elhoseny, M., Hassanien, A. E., Gabel, T., & Kumar, A. (2019). Intelligent Bézier curve-based path planning model using Chaotic Particle Swarm Optimization algorithm. *Cluster Computing*, *22*(s2), 4745–4766. https://doi.org/10.1007/s10586-018-2360-3.

79. Sayed, G. I., Darwish, A., & Hassanien, A. E. (2018). A New Chaotic Whale Optimization Algorithm for Features Selection. *Journal of Classification*, *35*(2), 300–344. https://doi.org/10.1007/s00357-018-9261-2.

80. Li, C., Chen, M. Z. Q., & Lam, J. (2012). On Exponential Almost Sure Stability of Random Jump Systems. *IEEE Transactions on Automatic Control*, *57*(12), 3064–3077. https://doi.org/10.1109/TAC.2012.2200369.

81. Deb, K., Pratap, A., Agarwal, S., & Meyarivan, T. (2002). A fast and elitist multiobjective genetic algorithm: NSGA-II. *IEEE Transactions on Evolutionary Computation*, *6*(2), 182–197. https://doi.org/10.1109/4235.996017.

82. Storn, R., & Price, K. (1997). Differential Evolution - A simple and efficient adaptive scheme for global optimization over continuous spaces. *Journal of Global Optimization*, *11*(4),341-359. https://doi.org/10.1023/A:1008202821328.

83. Nilakantan, J. M., Nielsen, I., Ponnambalam, S. G., & Venkataramanaiah, S. (2017). Differential evolution algorithm for solving RALB problem using cost- and time-based models. *International Journal of Advanced Manufacturing Technology*, *89*, 311–332. https://doi.org/10.1007/s00170-016-9086-2.

84. Han, F., Guo, X., & Gao, H. (2013). Bearing parameter identification of rotor-bearing system based on Kriging surrogate model and evolutionary algorithm. *Journal of Sound and Vibration*, *332*(11), 2659–2671. https://doi.org/10.1016/j.jsv.2012.12.025.

85. May, R. M. (1976). Simple mathematical models with very complicated dynamics. *Nature*, *261*(5560), 459–467. https://doi.org/10.1038/261459a0.

86. Arora, S., & Anand, P. (2019). Chaotic grasshopper optimization algorithm for global optimization. *Neural Computing and Applications*, *31*(8), 4385–4405. https://doi.org/10.1007/s00521-018-3343-2.

87. Arasomwan, A. M., & Adewumi, A. O. (2015). Comment on “an investigation into the performance of particle swarm optimization with various chaotic Maps. *Mathematical Problems in Engineering*, *2015*, Article ID 178959, 17 pages. https://doi.org/10.1155/2015/815370.

88. Yuan, X., Zhao, J., Yang, Y., & Wang, Y. (2014). Hybrid parallel chaos optimization algorithm with harmony search algorithm. *Applied Soft Computing*, *17*, 12–22. https://doi.org/10.1016/j.asoc.2013.12.016.

89. Demir, F. B., Tuncer, T., & Kocamaz, A. F. (2020). A chaotic optimization method based on logistic-sine map for numerical function optimization. *Neural Computing and Applications*, *9*, 1-13. https://doi.org/10.1007/s00521-020-04815-9.

90. Diakoulaki, D., Mavrotas, G., & Papayannakis, L. (1995). Determining objective weights in multiple criteria problems: The critic method. *Computers and Operations Research*, *22*(7), 763–770. https://doi.org/10.1016/0305-0548(94)00059-H.

91. Yu, D., Hong, J., Zhang, J., & Niu, Q. (2018). Multi-Objective Individualized-Instruction Teaching-Learning-Based Optimization Algorithm. *Applied Soft Computing*, *62*, 288–314. https://doi.org/10.1016/j.asoc.2017.08.056.

92. Keshavarz Ghorabaee, M., Amiri, M., Zavadskas, E. K., Turskis, Z., & Antucheviciene, J. (2017). A new hybrid simulation-based assignment approach for evaluating airlines with multiple service quality criteria. *Journal of Air Transport Management*, *63*, 45–60. https://doi.org/10.1016/j.jairtraman.2017.05.008.

93. Mahdiraji, H. A., Arzaghi, S., Stauskis, G., & Zavadskas, E. K. (2018). A hybrid fuzzy BWM-COPRAS method for analyzing key factors of sustainable architecture. *Sustainability*, *10*(5), 1–26. https://doi.org/10.3390/su10051626.

94. Mulliner, E., Smallbone, K., & Maliene, V. (2013). An assessment of sustainable housing affordability using a multiple criteria decision making method. *Omega*, *41*(2), 270–279.

95. Ju-Long, D. (1982). Control problems of grey systems. *Systems and Control Letters*, *1*(5), 288–294. https://doi.org/10.1016/S0167-6911(82)80025-X.

96. Kuo, Y., Yang, T., & Huang, G. W. (2008). The use of grey relational analysis in solving multiple attribute decision-making problems. *Computers and Industrial Engineering*, *55*(1), 80–93. https://doi.org/10.1016/j.cie.2007.12.002.
97. Kou, G., Yang, P., Peng, Y., Xiao, F., Chen, Y., & Alsaadi, F. E. (2020). Evaluation of feature selection methods for text classification with small datasets using multiple criteria decision-making methods. *Applied Soft Computing Journal*, *86*, 1-14. https://doi.org/10.1016/j.asoc.2019.105836.
98. Acır, A., Canlı, M. E., Ata, İ., & Çakıroğlu, R. (2017). Parametric optimization of energy and exergy analyses of a novel solar air heater with grey relational analysis. *Applied Thermal Engineering*, *122*, 330–338. https://doi.org/10.1016/j.applthermaleng.2017.05.018.
99. Ülker, E. D. (2017). An improved clonal selection algorithm using a tournament selection operator and its application to microstrip coupler design. *Turkish Journal of Electrical Engineering and Computer Sciences*, *25*(3), 1751–1761. https://doi.org/10.3906/elk-1603-73.
100. Kaur, A., Sharma, S., & Mishra, A. (2019). A Novel Jaya-BAT Algorithm Based Power Consumption Minimization in Cognitive Radio Network. *Wireless Personal Communications*, *108*(4), 2059–2075. https://doi.org/10.1007/s11277-019-06509-5.
101. Xia, C., Jiang, T., & Chen, W. (2017). Particle Swarm Optimization of Aerodynamic Shapes with Nonuniform Shape Parameter–Based Radial Basis Function. *Journal of Aerospace Engineering*, *30*(3), 1–12. https://doi.org/10.1061/(ASCE)AS.1943-5525.0000686.
102. Mohammadi-Balani, A., Dehghan Nayeri, M., Azar, A., & Taghizadeh-Yazdi, M. (2021). Golden eagle optimizer: A nature-inspired metaheuristic algorithm. *Computers and Industrial Engineering*, *152*, 1–30. https://doi.org/10.1016/j.cie.2020.107050.

List of Figures

Figure 22: Convergence curves of best performance histories accomplished by ECDE-based sinusoidal algorithm in Rastrigin and Schwefel 2.26 functions in experiment 1

Figure 13: Convergence curves of best performance histories accomplished by ECDE-based sinusoidal algorithm in Rastrigin and Griewank functions in experiment 2

Figure 24: Convergence curves of best performance histories accomplished by ECDE-based sinusoidal algorithm in Rastrigin and Griewank functions in experiment 3

Figure 25: Convergence curves of best performance histories accomplished by ECDE-based sinusoidal algorithm in Beale and three-hump camel functions in experiment 4

Figure 26: Convergence curves of best performance histories accomplished by ECDE-based sinusoidal algorithm in Beale and three-hump camel functions in experiment 5

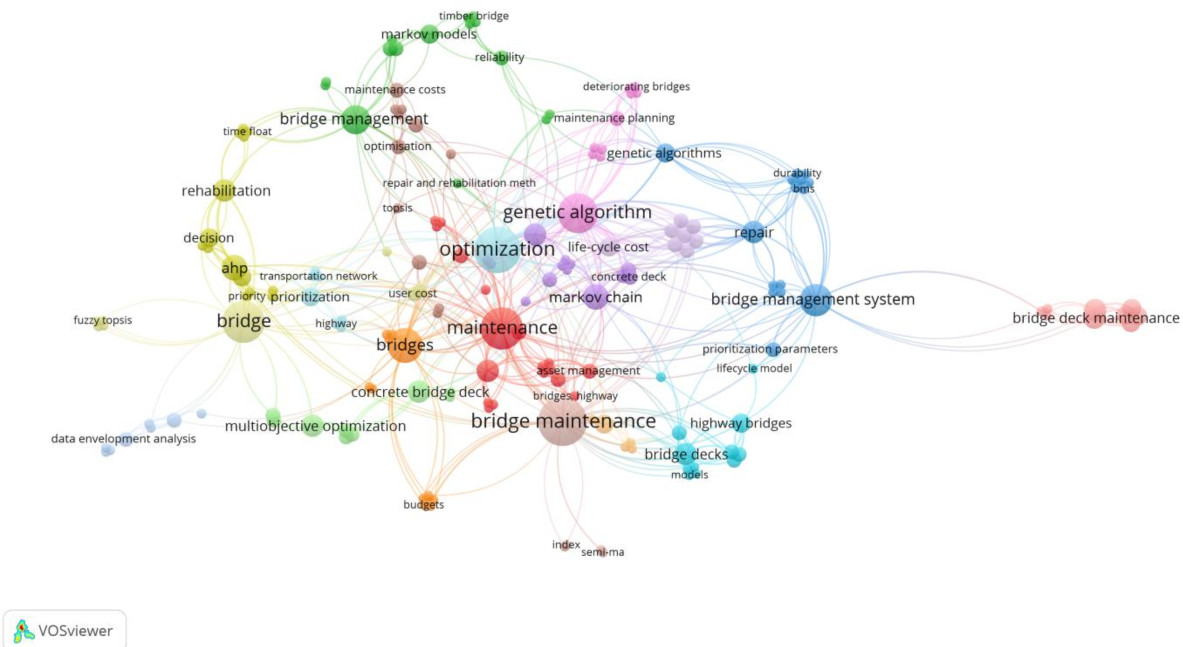

Figure 1: Bibliometric co-occurrence map of the maintenance planning models bridges

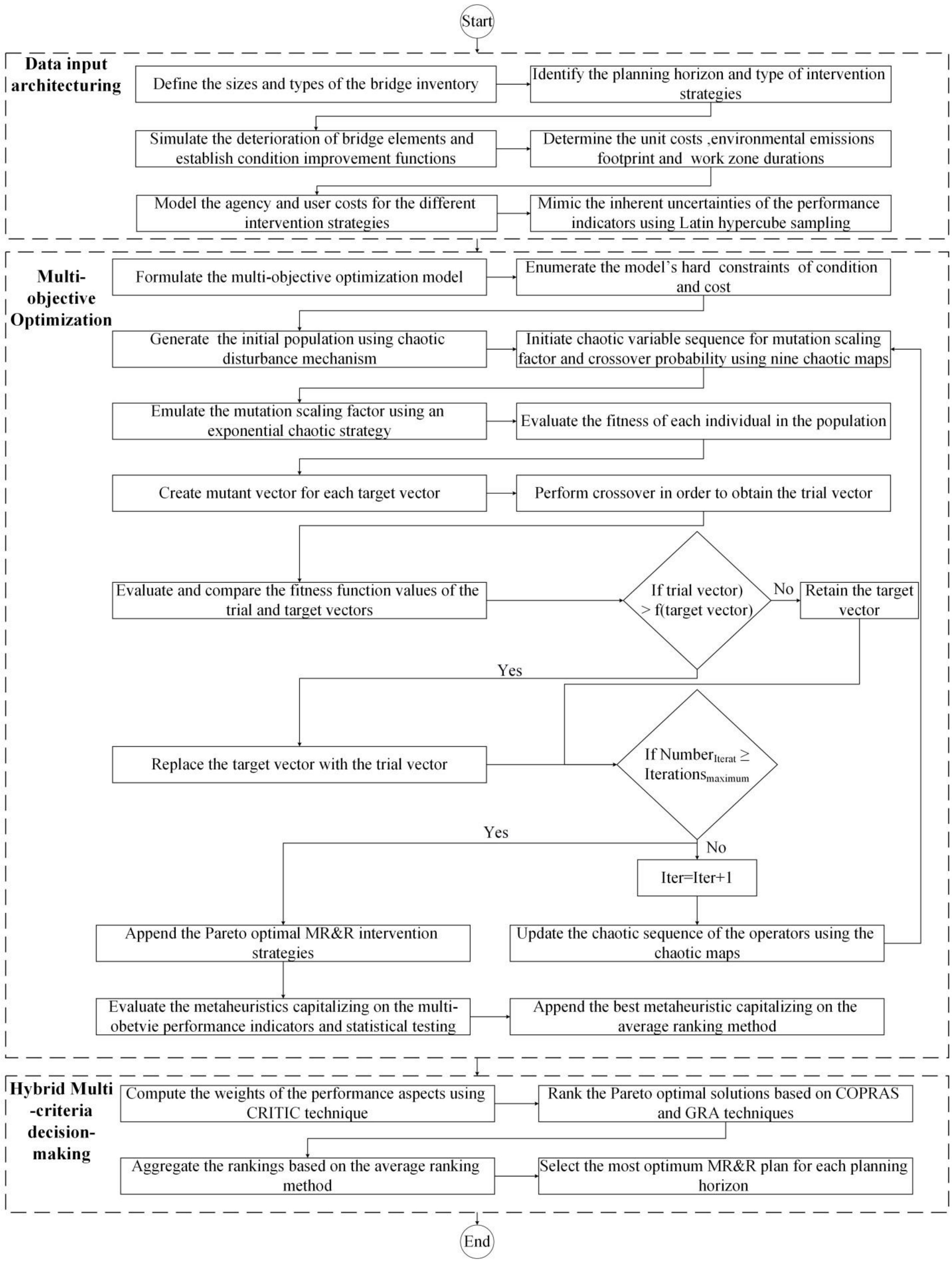

Figure 2: Framework of the proposed bridge maintenance planning method

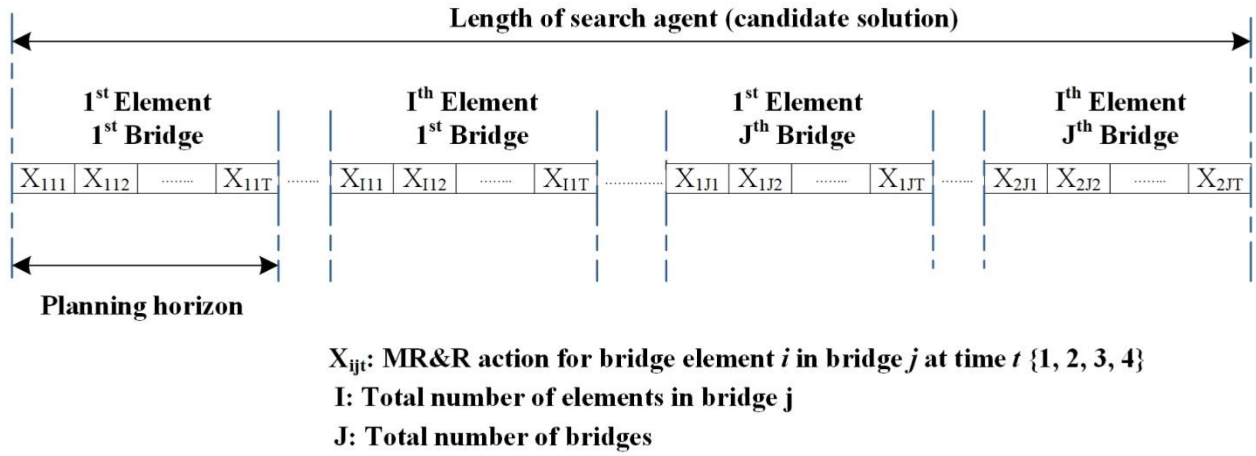

Figure 3: Schematic representation of a solution structure for a typical bridge network

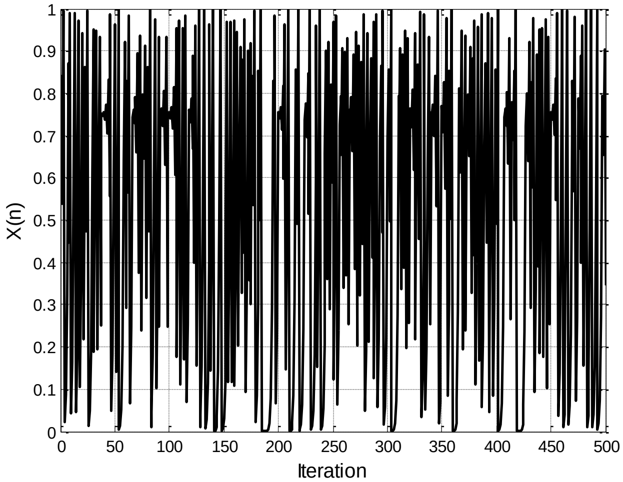

(a) Logistic map

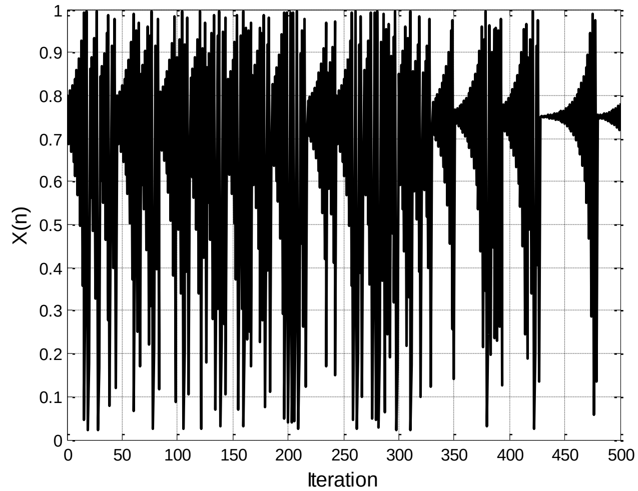

(b) Singer map

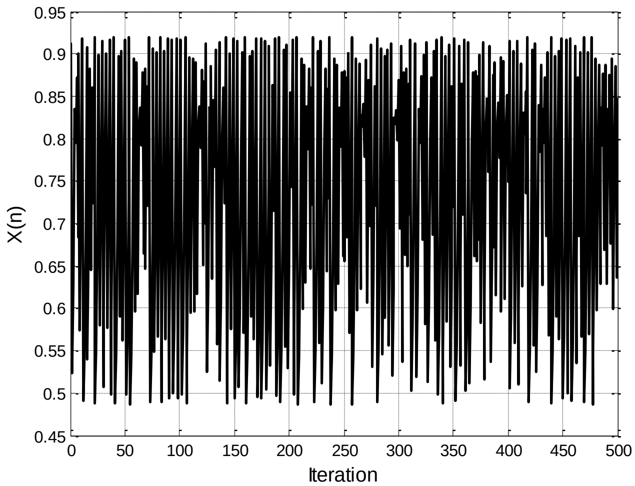

(c) Sinusoidal map

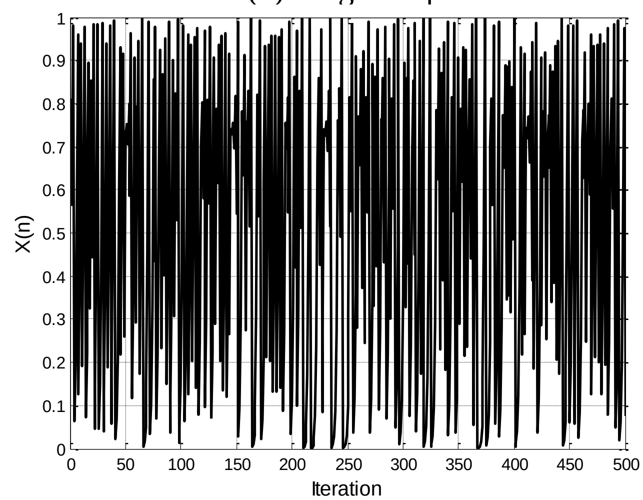

(d) Sine map

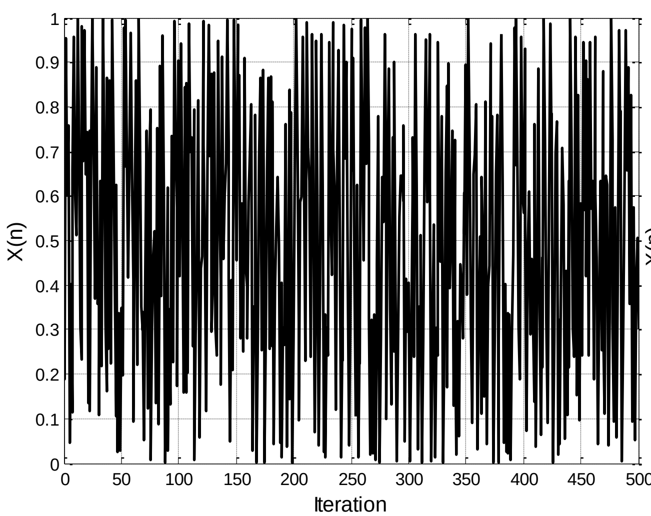

(e) Iterative map

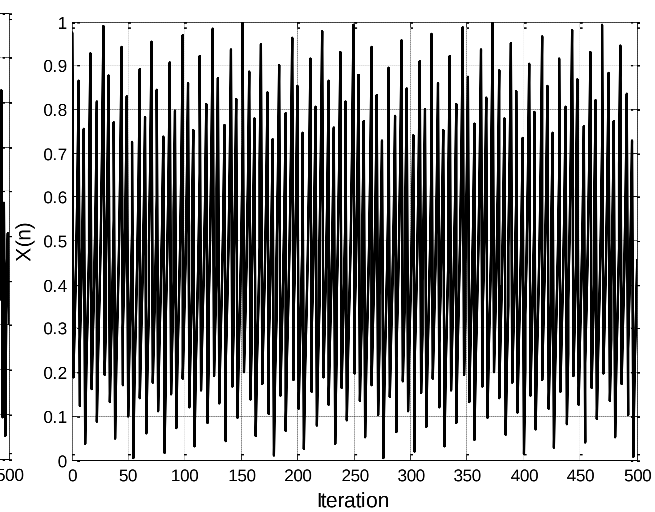

(f) Chebyshev map

Figure 4: Behavior of different chaotic maps

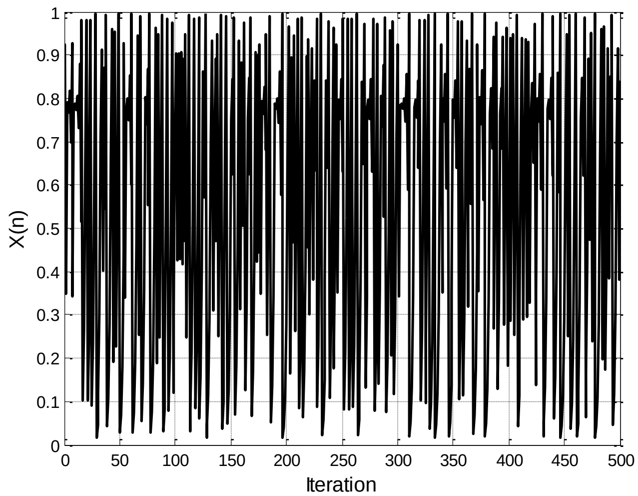

(a) Circle map

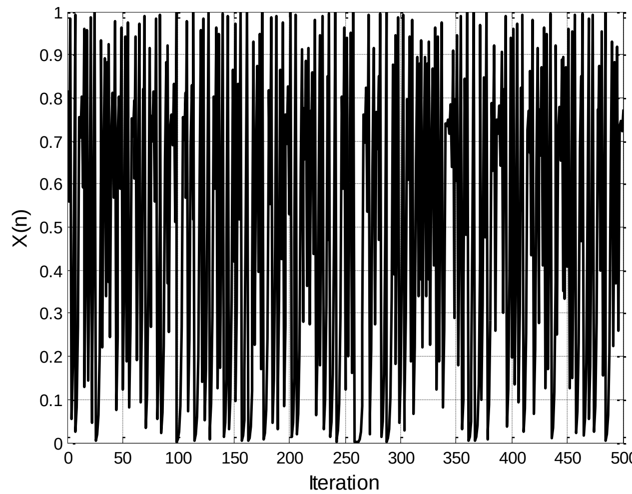

(b) Logistic-sine map

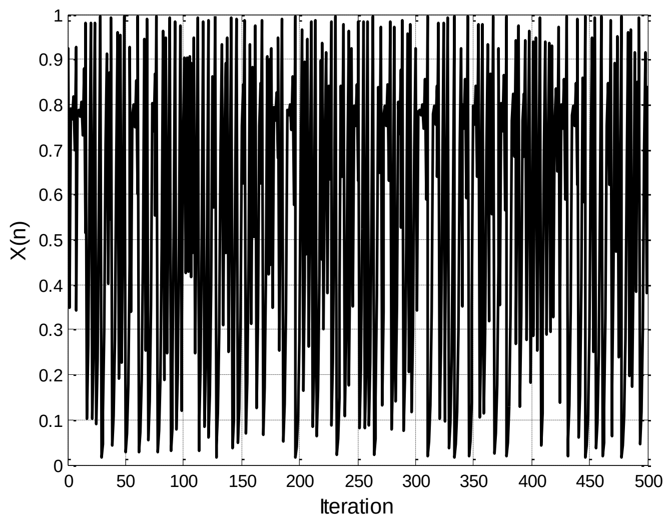

(c) Cubic map

Figure 5: Behavior of different chaotic maps (Continued)

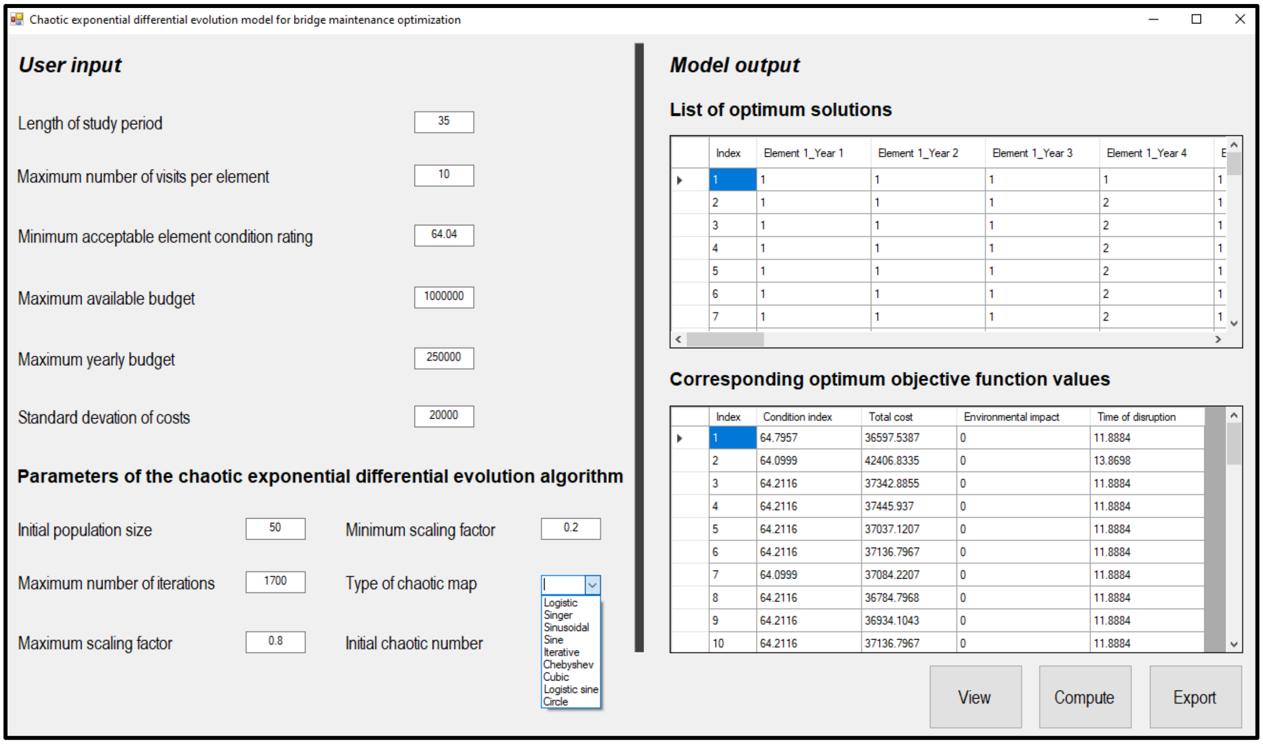

Figure 6: Interface of the proposed ECDE-based models for maintenance planning of bridge network

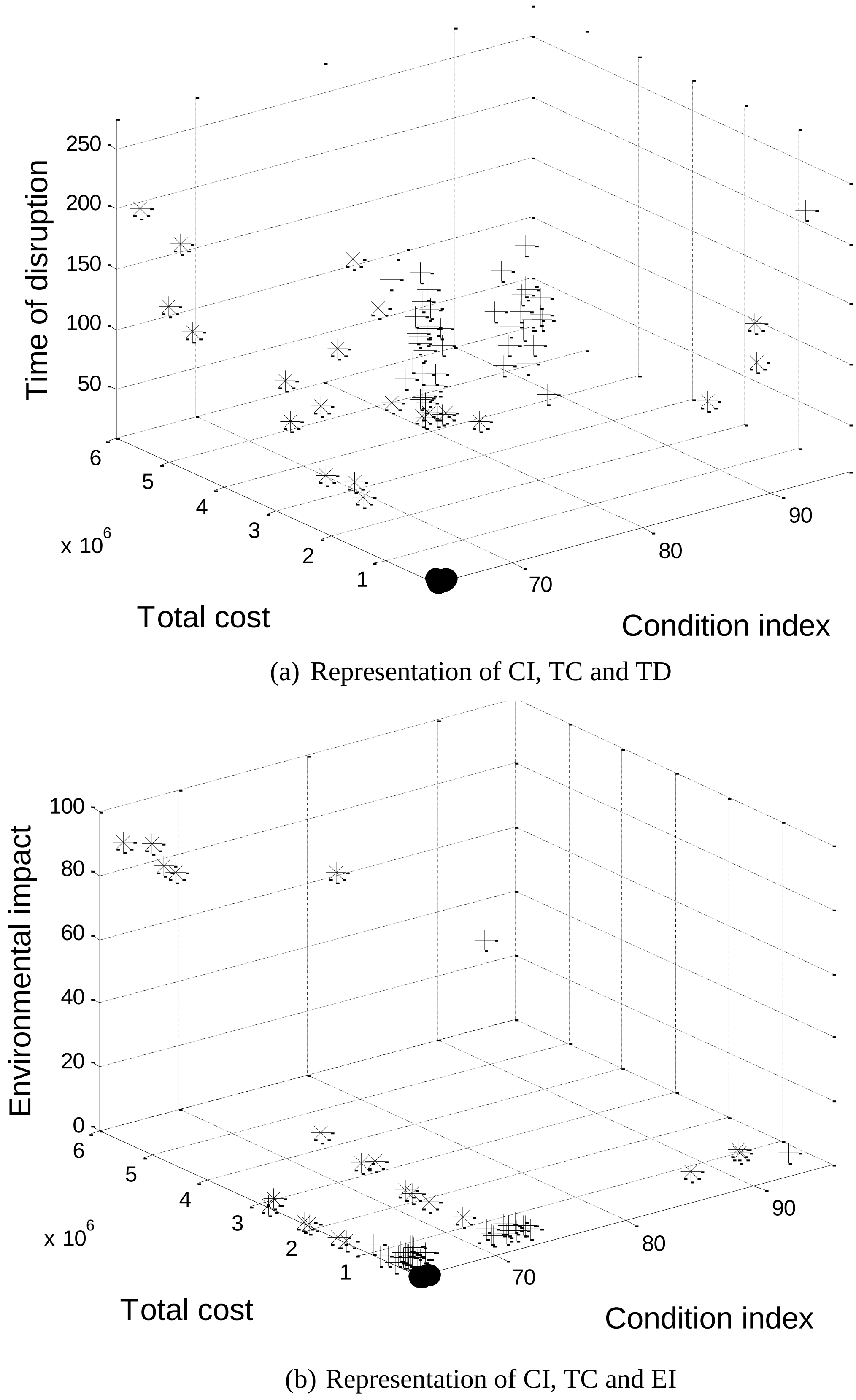

(a) Representation of CI, TC and TD

(b) Representation of CI, TC and EI

Figure 7: Optimum maintenance plans of the twenty five-year study period

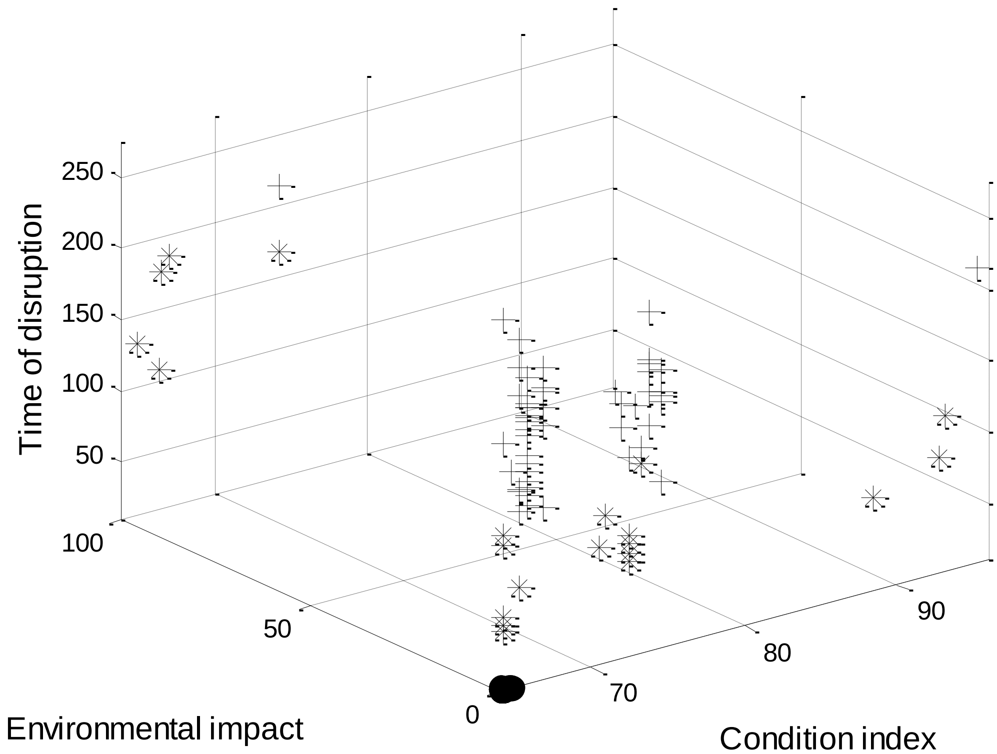

(a) Representation of CI, EI and TD

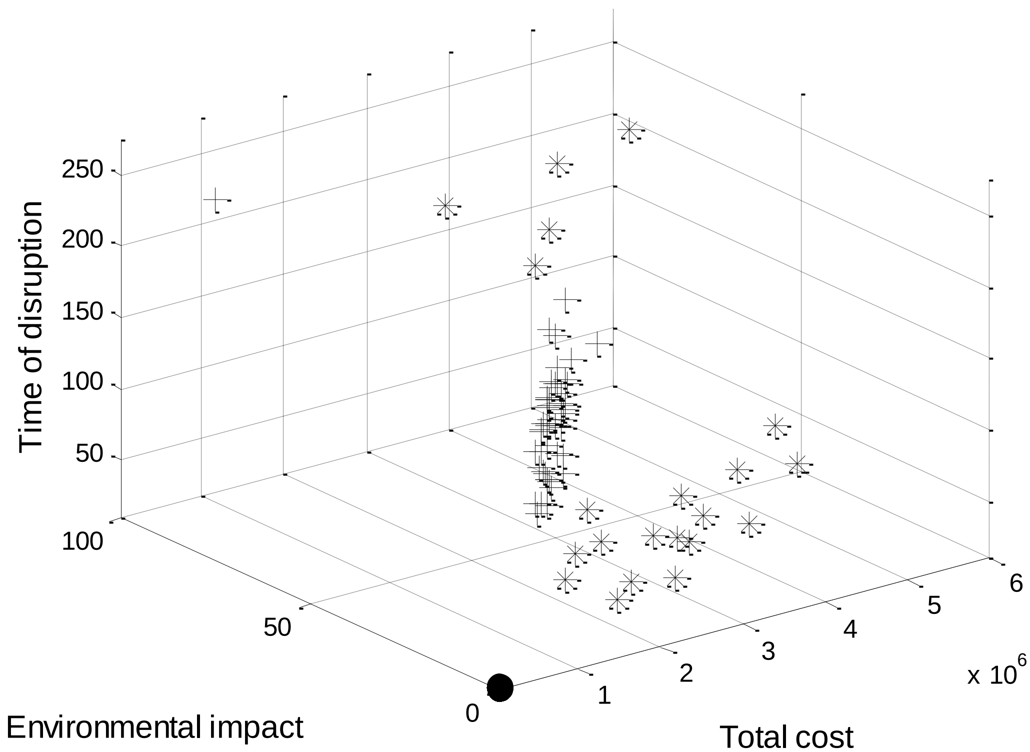

(b) Representation of TC, EI and TD

Figure 8: Optimum maintenance plans of the twenty five year-study period (Continued)

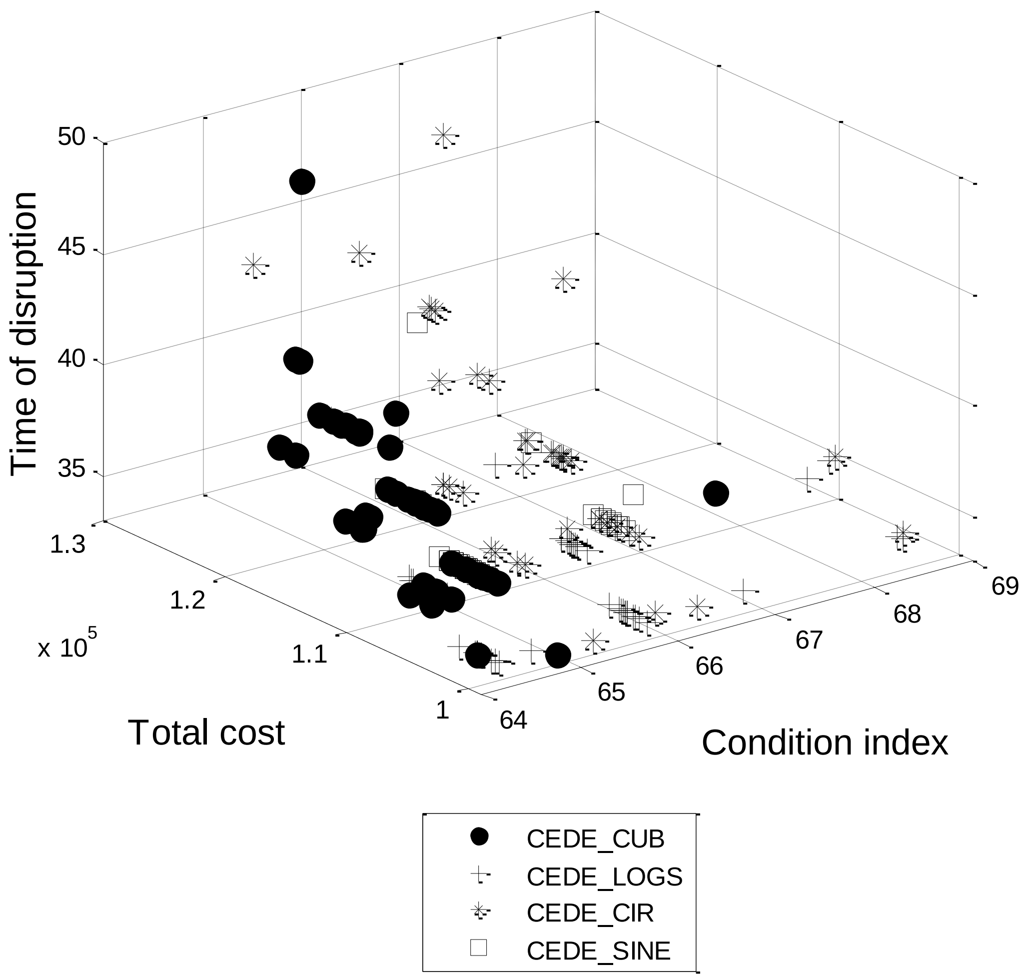

Figure 9: Optimum maintenance plans of the thirty five-year study period

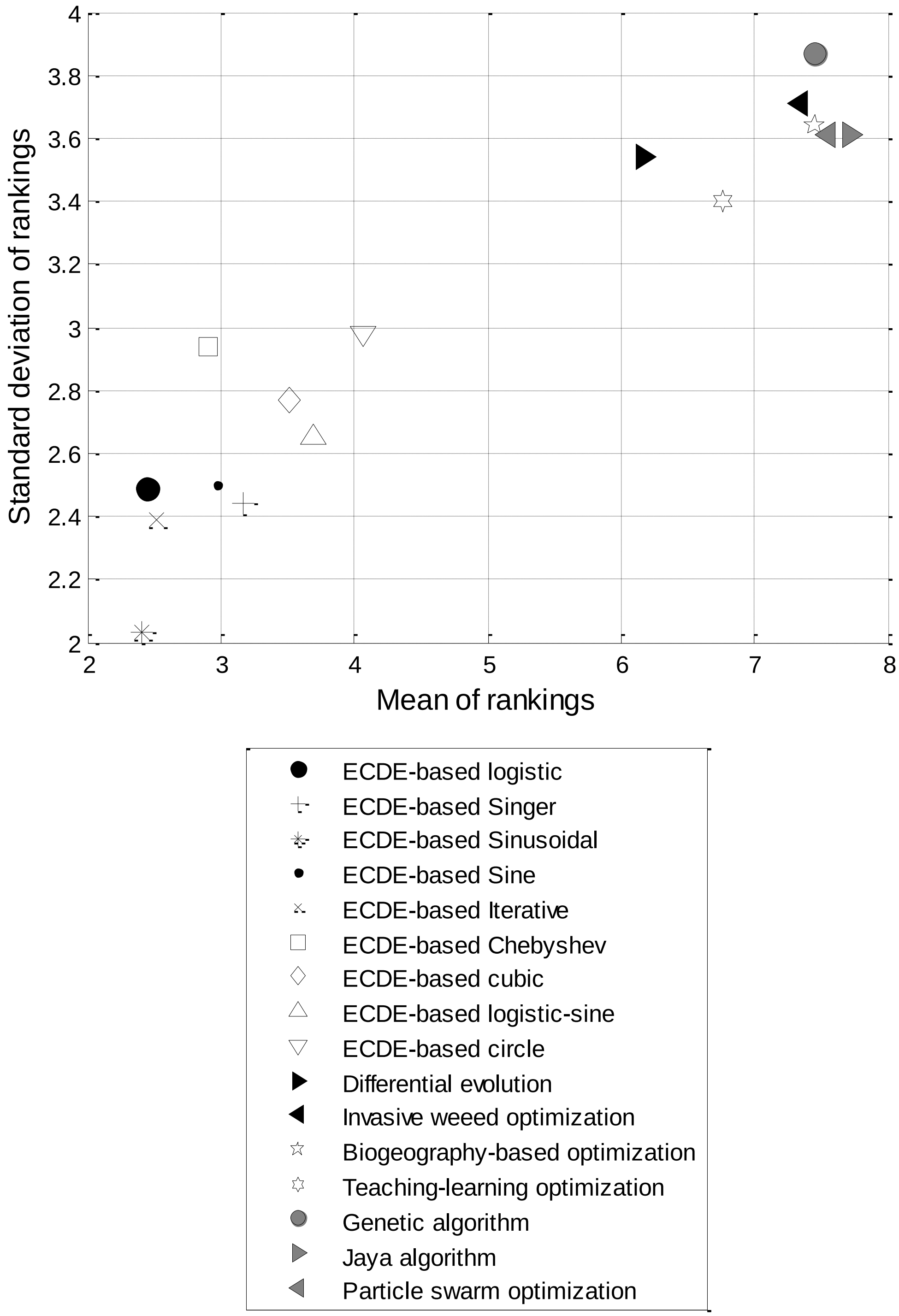

Figure 10: Plot of the average and standard deviation of rankings of the meta-heuristic-based optimization models

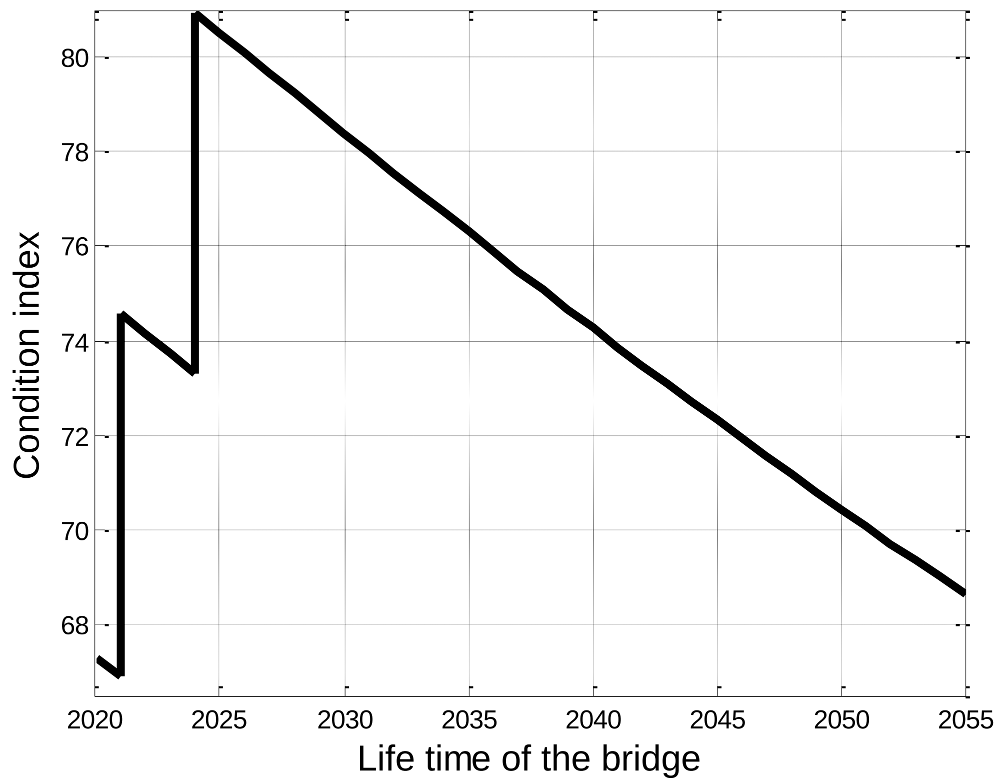

(a) Maintenance profile of bridge deck based on ECDE-based logistic-sine model

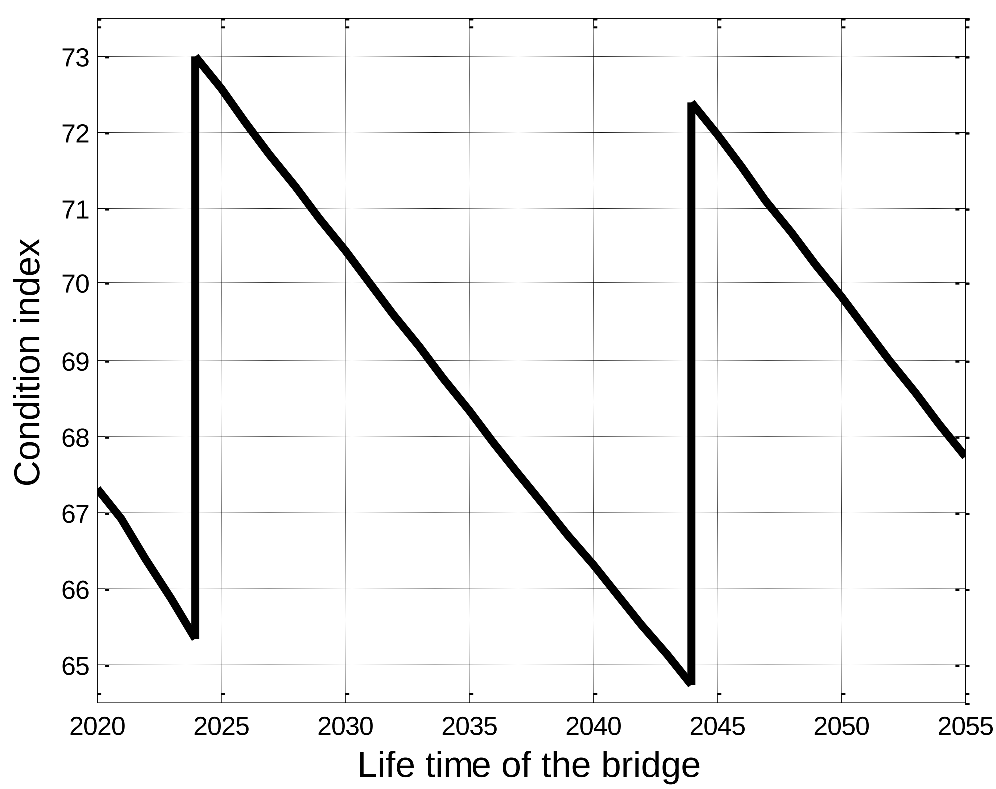

(b) Maintenance profile of bridge deck based on ECDE-based sinusoidal model

Figure 11: Maintenance profile of a bridge deck over a thirty five-year planning horizon

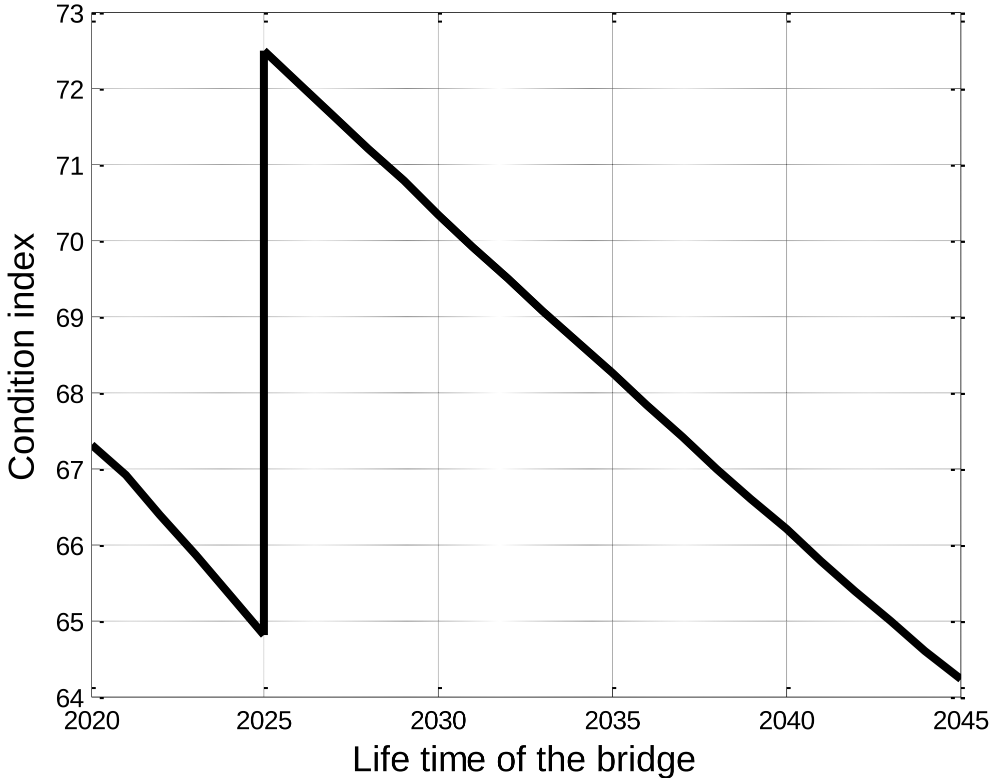

(a) Maintenance profile of bridge deck based on ECDE-based singer model

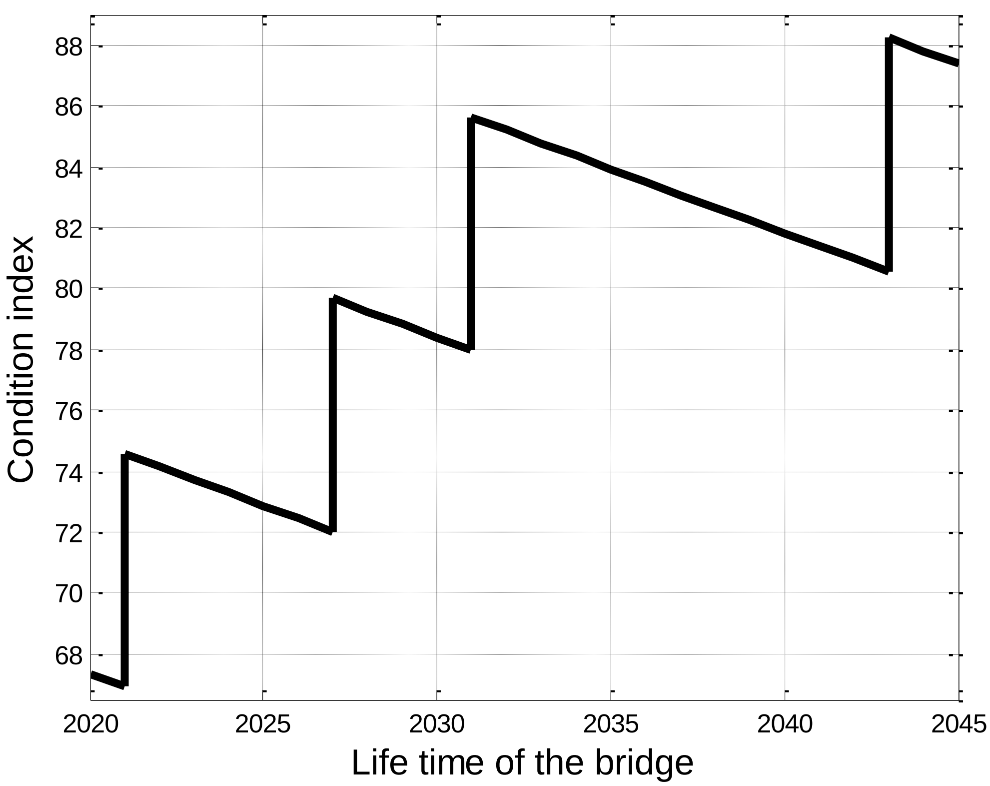

(b) Maintenance profile of bridge deck based on TLO model

Figure 12: Maintenance profile of a bridge deck over a twenty five-year planning horizon

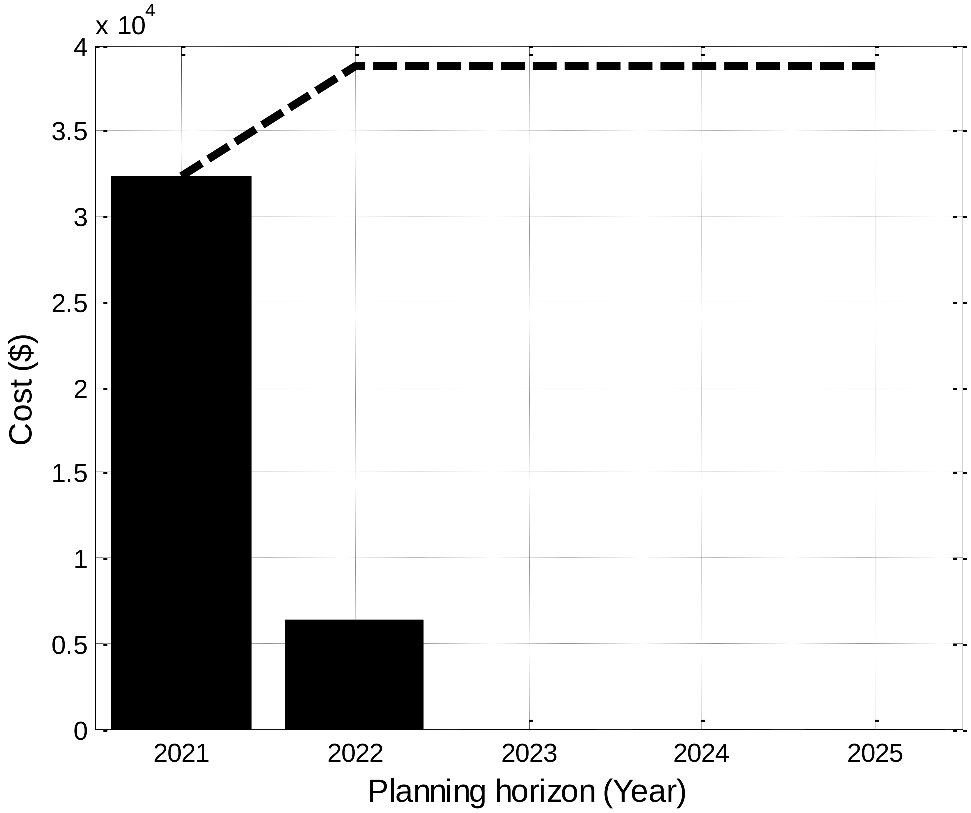

Figure 13: Cash flow of bridge network over a five-year planning horizon

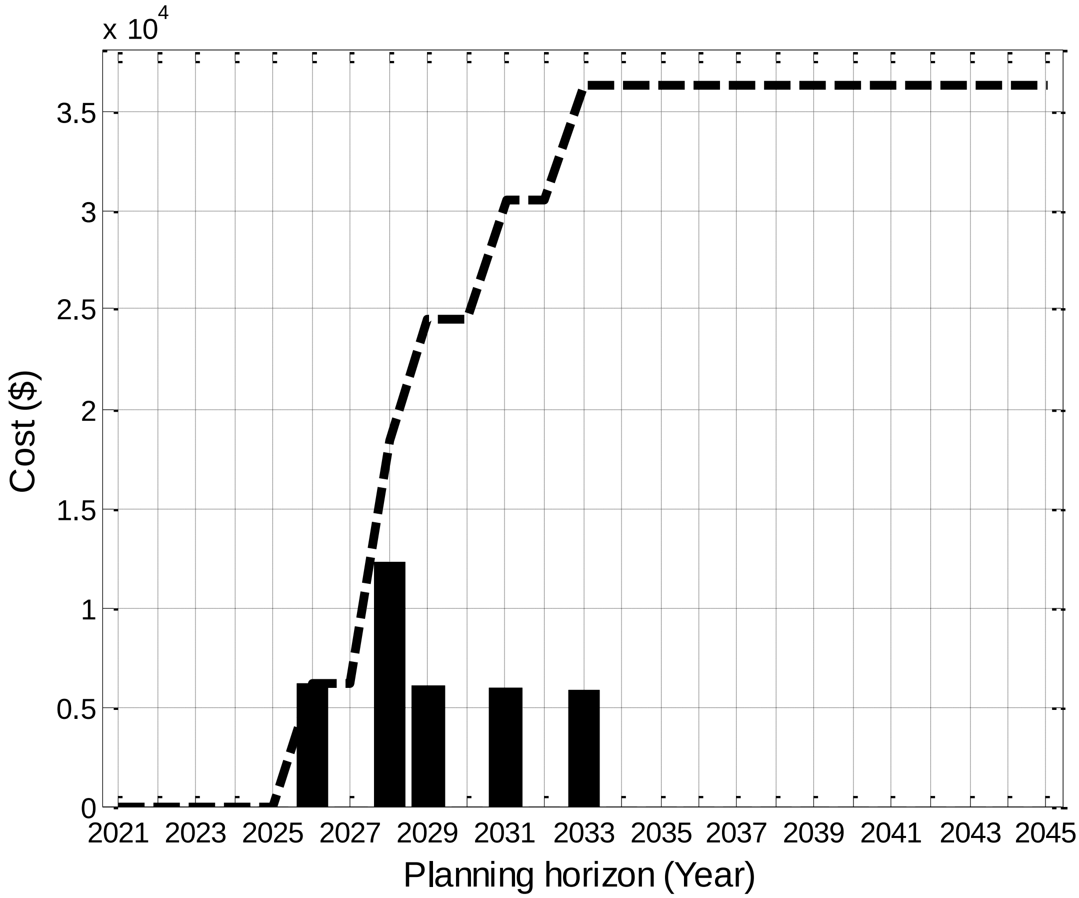

Figure 14: Cash flow of bridge network over a twenty five-year planning horizon

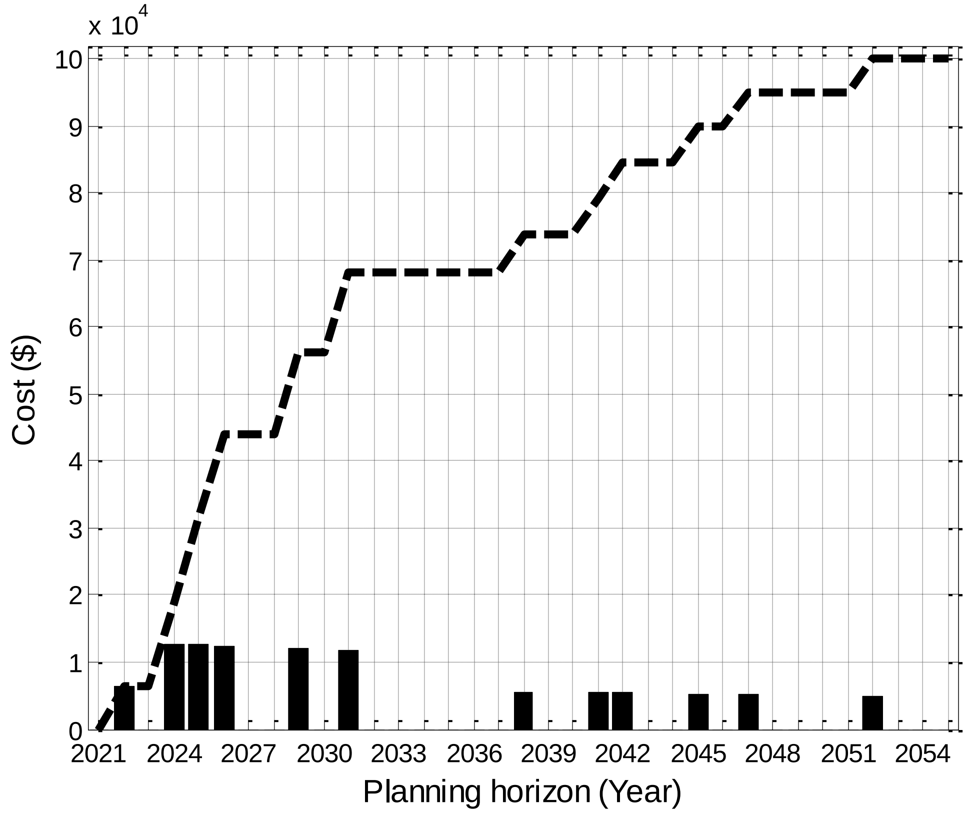

Figure 15: Cash flow of bridge network over a twenty five-year planning horizon

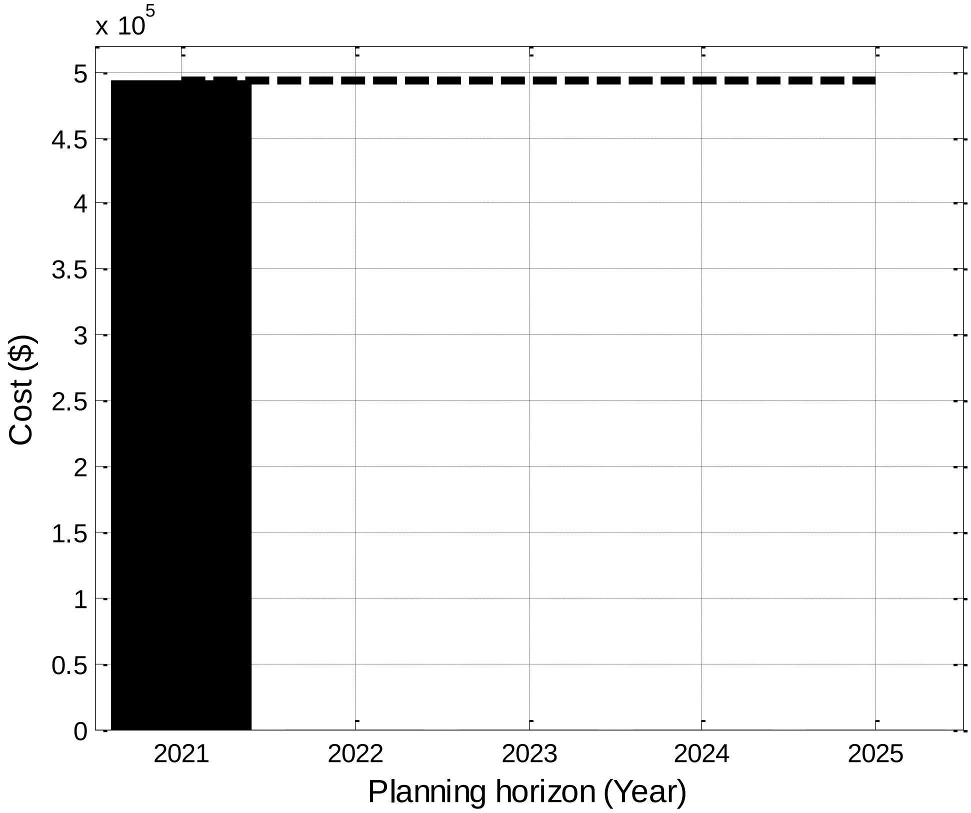

Figure 16: Cash flow of bridge network over a five-year planning horizon (girder case)

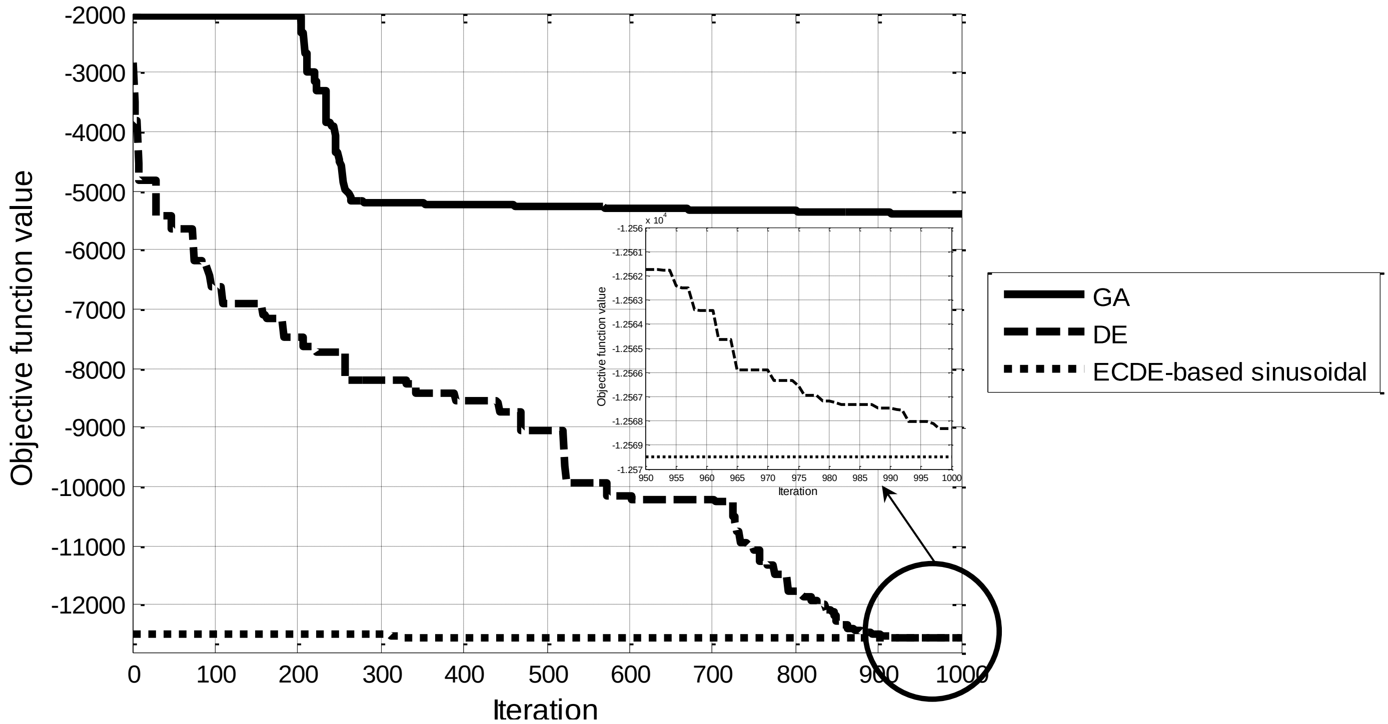

(a) Genetic, differential evolution and ECDE-based sinusoidal algorithms

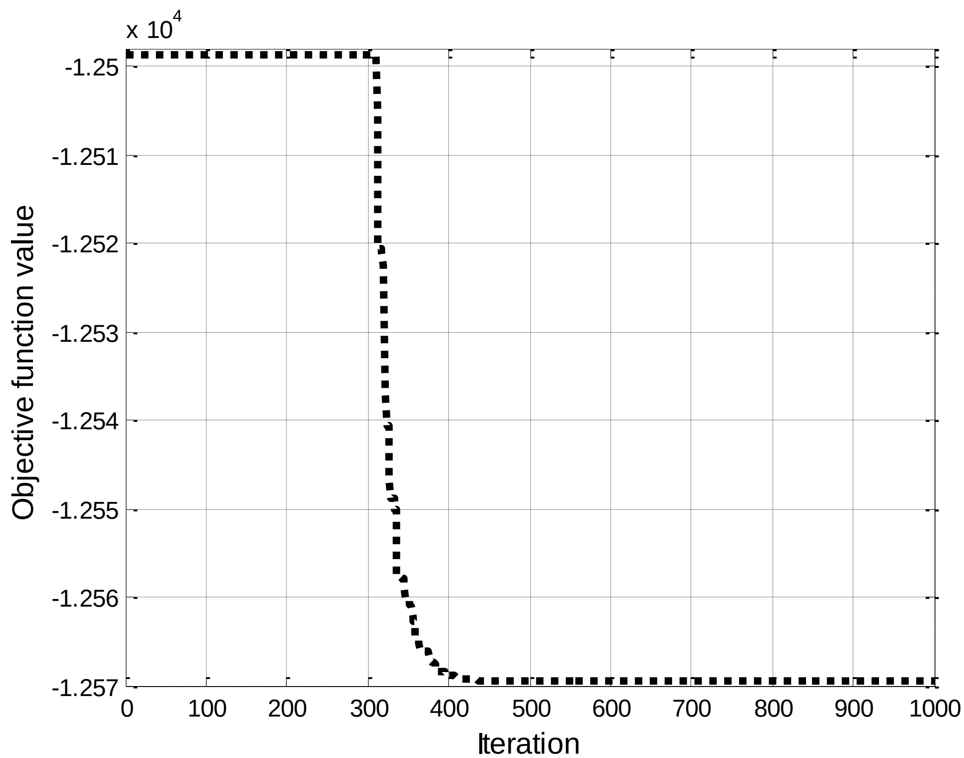

(b) ECDE-based sinusoidal algorithm

Figure 17: Convergence curves of the best performance histories accomplished by genetic, differential evolution and ECDE-based sinusoidal algorithms in Schwefel 2.26 function

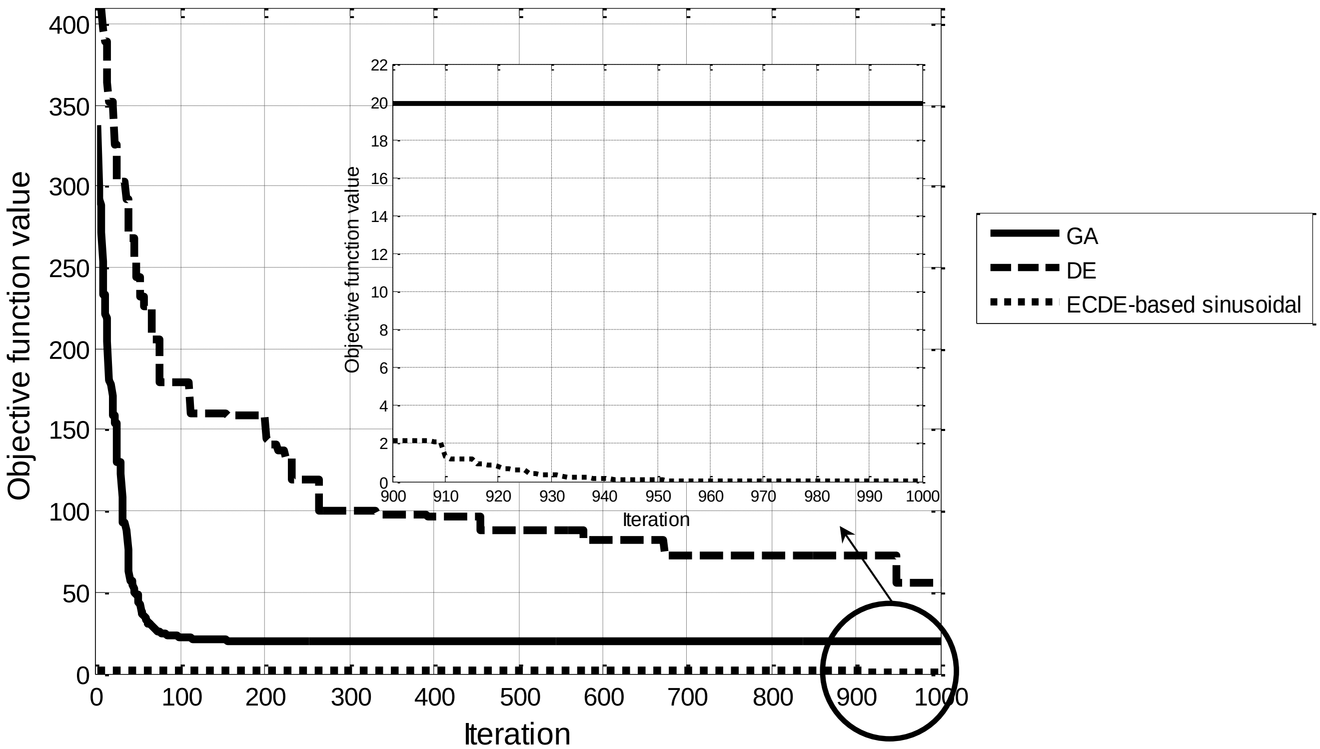

(a) Genetic, differential evolution and ECDE-based sinusoidal algorithms

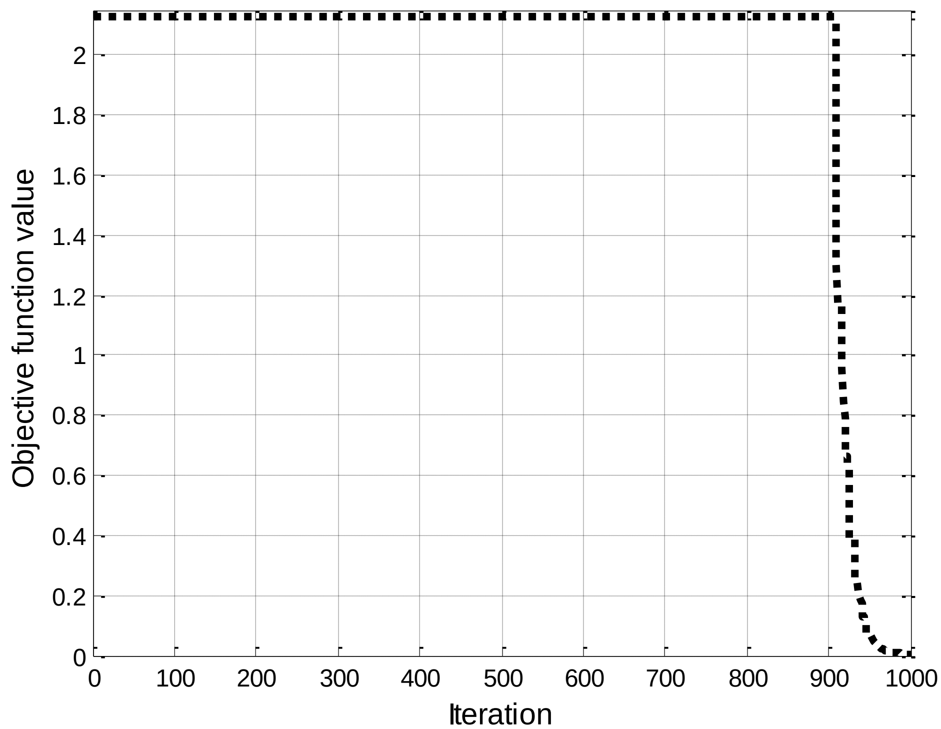

(b) ECDE-based sinusoidal algorithm

Figure 18: Convergence curves of the best performance histories accomplished by genetic, differential evolution and ECDE-based sinusoidal algorithms in Rastrigin function

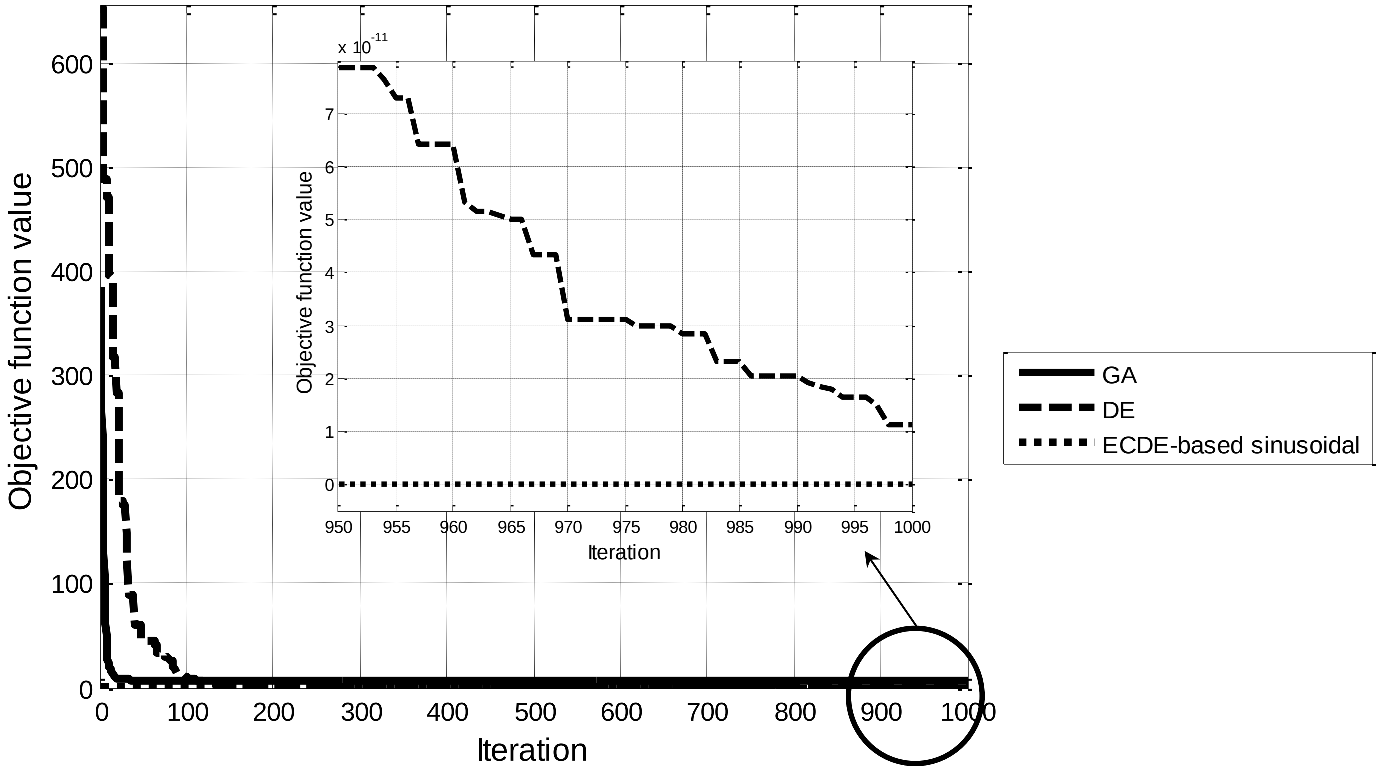

(a) Genetic, differential evolution and ECDE-based sinusoidal algorithms

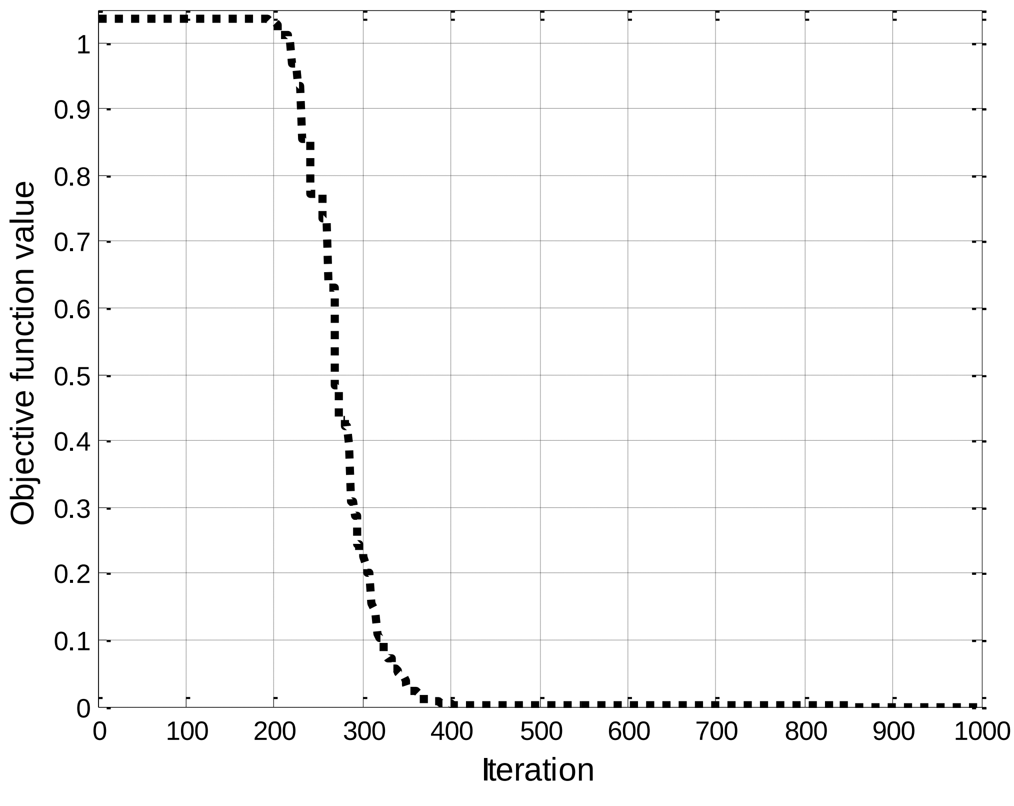

(b) ECDE-based sinusoidal algorithm

Figure 19: Convergence curves of the best performance histories accomplished by genetic, differential evolution and ECDE-based sinusoidal algorithms in Griewank function

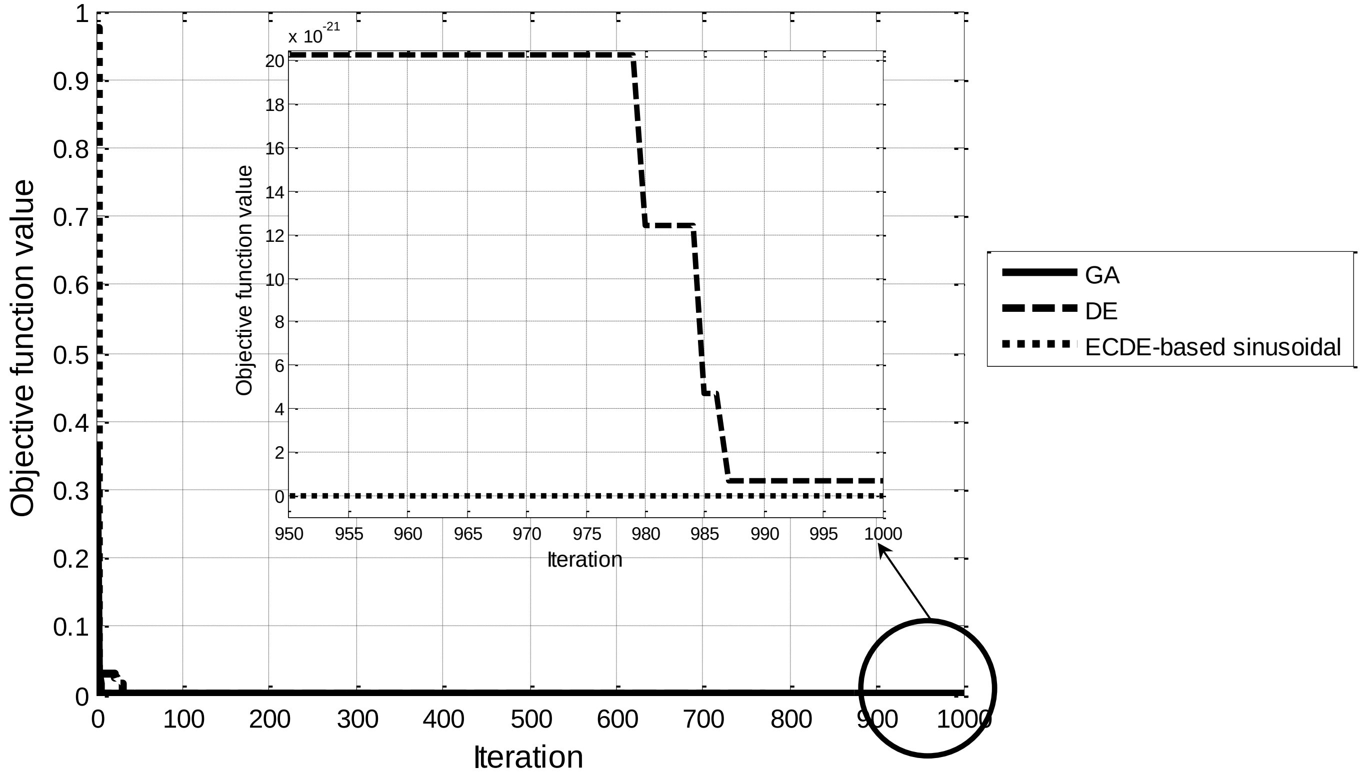

(a) Genetic, differential evolution and ECDE-based sinusoidal algorithms

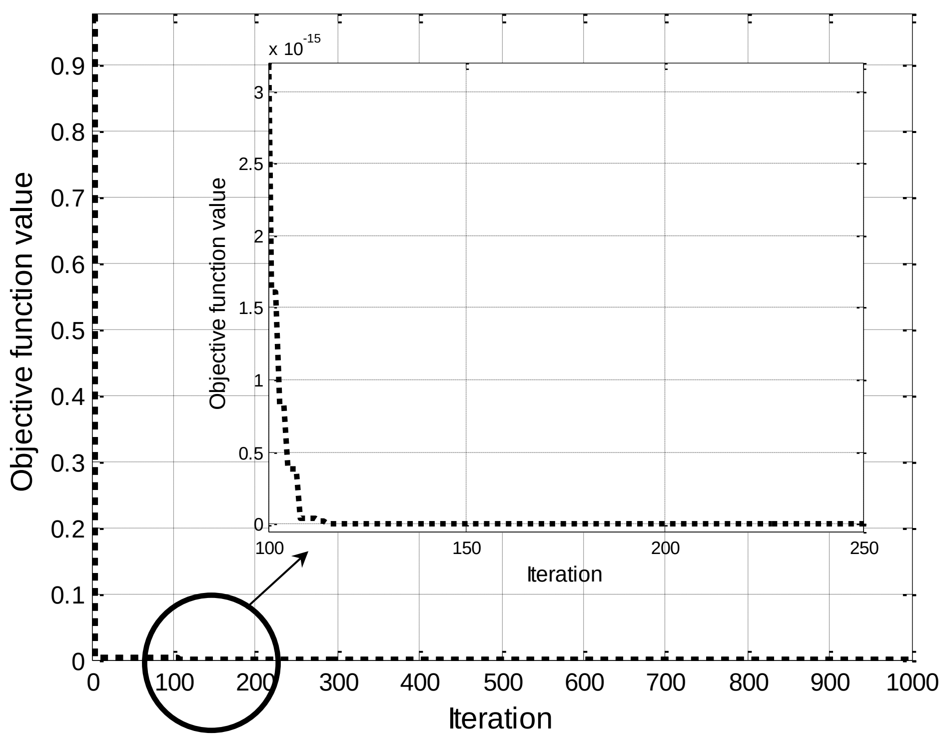

(b) ECDE-based sinusoidal algorithm

Figure 20: Convergence curves of the best performance histories accomplished by genetic, differential evolution and ECDE-based sinusoidal algorithms in Beale function

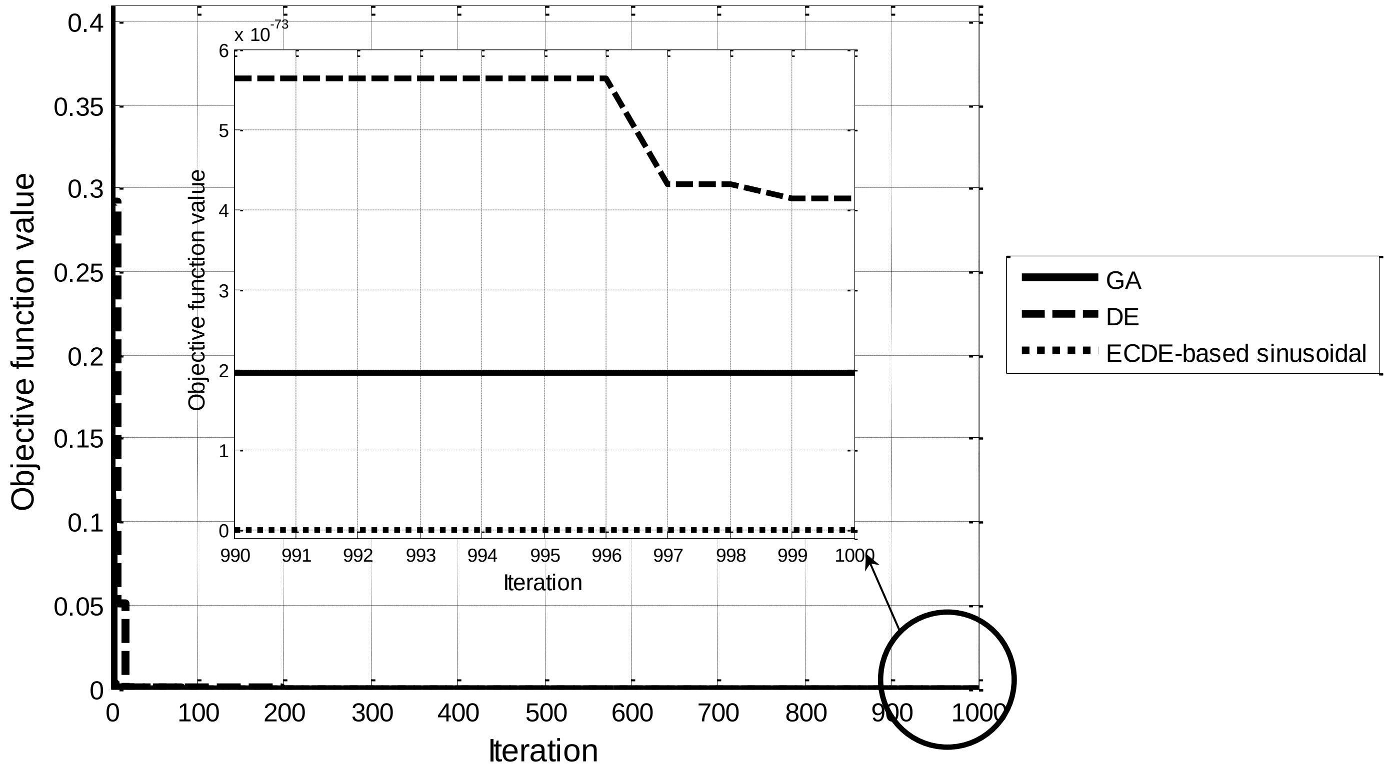

(a) Genetic, differential evolution and ECDE-based sinusoidal algorithms

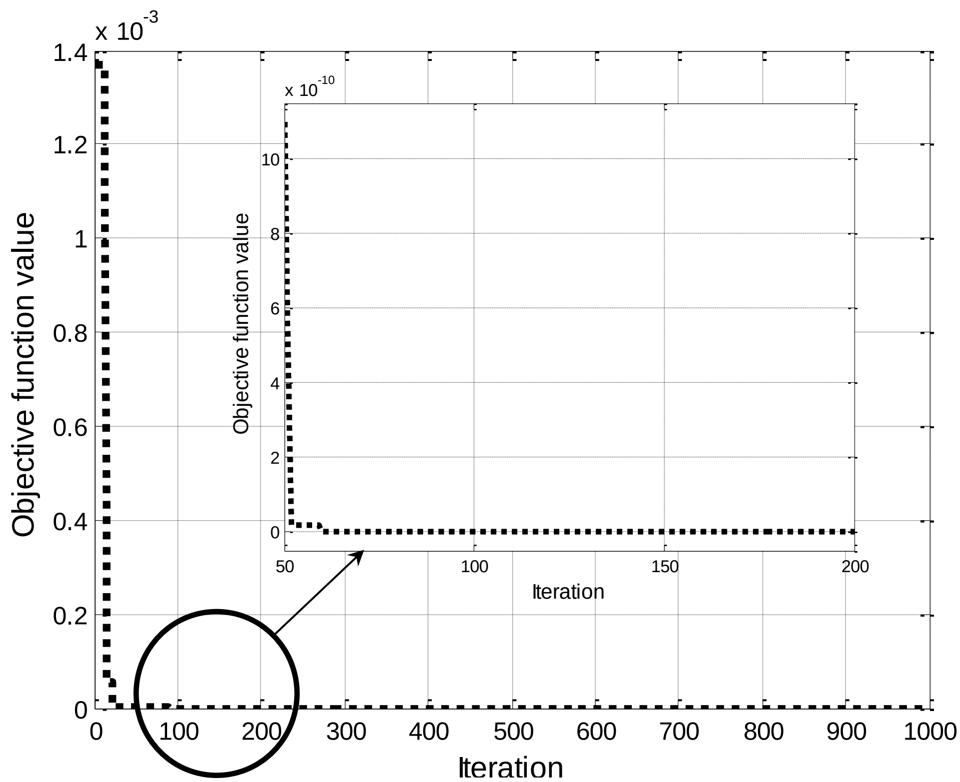

(b) ECDE-based sinusoidal algorithm

Figure 21: Convergence curves of the best performance histories accomplished by genetic, differential evolution and ECDE-based sinusoidal algorithms in three-hump camel function

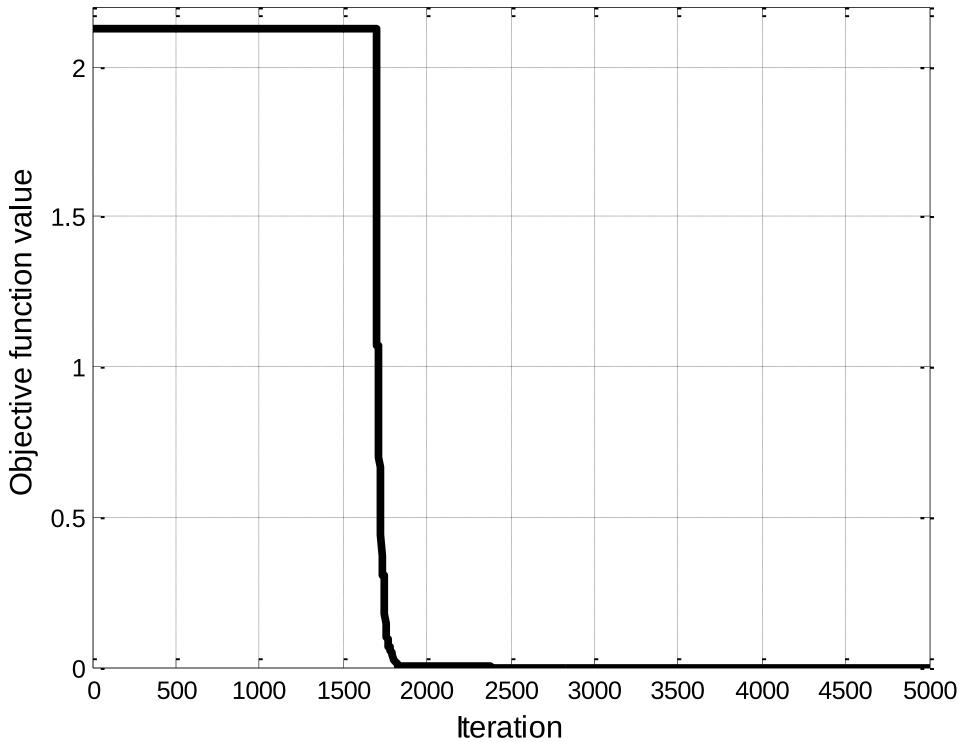

(a) Rastrigin function

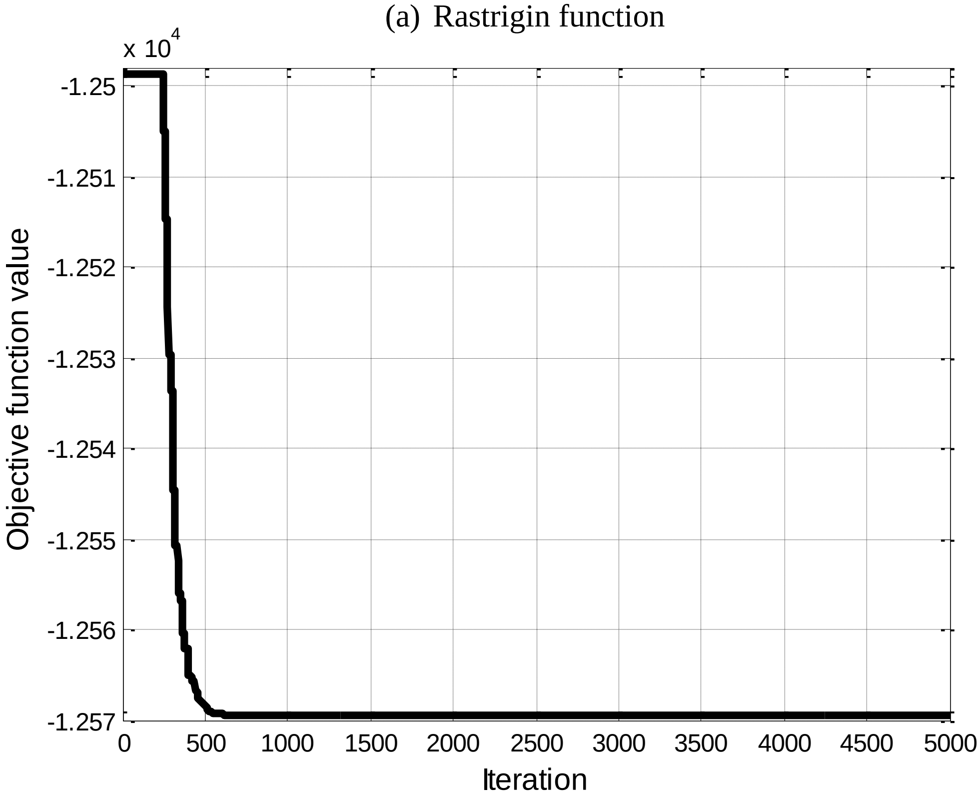

(b) Schwefel 2.26 function

Figure 22: Convergence curves of best performance histories accomplished by ECDE-based sinusoidal algorithm in Rastrigin and Schwefel 2.26 functions in experiment 1

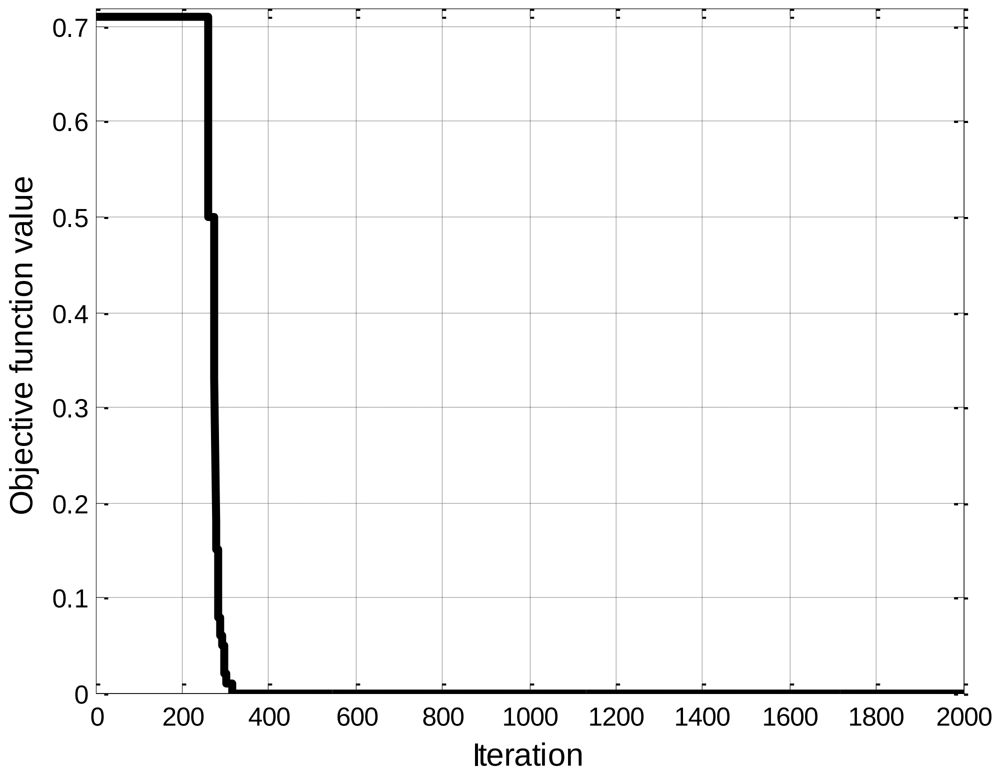

(a) Rastrigin function

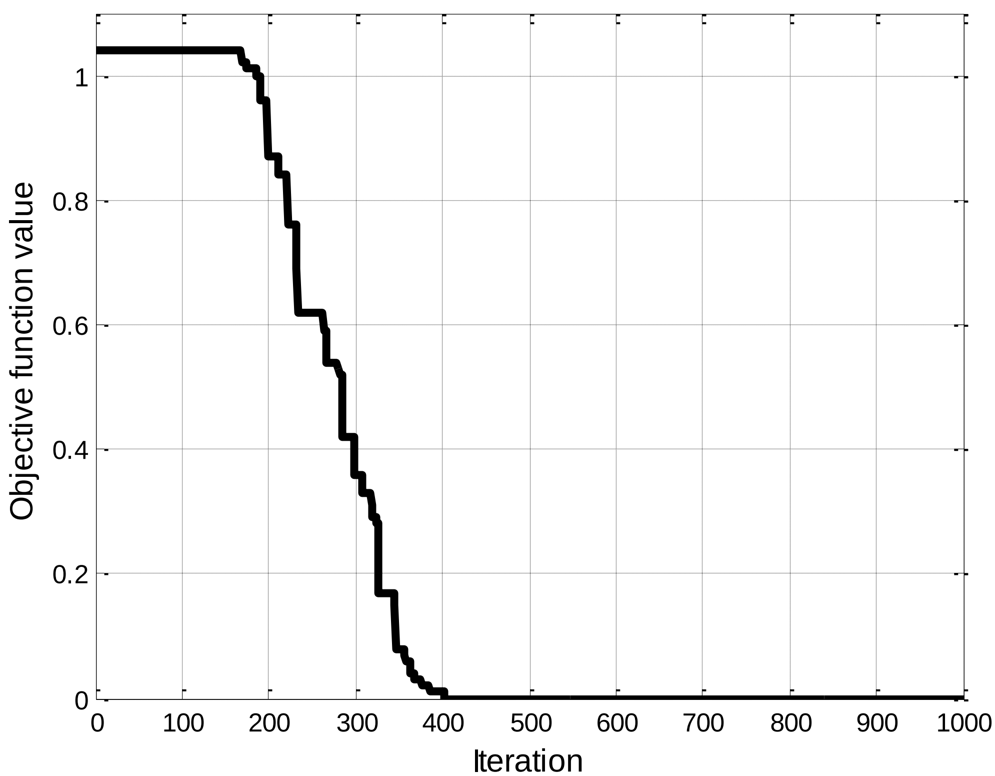

(b) Griewank function

Figure 23: Convergence curves of best performance histories accomplished by ECDE-based sinusoidal algorithm in Rastrigin and Griewank functions in experiment 2

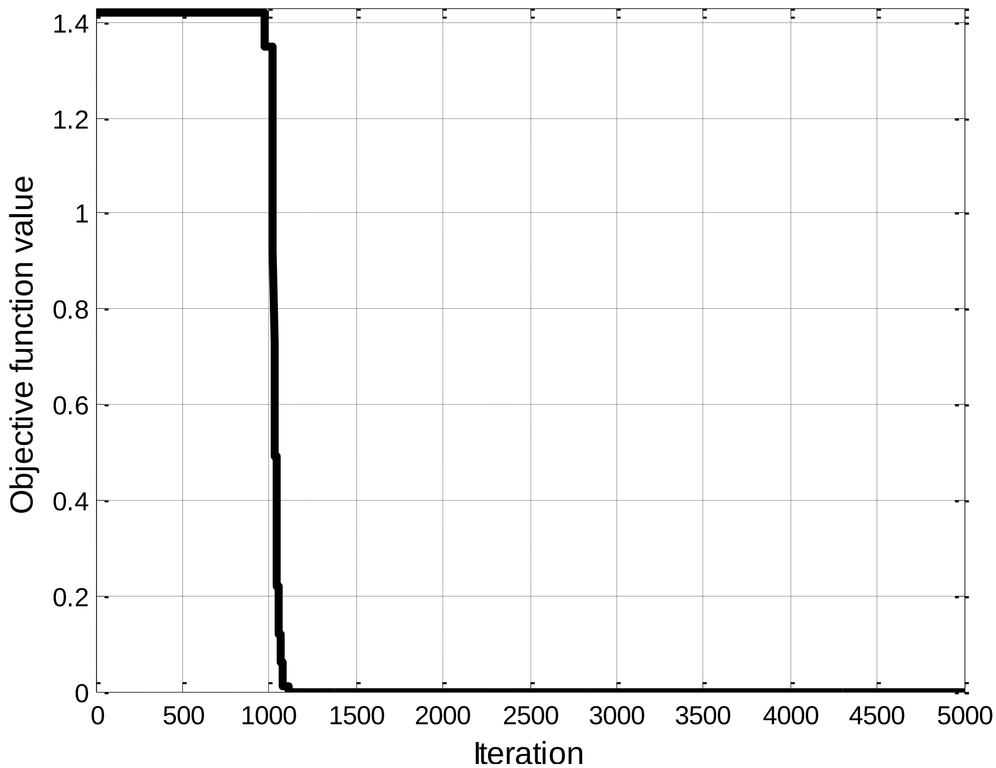

(a) Rastrigin function

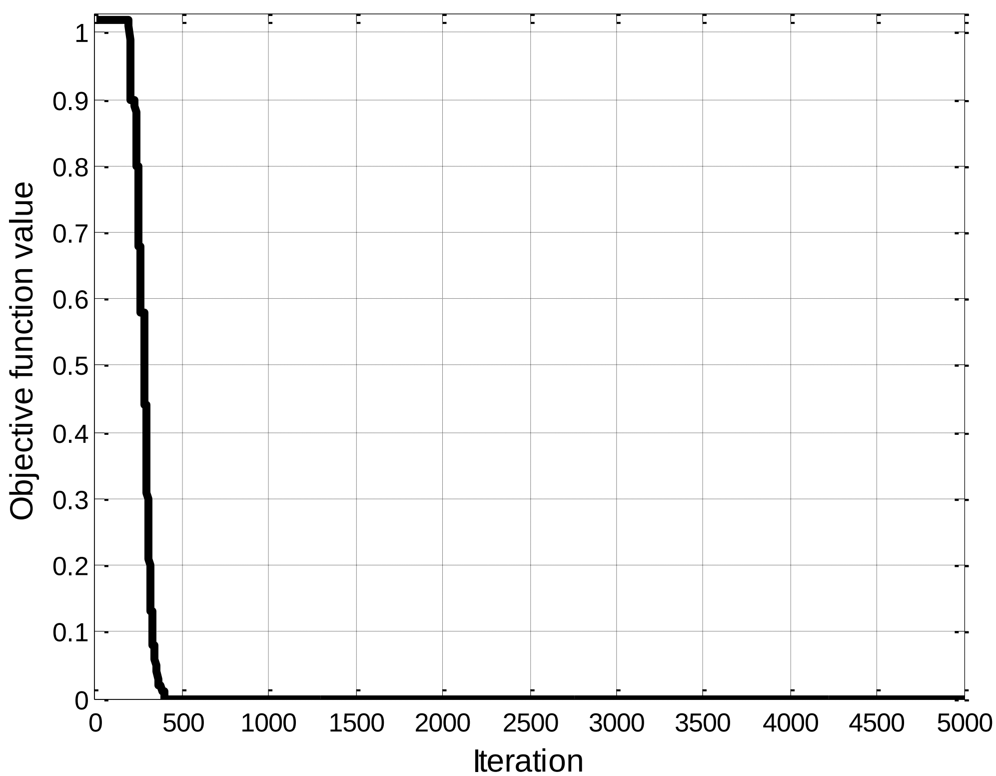

(b) Griewank function

Figure 24: Convergence curves of best performance histories accomplished by ECDE-based sinusoidal algorithm in Rastrigin and Griewank functions in experiment 3

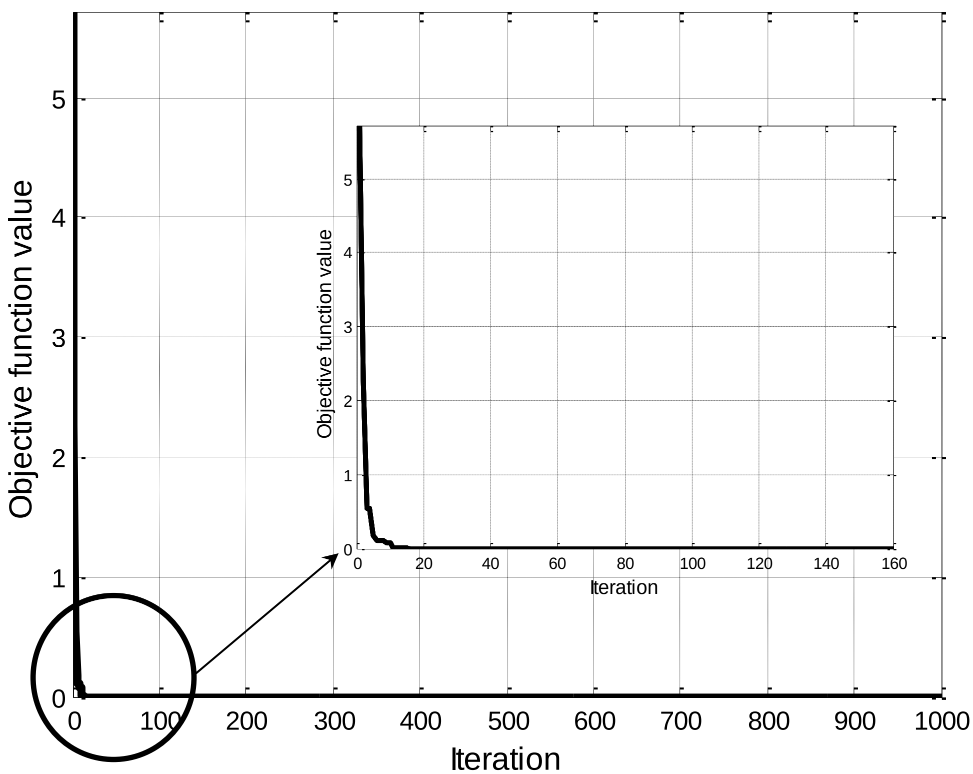

(a) Beale function

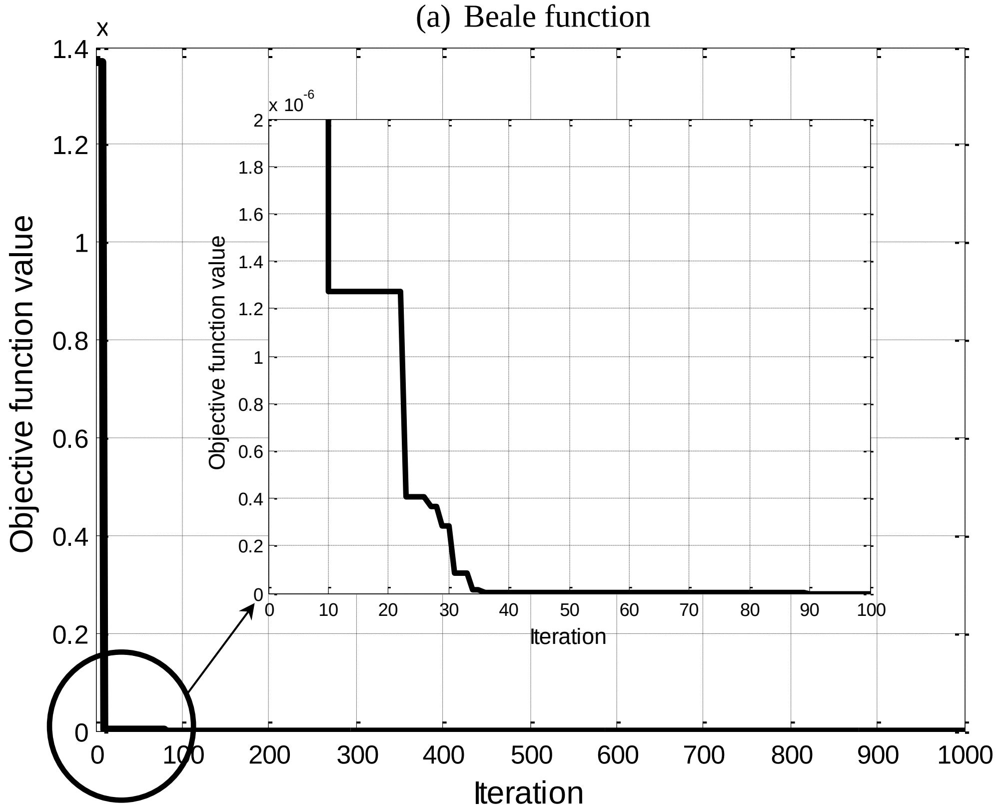

(b) Three-hump camel function

Figure 252: Convergence curves of best performance histories accomplished by ECDE-based sinusoidal algorithm in Beale and three-hump camel functions in experiment 4

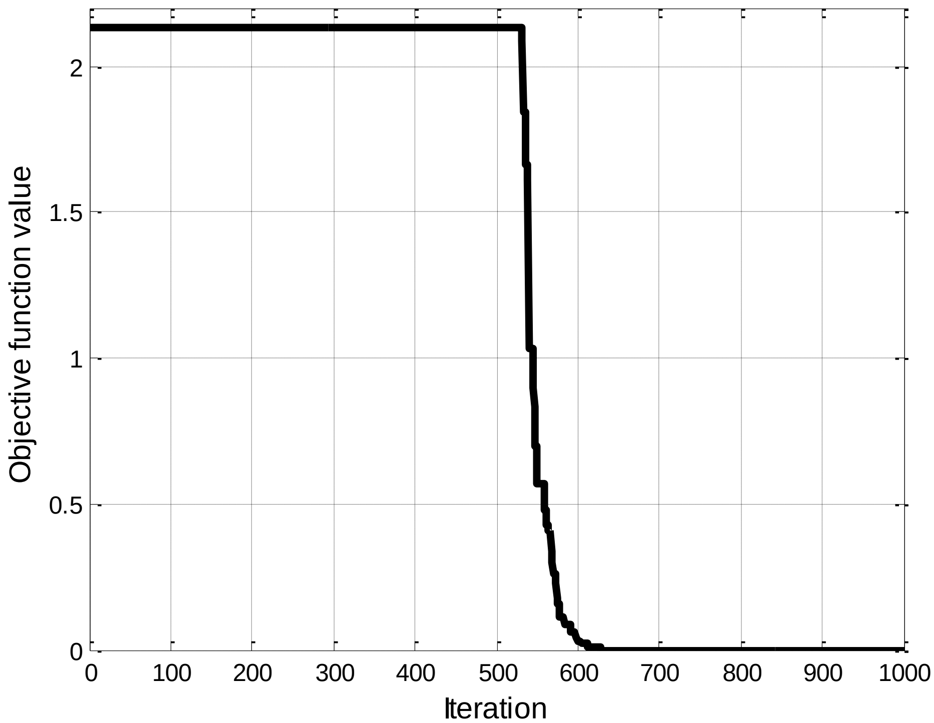

(a) Rastrigin function

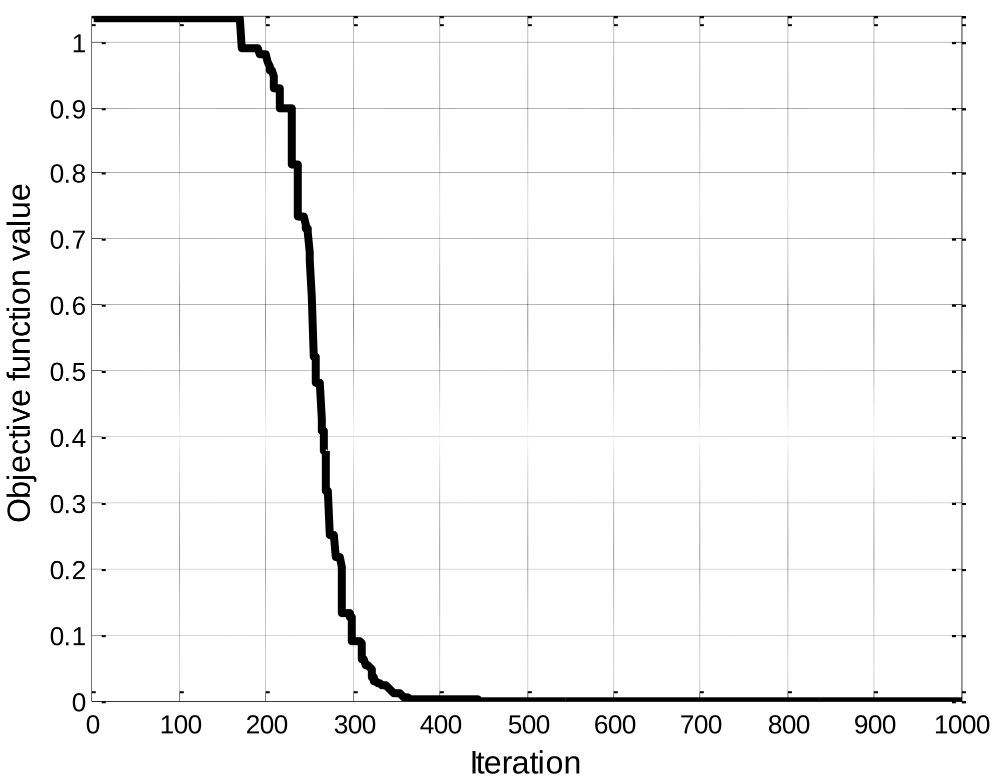

(b) Griewank function

Figure 26: Convergence curves of best performance histories accomplished by ECDE-based sinusoidal algorithm in Beale and three-hump camel functions in experiment 5

List of Tables

Table 1: Intervention actions and their corresponding unit costs for bridge deck

Type of intervention action	Unit cost ($/m^2)
Minor repair	107.19
Major rehabilitation	238.86
Replacement	695.76

Table 2: Performance comparison between the different multi-objective meta-heuristics for maintenance planning of the thirty five-year study period

Performance metric	Object. function	MOEDE Logistic	MOEDE Singer	MOEDE Sinusoidal	MOEDE Sine	MOEDE Iterative
Minimum	CR	**66.02**	64.3	65.11	64.81	65.85
	TLCC	108450.79	163632.75	99495.98	104997.22	109656.6
	TDTT	**0**	**0**	**0**	**0**	**0**
	TEI	37.65	39.63	**33.68**	35.67	37.65
Average	CR	66.02	64.3	65.11	65.2	65.85
	TLCC	108450.79	163925.64	**99495.98**	107554.82	109672.74
	TDTT	**0**	**0**	**0**	**0**	**0**
	TEI	37.65	39.63	**33.68**	36.06	37.65
Hypervolume indicator	…….	98	98	**98.4**	97.7	98
Generational distance	…….	**0**	79.17	**0**	451.25	5.91
Inverted generational distance	…….	**0**	292.89	**0**	2557.6	16.14
Spacing	…….	**0**	4.75×10^{-4}	**0**	**0**	**0**
Maximum Pareto front error	…….	**0**	2005.07	**0**	9020.5	138.19

Table 3: Performance comparison between the different multi-objective meta-heuristics for maintenance planning of the thirty five-year study period (Continued)

Performance metric	Objective function	MOEDE Chebyshev	MOEDE Cubic	MOEDE Logistic-sine	MOEDE Circle
Minimum	CR	64.81	64.1	64.08	64.81
	TLCC	**882308.26**	99394.74	, 110148.4	99810.6
	TDTT	**0**	**0**	**0**	**0**
	TEI	55.48	**33.68**	**33.68**	**33.68**
Average	CR	64.81	64.71	64.08	**66.12**
	TLCC	882308.26	110403.66	, 110148.4	111667.16
	TDTT	**0**	**0**	**0**	**0**
	TEI	55.48	37.65	34.56	37.93
Hypervolume indicator	…….	97.4	96.4	98	97.1
Generational distance	…….	**0**	1163.2	595.52	1120.3
Inverted generational distance	…….	**0**	6579.7	3214.05	5939.33
Spacing	…….	**0**	2.7×10-3	1.8×10-2	**0**
Maximum Pareto front error	…….	**0**	16866	12118	21382

Table 4: Final rankings of meta-heuristic optimization algorithms

Meta-heuristic algorithm	**Mean ranking (μ_a)**	**Standard deviation of ranking (σ_a)**	**Final ranking**
ECDE-based logistic	2.45	2.49	2
ECDE-based singer	3.17	2.44	6
ECDE-based sinusoidal	**2.41**	**2.03**	**1**
ECDE-based sine	2.97	2.50	5
ECDE-based iterative	2.52	2.39	3
ECDE-based Chebyshev	2.90	2.94	4
ECDE-based cubic	3.52	2.77	7
ECDE-based logistic-sine	3.69	2.65	8
ECDE-based circle	4.07	2.98	9
DE	6.17	3.54	10
IWO	7.34	3.71	12
BBO	7.45	3.64	13
TLO	6.76	3.40	11
GA	7.45	3.87	14
Jaya	7.72	3.61	16
PSO	7.55	3.61	15

Table 5: Quantity of information and final weights of attributes based on CRITIC algorithm

Index	CR	TLCC	TDTT	TEI
Q_j	0.3	0.2	0.26	0.23
W_j	30.07%	20.03%	26.68%	23.22%

Table 6: Sample of the solutions' rankings obtained from COPRAS, GRA and AR for the maintenance planning of five-year study period

Objective function values [CR, TLCC, TDTT, TEI]	Utility degree	Grey relational grade	Mean ranking (μ_a)	Final ranking
[72.87, 38805.06, 0, 11.89]	100	71.8	1	1
[73.28, 99628.99, 0, 33.83]	88.13	67.13	6	6
[73.72, 899921.57, 0, 41.6]	30.24	60.97	7	7
[74.15, 1313327.1, 0, 179.64]	47.34	48.86	8	8
[74.58, 374606.95, 0, 263.74]	20.83	47.3	9	9

Table 7: Sample of the solutions' rankings obtained from COPRAS, GRA and AR for the maintenance planning of twenty five-year study period

Objective function values [CR, TLCC, TDTT, TEI]	**Utility degree**	**Grey relational grade**	**Mean ranking (μ_a)**	**Final ranking**
[64.09, 36320.8, 0, 11.89]	99.81	86.13	2	1
[64.21, 36784.8, 0, 11.89]	99.63	86.04	6	5
[72.02, 2793796.51, 6, 81.68]	14.85	61.82	102.5	104
[65.86, 810025.81, 0, 194.91]	15.61	60.76	104	105
[72.45, 3927176.3, 6, 101.64]	14.15	57.92	116	116

Table 8: Sample of the solutions' rankings obtained from COPRAS, GRA and AR for the maintenance planning of thirty five-year study period

Objective function values [CR, TLCC, TDTT, TEI]	Utility degree	Grey relational grade	Mean ranking (μ_a)	Final ranking
[64.08, 110148.4, 0, 33.68]	100	74.69	1.5	1
[64.34, 100570.04, 0, 33.68]	98.72	71.85	24.5	24
[64.81, 106738.61, 0, 35.67]	94.72	66.27	104.5	106
[65.86, 109656, 0, 37.64]	92.09	62.65	141	141
[66.37, 114017.76, 0, 37.67]	66.92	62.75	154	152

Table 9: Comparison between meta-heuristics in optimizing bridge maintenance plans over five-year study period (girder case)

Meta-heuristic	Minimum condition rating	Total life-cycle maintenance cost	Total duration of traffic disruption	Total environmental impact	Number of intervention actions
ECDE-based sinusoidal	86.41	$493,551.56	0	126.14	10
DE	86.41	$1,0297,74.36	282.20	86.41	12
GA	90.62	$4,453,917.27	2.89	466.63	96

Table 10: Results of the ECDE-based sinusoidal, GA and DE algorithms for benchmark test functions

Test function	Search space	Global optimum solution	Metric	ECDE - based sinusoidal	GA	DE
Schwefel 2.26	[-500, 500]	-12569.5	Best	-12569.49	-5400.67	-12568.32
			Worst	-12569.49	-3258.75	-12449.04
			Average	-12569.49	-4509.28	-12531.73
			Standard deviation	0	864.44	45.61
Rastrigin	[-5.12, 5.12]	0	Best	3.6E-03	19.9	55.72
			Worst	2.13	27.86	68.05
			Average	1.7	22.88	61.81
			Standard deviation	0.85	3.33	5.18
Griewank	[-600, 600]	0	Best	0	6.11	1.12E-11
			Worst	5.55E-16	10.69	7.56E-11
			Average	1.11E-16	8.53	4.28E-11
			Standard deviation	2.22E-16	1.85	2.73E-11
Beale	[-4.5, 4.5]	0	Best	0	3.02E-11	6.53E-22
			Worst	0	8.40E-04	2.43E-19
			Average	0	2.30E-04	9.23E-20
			Standard deviation	0	3.22E-04	1.06E-19
Three-hump camel	[-5, 5]	0	Best	2.59E-244	1.96E-73	4.13E-73
			Worst	5.29E-239	8.99E-10	1.56E-66

			Average	1.06E-239	1.80E-10	3.36E-67
			Standard deviation	0	3.60E-10	6.12E-67

Table 11: Performance comparison of meta-heuristics in experiment 1

Test function	Metric	ECDE -based sinusoidal	ICSAT
Rastrigin	Best	0	9.84
	Average	1.33E-13	11.04
Schwefel 2.26	Best	-12569.49	3.76E-7
	Average	-12569.49	1.49E-5

Table 12: Performance comparison of meta-heuristics in experiment 2

Test function	Metric	ECDE -based sinusoidal	Jaya − Bat
Rastrigin	Best	0	1.17E-04
	Worst	2.34E-04	13.92
	Average	7.79E-06	4.94
	Standard deviation	4.2E-05	3.48
Griewank	Best	1.11E-16	2.9E-11
	Worst	5.53E-13	7.4E-03
	Average	4.03E-14	4.93E-04
	Standard deviation	1.27E-13	1.9E-03

Table 13: Performance comparison of meta-heuristics in experiment 3

Test function	Metric	ECDE -based sinusoidal	IPSO
Rastrigin	Average	0	3.54
Griewank	Average	0	2.53E-03

Table 14: Performance comparison of meta-heuristics in experiment 4

Test function	Metric	ECDE -based sinusoidal	GEO
Beale	Average	0	0
	Standard deviation	0	0
Three-hump camel	Average	8.88E-284	6.28E-126
	Standard deviation	0	1.73E-125
Rastrigin	Average	2.08E-01	1.09E01
	Standard deviation	5.53E-01	3.28
Griewank	Average	3.7E-18	5.01E-03
	Standard deviation	1.99E-17	5.53E-03